UNIVERSITY OF BELGRADE
FACULTY OF MEDICINE

Marko Đ. Vorkapić

SPECTRAL, BIOTIC AND FRACTAL ANALYSIS OF EEG AND ECG SIGNALS IN EXPERIMENTAL MODELS OF MYOCARDIAL INFARCTION AND EPILEPSY

doctoral dissertation

Belgrade, 2024

UNIVERZITET U BEOGRADU
MEDICINSKI FAKULTET

Marko Đ Vorkapić

SPEKTRALNA, BIOTIČKA I FRAKTALNA ANALIZA EEG I EKG SIGNALA U EKSPERIMENTALNIM MODELIMA INFARKTA MIOKARDA I EPILEPSIJE

doktorska disertacija

Beograd, 2024

MENTORS/PhD ADVISORS

1. **Prof. Dr. Dragan Hrnčić**, Associate Professor and Principal Research Fellow, Faculty of Medicine, University of Belgrade.

2. **Prof. Dr. Milica Janković**, Associate Professor
   University of Belgrade – School of Electrical Engineering

MEMBERS OF THE COMMITTEE

1. **Prof. Dr. Olivera Stanojlović**, Full Professor,
   Faculty of Medicine, University of Belgrade

2. **Prof. Dr. Predrag Mitrović**, Full Professor,
   Faculty of Medicine, University of Belgrade

3. **Prof. Dr. Aleksandar Ristić**, Assistant Professor,
   Faculty of Medicine, University of Belgrade

4. **Dr. Andrej Savić,** Senior Research Associate,
   University of Belgrade – School of Electrical Engineering

5. **Prof. Dr. Vojin Ilić**, Full professor,

   University of Novi Sad, Faculty of Technical Sciences

DATE OF DEFENSE: _____

MENTORI

1. **Prof. dr Dragan Hrnčić**, vanredni profesor i naučni savetnik,
   Medicinski fakultet, Univerzitet u Beogradu

2. **Prof. dr Milica Janković**, vanredni profesor
   Elektrotehnički fakultet, Univerzitet u Beogradu

ČLANOVI KOMISIJE

1. **Prof. dr Olivera Stanojlović**, redovni profesor
   Medicinski fakultet, Univerzitet u Beogradu

2. **Prof. dr Predrag Mitrović**, redovni profesor,
   Medicinski fakultet, Univerzitet u Beogradu

3. **Prof. dr Aleksandar Ristić**, docent
   Medicinski fakultet, Univerzitet u Beogradu

4. **Dr Andrej Savić**, viši naučni saradnik
   Elektrotehnički fakultet, Univerzitet u Beogradu

5. **Prof. dr Vojin Ilić**, redovni profesor
   Fakultet tehničkih nauka, Univerzitet u Novom Sadu

DATUM ODBRANE:_____

Firstly, I must thank p*rof. Olivera Stanojlović* for the unwavering faith she always had for all of the doctoral students as well as our mentors, even when, at times, we may have lost faith ourselves. Also, it would be impossible, not to remember that decisive moment during the second year Physiology exam we crossed paths, a moment which has paved the way for everything that was later to come, and that in some way still steers my course through the waters of professional life. In a word: thank you, professor.

To *prof. Nela Puškaš* of the Institute of Histology and Embryology "Aleksandar Đ. Kostić" I extend thanks for her expertise in histological techniques and given support.

To *prof. Aleksandra Rašić Marković* I express my gratitude for the valuable advice that helped guide the methodology used during the experimental process. *Dr Andrej Savić* I must especially thank for all the engineering, scientific knowledge as well as invaluable advice that played a key role in shaping the signal analysis segments of this research.

Further, to *Andrijana Pušica, Milica Isaković and Milica Badža Atanasijević,* former students of School of Electrical Engineering and now engineers in their own right, I am grateful for the contribution to signal processing and analysis techniques used during our study.

To dearest colleagues from the Institute of Medical Physiology "Richard Burian", *dr sci med Nikola Šutulović, dr sci med Željko Grubač and dr Nikola Useinović* I am grateful for help and support during the long hours of lab work.

Prof. Milica Janković I cannot thank enough and cannot possibly list all the numerous ways she has helped make this thesis a reality: from the conceptualization of the experimental method through the realization of electrophysiologic experiments all the way to biosignal analysis. Leaving aside her professional contribution I must extend a heartfelt thanks for the impeccable personal relation and support she has afforded me over the years.

Finally, to *prof. Dragan Hrnčić* I must give the most heartfelt of thanks, not only for all he has taught me, first as an assistant of Physiology during my graduate studies, then as a mentor, not only for his extraordinary contribution to every aspect of this dissertation but first and foremost for all of the honest and dedicated support he provided me over the years that far surpasses mere mentoring, and can be defined only, as friendship.

Belgrade, 2024

Also, I must express gratitude to the coauthors of the publications that have been produced as a result of this research for the following contributions:

1. Thesis conceptualization: *prof. Dragan Hrnčić*, *prof. Milica Janković, dr Andrej Savić;*

2. Data collection: *dr Nikola Useinović; dr Anida Ademović, dr Aleksa Leković, dr Željko Grubač, dr Nikola Šutulović*

3. Data curation: *prof. Olivera Stanojlović,* p*rof. Dragan Hrnčić*, *prof. Milica Janković, dr Andrej Savić*, *prof. Nela Puškaš, Milica Isaković; prof. Aleksandra Rašić Marković*

4. Formal analysis: *Milica Isaković, prof. Dragan Hrnčić, prof. Milica Janković;*

5. Methodology: *prof. Dragan Hrnčić*, *dr Andrej Savić, prof. Milica Janković, Milica Isaković;*

6. Supervision: *prof. Dragan Hrnčić, prof. Milica Janković, prof. Olivera Stanojlović;*

7. Writing: *prof. Dragan Hrnčić, prof. Milica Janković, prof. Olivera Stanojlović, dr Andrej Savić.*

Title of doctoral dissertation

SPECTRAL, FRACTAL AND BIOTIC ANALYSIS OF EEG AND ECG SIGNALS IN EXPERIMENTAL MODELS OF MYOCARDIAL INFARCTION AND EPILEPSY

Abstract

Acute myocardial infarction (AMI) and epilepsy are responsible for significant morbidity and mortality. Besides clinical significance, another thread connecting AMI and epilepsy is the importance of signal analysis in establishing diagnosis as well as assessing risk for disease progression.

The objectives of this study were to investigate spectral, fractal and biotic characteristics of the EEG and ECG signals in animal models of AMI and epilepsy.

We used the rat model of isoprenaline-induced AMI and registered concomitantly ECG and EEG signals in baseline conditions and up to 24h after isoprenaline administration. Histological myocardium evaluation was done at the end of registration period to assess AMI development morphology. The spectral, fractal and biotic characteristics of the EEG and ECG were analyzed.

Lindane-induced generalized seizures in rats were used herein as experimental model of epilepsy. EEG and ECG signals were recorded simultaneously before and after lindane administration. Ictal EEG parameters were detected and analyzed. EEG, as well as ECG features were extracted using spectral, fractal and biotic analyses and neural networks were constructed in order to test the possibility of automatic detection of seizures.

Development of AMI has been confirmed by presence of ST elevation in ECG and histological findings of myocardial necrosis. Significant alterations were determined in EEG spectral power in the alpha, beta and theta bands upon isoprenaline administration. These alterations were significantly correlated with ST elevation. We found significant changes in biotic, fractal and time domain analyses of ECG before and after isoprenaline administration. All perceived changes returned to baseline averages after 24h denoting acute effects. In the epilepsy model, we saw significant changes in spectral EEG power and band power dominance in ictal vs baseline periods. EEG and ECG features based on spectral, fractal and biotic analyses were extracted and neural networks for detection of ictal periods were trained. Neural network based on our features for detection of ictal events showed favorable performances.

Key words: EEG, ECG, HRV, nonlinear, Epilepsy, AMI, signal analysis, Bios, Isoprenaline, Lindane.

Scientific field: Medicine

Scientific subfield: Physiological Sciences

UDC number: _____

Naziv doktorske disertacije

SPEKTRALNA, BIOTIČKA I FRAKTALNA ANALIZA EEG I EKG SIGNALA U EKSPERIMENTALNOM MODELU INFARKTA MIOKARDA I EPILEPSIJE

Sažetak

Akutni infarkt miokarda (AMI) i epilepsija su bolesti odgovorne za značajan morbiditet i mortalitet u populaciji. Pored njihovog klničkog značaja, još jedna važna veza AMI i epilepsije ogleda se u značaju analize signala za uspostavljanje dijagnoze, procenu rizika i praćenje progresije bolesti.

Ciljevi ove studije bili su da ispitaju spektralne, fraktalne i biotičke karakteristike EKG i EEG signala u animalnom modelu AMI i epilepsije.

Koristili smo model Isoprenalinom indukovanog AMI kod pacova i paralelno registrovali EKG i EEG signale pre administracije kao i do 24h nakon administracije Isoprenalina. Radi procene razvoja AMI učinjena je histološka evaluacija miokarda na kraju perioda registrovanja signala. Analizirane su spektralne, fraktalne i biotičke karakteristike EEG i EKG signala.

Za modelovanje epileptičkih napada korišćen je Lindanski model kod pacova. EEG i EKG signali su registrovani pre i nakon administracije Lindana. Iktalni EEG parametri su detektovani i analizirani. Koristeći spektralne, fraktalne i biotičke analize, izvučene su EEG i EKG karakteristike koje su nakon toga korišćene za treniranje neuralne mreže u svrhu automatske detekcije i predikcije pojave epileptičkih napada.

Razvoj AMI potvrđen je pojavom ST elevacije i karakterističnim histološkim nalazom nakon nekroze miokarda. Nakon administracije isoprenalina registrovane su značajne promene u EEG spektru alfa, beta i gama frekventnih opsega. Navedene promene su značajno korelisale sa ST elevacijom. Takođe, našli smo značajne promene u biotičkim i fraktalnim parametrima i paramterima vremenskog domena EKG signala pre i nakon administracije Isoprenalina. Sve promene su se povukle nazad na osnovne vrednosti nakon perioda od 24h što ukazuje na akutne efekte.

U modelu epilepsije registrovane su značajne promene u snazi EEG spektra kao i u dominaciji snage pojedinih frekventnih opsega u iktalnoj u odnosu na osnovne vrednosti. Nakon izolovanja EEG i EKG karakteristika, trenirali smo neuralne mreže koje su potom dale zadovoljavajuće rezultate u automatskoj detekciji i predikciji iktalnih fenomena.

Ključne reči: EEG, ECG, HRV, nelinearne metode, Epilepsija, AMI, analiza signala, Bios, Izoprenalin, Lindan.

Naučna oblast: Medicina

Uža naučna oblast: Fiziološke nauke

UDK broj:_____

Contents

1. INTRODUCTION 11
1.1 Epilepsy 12
Pathophysiological, epidemiological and diagnostic aspects of epilepsy 12
Experimental models of epilepsy 13
1.2 Acute myocardial infarction 14
Patophysiological, epidemiological and diagnostic aspects of myocardial infarction 14
Experimental models of myocardial infarction 15
1.3 The heart brain axis: a focal point of autonomic regulation 16
1.4 Neurophysiological basis of ECG and EEG 18
Cardiac conduction system and origin of ECG 18
Neuronal electrophysiology and origin of EEG 20
1.5 Acquisition and advanced analysis of biological signals 22
Significance of EEG in clinical practice and experimental research 22
Significance of ECG in clinical practice and experimental research 23
Advanced EEG signal analysis 24
Advanced ECG signal analysis 25
1.6 Artificial neural networks 27
1.7 Biological signals as digital biomarkers 28
2. STUDY GOALS 30
3. MATERIALS AND METHODS 32
3.1 Experimental animals 33
3.2 EEG and ECG registration set-up and analysis 33
Electrode implantation 33
Data acquisition 33
ECG and EEG signal analysis: general aspects 34
3.3. Experiment I: model of AMI 35
AMI induction and experimental design 35
Heart tissue sampling and histopathological evaluation 35
Data recording and processing details 35
3.4 Experiment II: model of epilepsy 36
Epilepsy induction and registration 36
Analysis of spectral ictal EEG data 37
HRV based seizure prediction using neural networks 37
Biotic EEG based seizure detection using neural networks 38
3.5 Statistical analysis 41

4. RESULTS 42
4.1 Isoprenaline induced acute myocardial infarction model 43
4.1.1 Isoprenaline - induced ECG and histological changes 43
4.1.2 Medial prefrontal cortex EEG signal characteristics during AMI 44
EEG power spectrum analysis 44
Correlation analysis of EEG frequency band relative power and ST elevation 48
4.1.3 ECG characteristics during AMI 49
Time domain HRV features 49
Frequency domain HRV features 55
Nonlinear HRV features 59
4.2. Lindane induced epilepsy model 70
4.2.1 Linear EEG signal characteristics during lindane induced epilepsy model 70
4.2.2 Seizure recognition using neural networks in lindane induced epilepsy model. 72
5. DISCUSSION 74
6. CONCLUSIONS 82
7. LITERATURE 84

1. INTRODUCTION

1.1 Epilepsy

Pathophysiological, epidemiological and diagnostic aspects of epilepsy

Epilepsy has, since ancient times been known as an extremely debilitating but often misunderstood neurological disorder. The total prevalence of epilepsy, according to modern research is around 1% which along with its debilitating and unpredictable nature makes it one of the diseases with the greatest morbidity burden. [Rao VR et al., 2015].

Paroxysmal occurrence of seizures caused by intermittent hypersynchronous neuronal activity, classically within the cortex of the brain, is regarded as the defining characteristic of epilepsy. Extent, as well as cortical region localization of hypersynchronous neuronal activity provides criteria for classification as well as pathophysiological explanation for seizure clinical manifestation.

If hypersynchronous neuronal activity is localized to a single cortical region, such as the temporal lobes, the clinical manifestation will be as partial seizures (i.e. temporal lobe epilepsy). If hypersynchronous activity engulfs the entire cortex, the resulting seizure will have of grand-mal tonic-clonic type (GTSC) characteristics [Moshé SL et al., 2014]. The cornerstone of epilepsy pathophysiology, is neuronal hyperexcitability with impaired functional connectivity in the cortex and/or deep gray matter structures. The seizures have a characteristic bioelectrical signature detected as interictal epileptiform discharges (IEDs) and recorded using surface and/or deep electroencephalography (EEG) signal registering. Numerous different epileptic EEG signal isoforms are described in the literature, including sharp waves, sharp, transient spikes; polyspikes or spike-wave complexes [Werhahn KJ et al., 2015].

The gold standard in diagnosis of epilepsy is defined as a characteristic spike wave pattern EEG signal recorded during a seizure, assessed by an experienced neurologist/neurophysiologist in coordination with the clinical symptoms [Nashef L et al., 2009]. As it is commonly the case with gold standards, this technique has its drawbacks. Firstly, there is the issue of -significant inter observer variability when it comes to EEG signal analysis and interpretation weather subjective (due to individual observer characteristics) or objective (since background noise, muscle and electrocardiography (ECG) artifacts can mimic the pattern characteristic for epileptic activity). Secondly, the classical technique of EEG recording and analysis oftentimes includes the necessity for multiple day video-EEG monitoring in order to document the seizure, which is neither convenient nor cost effective [Tzallas AT et al., 2012].

Furthermore, problems in epilepsy treatment become acutely evident if we take into account its stochastic, i.e. paroxysmal, unpredictable nature. Due to the paroxysmal nature of epilepsy, antiepileptic drug therapy, the cornerstone of epilepsy treatment, is necessarily chronic in nature. On the other hand, the possibility of predicting seizure onset and consequently acting with medications in the hours or minutes before the seizure, is rightfully considered the holy grail of treatment research [Netoff T et al., 2009].

Thus, contemporary epileptology is faced with a difficult task of integrating seizure diagnosis, prediction, prevention and treatment in order to avoid life threatening outcomes caused by an unpredictable and paroxysmal disease. In this task, a multidisciplinary approach and automation are two paths that afford great promise.

Experimental models of epilepsy

Understanding the complex mechanisms of epileptogenesis that underlie seizure generation cannot be achieved exclusively through human studies. The stochastic nature of epilepsy and ethical constraints that are imposed on human studies make necessary the use of appropriate animal models [Stanojlović O et al., 2004]. Ideally, the goal of these models is to replicate the natural history of symptomatic focal as well as generalized epilepsy as close as possible. This pursuit involves replication of an initial epileptogenic insult, followed by an apparent latent period and subsequently a period of spontaneous chronic seizures [Kandratavicius L et al., 2014].

There have been multiple experimental animal models developed for contemporary epilepsy research. They are categorized by the timing of associated symptoms in to models of chronic epilepsy and models of acute seizures and by method of induction in to chemo convulsant, electrically or sound and traumatic brain injury induced models [Lévesque, M et al., 2016]. There are also models created for more specialized uses such as genetic models useful in examining absence seizures, models of status epilepticus as well as seizures and in the immature brain [Lothman EW et al., 1993].

The first created and still most commonly used animal epilepsy models are the chemoconvulsant models. One of the first chemoconvulsant substances used to model epilepsy in rodents was Kainic acid [Sharma AK et al., 2007]. Kainic acid is an L-glutamate analog with forceful depolarization effects. When kainic acid is systemically administrated it leads to neuronal toxicity and seizures, especially targeting the hippocampus [Nadler JV et al., 1978]. After the kainic acid model success many other chemoconvulsant models were developed. Pilocarpine is an antagonist of muscarinic acetylcholine receptors. Systemic administration of pilocarpine causes hypersynchronized activity of neurons in the limbic system [Furtado MA et al., 2002; Turski WA et al., 1983]. There are multiple other compounds widely used in acute seizure models. They include strychnine, pentylenetetrazol (PTZ), tetanus toxin, and others. The key distinction between chronic vs acute seizure models is that latter are useful for studying seizure activity and antiepileptic drug effects but do not necessarily result in chronic epilepsy [Barkmeier DT et al., 2003].

Another compound used to model seizures is lindane, an organochloride pesticide. Lindane provokes neuronal hyperexcitability and consequently convulsions in most part by inhibiting gamma-aminobutyric acid A ($GABA_A$) receptors. It is postulated that lindane interacts with the picrotoxin site within the $GABA_A$ receptor chloride channel which suppresses chloride influx (Sunol et al., 1998; Anand et al., 1998). When administered intraperitoneally, lindane evokes grand mal seizures in a dose-dependent manner. There are numerous studies that describe the characteristics of lindane induced seizures and the model is well established within the literature [Vucevic D et al., 2008; Hrncic D et al., 2011].

1.2 Acute myocardial infarction

Patophysiological, epidemiological and diagnostic aspects of myocardial infarction

Acute chest pain is one of the most common complaints in emergency departments. US statistics estimate this burden accounts for an estimated five million visits. The highest morbidity and mortality of acute chest pain etiologies belongs to myocardial infarction (MI). Over 800,000 people yearly experience an acute MI (AMI), and mortality rates are estimated to be at around 27%. It is relevant to point out that most of the mortality is accounted for by deaths before hospital arrival due to arrhythmic events [Boateng S et al., 2013.] Although these statistics appear dismal, they are in fact the result of multiple decades worth of improvement in mortality.

Since 1970s significant strides have been achieved in reducing MI deaths due to advances in diagnosis and management. During this time, the clinical definition of MI was changed multiple times in keeping with an increase in precision of diagnostic tests and development of more efficient clinical protocols. The current, fourth universal definition of MI consists of two main propositions. To arrive at a diagnosis there must firstly be a change (rise or fall) in the blood level of specific cardiac markers indicative of muscle damage (troponin I or T) with at least one value above the 99th percentile of the upper reference limit [Chapman AR et al., 2017]. Secondly this must be correlated with clinical parameters indicative of AMI. These clinical parameters include angina and angina equivalents, electrocardiographic evidence such as ST segment changes or new left bundle branch block or development of pathological Q waves and echocardiographic evidence such as new wall motion abnormalities or a combination of these [Thygesen K et al., 2018]. On the other hand, the pathophysiological definition of MI remains largely unchanged. The simplest and most encompassing definition of MI is as myocardial cell death caused by prolonged ischemia [Saleh M et al., 2018].

The classification of MI has also changed significantly over the past decades. From the division to transmural MI versus non-transmural MI through Q wave and non-Q wave to the contemporary ST elevation and non-ST elevation MI. Transmural MI is defined as myocardial necrosis caused by an ischemic event affecting the entire thickness of the myocardial muscle. The ischemic event is most commonly caused by complete occlusion of a major coronary artery by a blood clot (thrombus) creating a decrease or completely cutting of blood supply to the full thickness of the heart muscle. Non-transmural MI is defined as ischemic myocardial injury that does not affect the full thickness of the heart muscle, commonly not involving the epicardium. Both Q wave and non-Q wave MI are confirmed by histopathological findings of ischemic injury. The findings consist of necrotic myocardium (pyknotic nuclei, hyper-eosinophilia and inflammatory cell infiltration) and a penumbra area of inflammation [Michaud K et al., 2020]. The change of classification to Q wave and non-Q wave MI instead of transmural and non-transmural did not hold up to scrutiny and has been since abandoned [Gorlin R et al., 1986]. As opposed to the previous classification reflecting pathoanatomic changes (transmural/non-transmural MI) and chronic ECG changes (Q wave/non-Q wave MI) the modern classification relies on acute ECG changes reflecting the need for fast therapeutic decisions reflecting the primary PCI era [Zimetbaum PJ et al., 2003].

Although morbidity and mortality of MI has been successfully lowered by advances in treatment and management, MI still presents a large burden to patients and health systems worldwide. It has been shown that environmental and genetic risk factors have a significant modifying effect on the clinical course of MI. Furthermore, psychosocial stressors have been related to higher risk of heart diseases such as acute myocardial infarction (AMI) in large case

control studies [Rosengren A et al., 2004]. The connection between mood disorders, primarily depression with AMI has also been well documented [Pozuelo L et al., 2009; Frasure-Smith N et al., 2010; Pratt LA et al., 1996] and even cognitive decline can be attributed to cardiovascular events since it is significantly faster in elderly patients with heart failure while EEG studies have shown changes similar to those in Alzheimer's disease [van der Wall EE et al., 2011].

Experimental models of myocardial infarction

As is the case in epilepsy and other human diseases, animal models of myocardial infarction have an indispensable role in exploring new avenues of MI prevention, diagnosis, and therapy [Goldman S et al., 1995]. Animal models are unavoidable in the preclinical phase of drug development as no other type of study can provide such depth and breadth to understanding disease pathophysiology and complement or amend existing approaches to diagnosis and treatment of disease [Zaragoza C et al., 2011]. Although most laboratory animals used in research have physiology similar to that of a human and thus an intense translational capability from "bench to bed", due to its convenience and standardization, the most commonly used model for acute MI is the rodent model. For more than a century, the rat has been the animal model of choice for most experimental MI research with the mouse coming in as close second, although this trend has recently begun to reverse [Aitman TJ et al., 2008].

The most commonly used rat model of MI is the surgical ligation model. This is a highly invasive model that requires total anesthesia, ideally with the use of a respirator. After a sternotomy and pericardiectomy to liberate the heart, the anterior descending coronary artery is isolated and ligated which produces ischemia in its myocardial vascular bed. The high cost and need for specific instruments, such as a respirator, have restricted the use of this model to highly specialized laboratories while improper use or suboptimal placement of the respirator along with prolonged opening of the chest greatly contribute to complications including the death of the animal [Zhang R et al., 2004].

Isoproterenol (ISO) or isoprenaline induced acute MI model is a reliable and highly developed non-surgical animal model in rats [Kannan MM et al., 2013; Brooks WW et al., 2009]. The pathophysiological mechanisms of ISO induced MI are numerous and consist of increased and prolonged myocyte contraction stimulus coupled with auto oxidation of ISO into reactive oxygen species altering membrane permeability, and decreasing the endogenous antioxidant enzyme levels [Zaafan MA et al., 2013; Haleagrahara N et al., 2011]. Relative ischemia with resulting oxidative stress leading to intracellular calcium overload, metabolic changes and alteration in concentration of electrolytes are considered as plausible mechanism of ISO induced MI [Upaganlawar A et al., 2011].

ISO induced model of MI has several advantages over the coronary artery ligation model such as low mortality rate, non-surgical technique, thus no postsurgical infections as well as simplicity and cost-effectiveness. Furthermore, in our study it was essential to avoid all confounding factors inherent in major surgery such as anesthesia and trauma in order to get HRV and EEG signals representative of MI. Therefore, we used in our study ISO-induced MI as an experimental model of AMI.

1.3 The heart brain axis: a focal point of autonomic regulation

The heart brain axis is a term used to define the interrelations of higher brain centers as well as lower order centers with autonomic and intrinsic neural networks organizing heart function. The cardiac autonomic nervous system (CANS) is an important part of the heart brain axis and consists of neural networks at multiple functional levels [Fedele and Brand, 2020]. As is the case with autonomic regulation of other organs, autonomic heart regulation comprises of central nervous system and peripheral, ganglionic gray matter centers. This system enables the exertion of autonomic, sympathetic and parasympathetic nervous influences that are core to heart regulation [Levy and Schwartz, 1994; Shivkumar et al., 2016]. Due to its inherent complexity, the CANS is hierarchically organized and it can be subdivided into three levels (Fig 1.1).

Level 1 refers to brainstem and spinal cord neurons that are controlled by higher CNS centers such as medial prefrontal cortex, insular cortex etc [Jaenig W, 2016]. Level 2 consists of intrathoracic extracardiac ganglia and level 3 is located in the epicardium proper, forming the intrinsic cardiac nervous system (ICNS). The ICNS is located in the epicardial layer and is comprised of cardiac ganglia [Paintal, 1963; Schwartz et al., 1973]. ICNS, which is also referred to as as the "little brain" of the heart [Armour JA 2008] processes afferent information and provides efferent input to the myocardium. The ICNS is also under constant tonic modulation of higher order CANS centers (in level 1 and 2). Besides its role as the "final common pathway" for the CANS its role is also in tightly modulating regional cardiac function, even when disconnected from the higher levels [Ardell JL et al., 2016].

Sympathetic and parasympathetic branches of the ANS are key regulatory pillars for the CANS. Both sympathetic and parasympathetic systems have the characteristic structure consisting of two neuron orders. The sympathetic branch has its first order neuron in the spinal cord (intermediolateral column), from where it projects to second order sympathetic neurons residing in intrathoracic ganglia (cervical and stellate ganglia) [Ardell JL et al., 2016]. A small number of first order sympathetic neurons also form synapses with sympathetic post-ganglionic neurons in the ICNS [Ardell JL et al., 2016]. Parasympathetic first order neurons reside mainly in the nucleus ambiguous of the brainstem and project to neurons located in the ICNS ganglia [Armour JA, 2008].

The CANS operate by integrating various cardiothoracic reflexes. Reflex transduction can be initiated in local afferent neurons of thoracic and or cardiac ganglia as well as neurons in the dorsal root, spinal cord, and nodose ganglia. Even cortical centers can play a role in initiating reflex arcs [Ardell JL et al., 2016]. The main sensory modalities of afferent stimulus are mechanical (mechanosensory) and chemical (chemosensory) stimuli, with the majority of intrinsic cardiac afferent neurons being polymodal. [Armour JA et al., 2004].

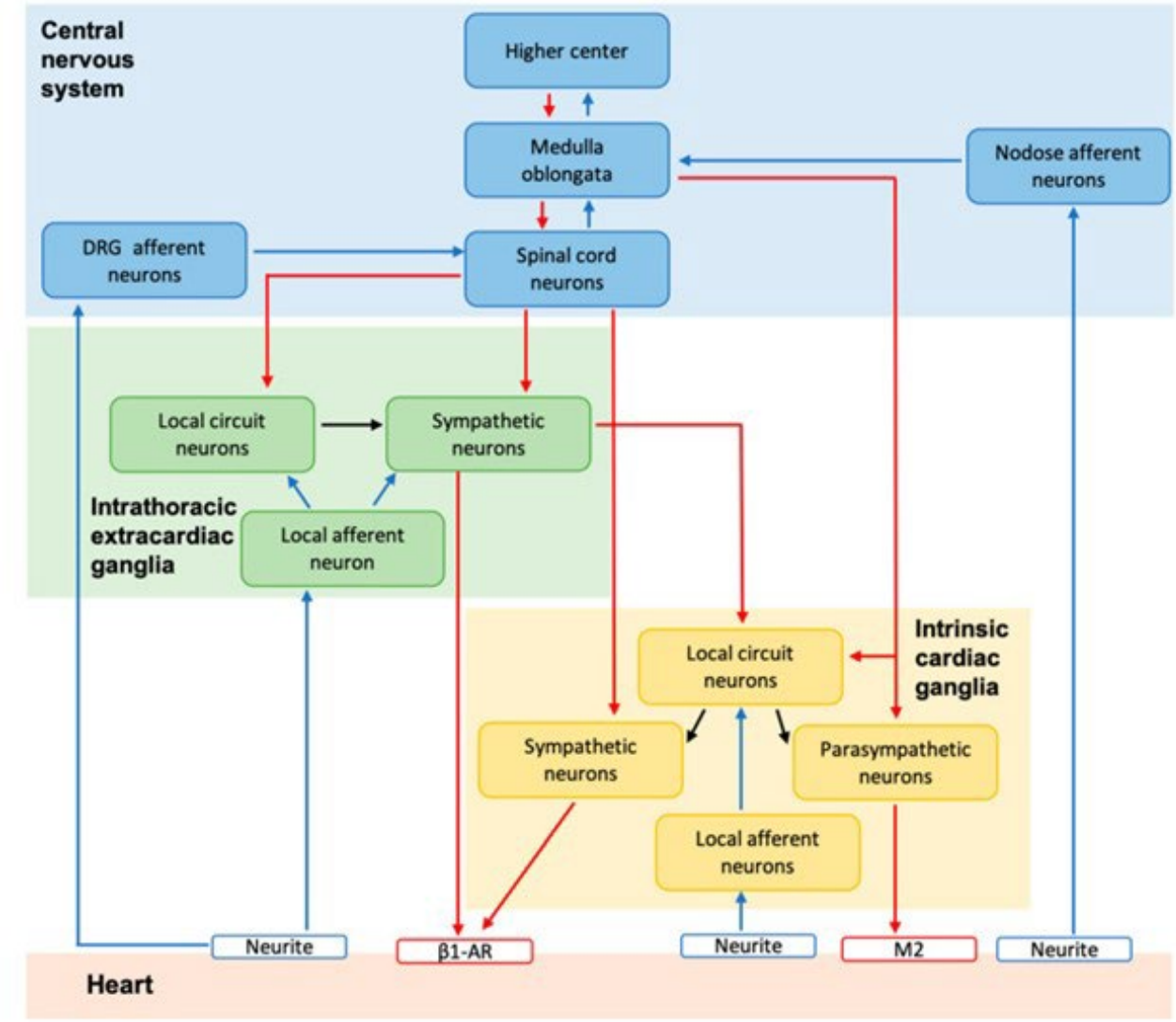

Fig. 1.1 Schematic illustration of CANS components and their functional connections

Adapted from Fedele L and Brand T. (2020)

Although not considered part of the CANS in the narrow sense, several cortical regions play a key regulatory role in the system. The insular cortex (IC) [Verberne AJ et al., 1998; Tokgozoglu SL et al., 1999; Oppenheimer SM et al., 1990] and the medial prefronal cortex (PFC) [Cerqueira JJ et al., 2008; Tavares RF et al., 2009; Hilz MJ et al., 2006] are seen as the most prominent. Insular cortex has one of the simplest neural structures of all cortical centers pointing to an older origin and more archaic roles such as limbic and autonomic regulation. The mPFCs role in CANS regulation is more surprising. The traditional role of medial PFC is primarily in higher brain functions: decision making, executive control, social interaction etc. However, its effects on heart regulation have recently become more recognized [Resstel LBM et al., 2006].

As a whole, the CANS plays a fundamental role in modulating heart wall contractility/relaxation dynamic, heart impulse conduction speed, heart rate, and even myocyte cohesion. Therefore. an intact and harmonious functioning of the CANS at all levels of integration is key for both the electrophysiology and hemodynamic regulation of the heart [Zipes DP et al., 2018].

1.4 Neurophysiological basis of ECG and EEG

Cardiac conduction system and origin of ECG

The cardiac conduction system is key in initiation and coordination of cardiac electrophysiology. It is composed of the sinoatrial (SA) node, internodal pathways, the atrioventricular (AV) node and the His–Purkinje system [Zipes DP et al., 2018; Bennet DH et al., 2013]. The SA node is the primary pacemaker of the conduction system. It resides in the inflow tract of the right atrium, from where it initiates the cardiac action potential. After being generated in the SA node, the electrical impulse travels to the AV node through the internodal pathways. Under physiological conditions, the only direction for impulse conduction is from the atria to the ventricles via the AV node-His bundle pathway. The AV node's role is in slowing conduction of the action potential from the atria to the ventricles by approximately 0.13 s creating time between atrial and ventricular contraction. The AV node can also take over the role of pacemaker in case of SA node failure. The His-Purkinje system begins in the AV node as a common bundle that after passing through the interventricular septum branches into the left and right hemi bundles. In the myocardium proper the hemi bundles further branch out to networks of Purkinje fibers. The low conduction velocity of the ventricular Purkinje system (approximately 0.06 to 0.1 s for full ventricular depolarization) allows for a coordinated action potential propagation and consequent ventricular contraction. [Huang CL et al., 2017; Pappano AJ et al., 2019].

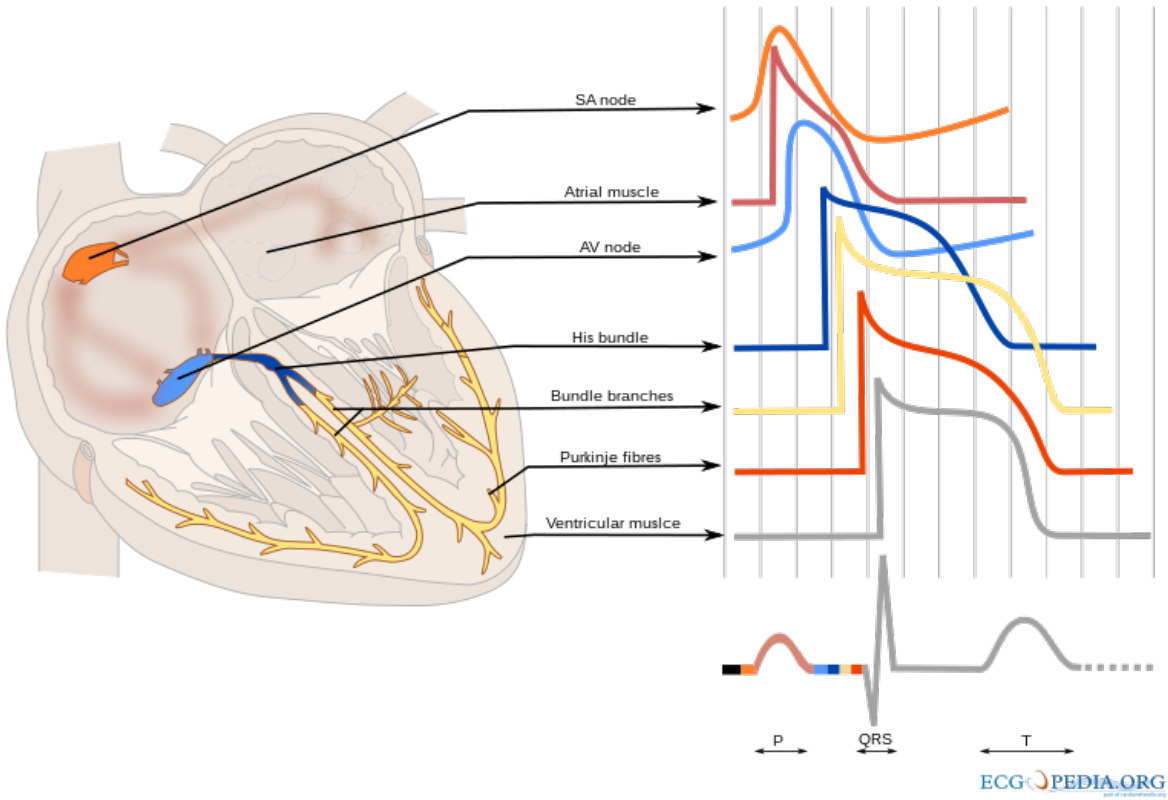

Fig. 1.2 Schematic illustration of cardiac conduction system components and action potentials elicited at different levels of the system

Adapted from https://www.textbookofcardiology.org/wiki/File:Conductionsystem.svg

The cornerstone of the conduction system and cardiac physiology as a whole is the ventricular myocyte. The ventricular myocyte has a triple mandate. It can initiate action potentials, (most importantly in the SA and AV node), conduct action potentials (in the conduction His-Purkinje system) and finally provide cardiac contraction. In order to achieve the necessary goals, cardiomyocytes at various levels of organization are structurally and functionally specialized. There are two types of cardiac action potential [Pappano AJ et al., 2019]. The action potential formed in the SA and AV nodes has a slow upstroke and is brief in length while the action potential formed in the myocardium proper and Purkinje fibers has a quick onset and longer duration with a pronounced plateau (also called plateau AP). The slow and short nature of SA and AV node AP serves to ensure pacemaker dominance, preserving optimal impulse propagation while the fast and long AP of the conduction system and ventricular myocardium is geared towards fast conduction and optimal ventricular contraction [Hall JE, 2020].

The most important diagnostic tool for quick clinical assessment of cardiac conduction system function is the ECG. It was introduced as the string galvanometer in 1924. by Willem Einthoven and later evolved in to the 12-lead electrocardiogram [Einthoven W et al., 1902, Kligfield P, 2002]. The ECG is recorded using electrodes placed on the skin and an ECG recording is a time series of average myocyte electrical activity underneath an ECG electrode. It is important to understand that the ECG does not measure contraction of the cardiac muscle, rather it reflects changes in myocyte membrane ion channel activity giving rise to voltage changes. The membrane voltage changes can also be extrinsic, caused by the cardiac conduction system as well as intrinsic: caused by intracellular signaling stemming from myocyte biochemical and metabolic processes [Farraj AK et al., 2011].

The ECG consists of deflections (waves) and intervals. There are three distinct waves: the P wave, the QRS complex, and the T wave representing atrial depolarization, ventricular depolarization, and ventricular repolarization, respectively. There are also two intervals: the PR interval represents the time required for the impulse to travel from the SA node to the ventricles and the QT interval is representative of the time required for ventricular depolarization and repolarization. The ST segment is a specific structure with important diagnostic purposes. It spans from the end of the QRS complex to the beginning of the T wave and represents the period of the plateau phase in ventricular myocytes [Bennet DH, 2013; Hall JE, 2020]. Since the ECG reflects spatiotemporal alignment of extracellular voltage in the heart we are able to infer multiple variables of heart health and function from the ECG. Firstly, rhythm and conduction disturbances are based on changes in cardiac electrical properties. Furthermore, heart anatomical orientation can be assessed from analysis of the cardiac conduction vector. The presence of acute or chronic coronary insufficiency is reflected in the ECG and so is cardiac injury, alteration in electrolyte concentrations, nutritional deficiencies as well as effects of some drugs and diseases. [Tse G, 2016; Detweiler DK, 1997].

Neuronal electrophysiology and origin of EEG

The human brain consists of more than 100 billion neurons, which are all part of an interconnected network. The varying roles neurons play within the nervous system dictate the difference in size and shape as well as position within the network. No matter the role, major components of a standard neuron are always the same: the dendrites receive information; the cell body (soma) integrates the information and tends to the metabolic needs of the cell and the axon conducts signals to other regions of the brain or periphery [London M et al., 2005; Li L et al., 2015]. Functionally, the structure of a neuron is represented by two domains. The first domain is the somatodendritic domain: soma, multiple dendrites and a short region of the proximal axonal segment (axon hillock). The second is the axonal domain: a long projection away from the axon hillock and toward the next neuron or a target tissue [Luo J et al., 2016; Kirkcaldie MT et al., 2016].

Neuronal structure dictates the information flow within the nervous system. Information flows from the somatodendritic domain, where synaptic input from neighboring or distant neurons is received and integrated to be subsequently transmitted to the axonal domain [Jones SL et al., 2016]. Neurons are locally organized into circuits, smaller networks, tasked with processing specific information. Neurons that carry information into the circuit are dubbed afferent neurons, whereas neurons signaling information away from the circuit are referred to as efferent neurons. Nerve cells that integrate the function of local network communication of a circuit are called interneurons. Processing circuits are combined to form systems that serve a broader function, such as association, memory, vision, etc. [Shipp S, 2007; Briggs F, 2010].

Communication between neurons is established through synapses. Synapses can connect at the cell body, dendrites or the axon. There are two fundamental types of synapses: electrical or chemical. Electrical synapses are mainly found in the heart and smooth muscle but there are also instances of electrical synapses in the CNS while chemical synapses dominate CNS and PNS circuits. Electrical synapses are continuous, i.e. there is a cytoplasmic continuity between the communicating neurons (also called gap junction). Chemical synapses, on the other hand, function via the excretion of chemical substances (neurotransmitters) from the presynaptic neuron in to the intercellular space. The vesicles containing a chemical neurotransmitter are activated through an electrical potential arriving at the axonal terminal and induced to release the neurotransmitter. The neurotransmitter spreads in the intercellular space (synaptic cleft) binding to the receptors at the postsynaptic membrane and initiating the opening (or closing) of ionic channels in which modifies the membrane potential [Roux Bet al 2017]. Flow of electrical current across the cell membrane is accomplished by both cations (mainly Na+ and K+) and anions (Cl-) [Kandel ER et al., 2018; Holm TH et al., 2016].

The change of ionic conduction and thus neuronal membrane permeability modifies the probability of triggering an action potential in the postsynaptic cell. Because the initial, base state of the inner cell membrane is negatively charged the movement of cations initiates depolarization (reduction of intracellular negative charge leading to less negative membrane potential) and triggers AP. If the change in membrane polarization is in the positive direction-towards depolarization, the resulting potential is dubbed an excitatory postsynaptic potential (EPSP). On the other hand, if the resulting effect is hyperpolarization, the potential is called an inhibitory postsynaptic potential (IPSP). In other words, EPSPs elevate the membrane potential closer to threshold for action potential generation, while IPSPs lower the membrane potential further from the threshold potential. In chemical synapses, the main determinant of whether synaptic communication results in an EPSP or IPSP is the nature of neurotransmitter released

as well as the type of postsynaptic receptor present. In the cerebral cortex, the dominant neurotransmitter is glutamate the synthesis and signaling, of which constitutes 90% of neurotransmitter activity making it the principal excitatory neurotransmitter. The principal inhibitory neurotransmitter of the cortex is gamma amino butyric acid (GABA). [Holmes et al 2007]

Neurons transmit signals by generating action potentials (AP). When enough EPSPs reach the neuronal soma to trigger depolarization action potentials are triggered. On the other hand IPSP return membrane polarization in to its negative, steady state slowing or ending AP [Lacroix JJ et al., 2013].

Electroencephalography (EEG) is a method of recording bioelectric activity of the brain using scalp or implanted electrodes [Olejniczak P, 2006]. Electrical activity of large neuronal networks is detected via extracellular recordings; in this case, called field potentials. The EEG recording is a result of field potentials generated by the spatial summation of dendritic postsynaptic potentials (EPSPs and IPSPs) while APs are not detected due to much lower impact on electrical field changes. It is a dynamic, temporal representation, as the potential difference is plotted as a function of time. The actual postsynaptic potentials detected are currents flowing in the cortical structures during synaptic activation of dendrites of a neuronal network. Although action potentials having individually larger electrical potential may appear to be the obvious source of electrical flows recorded, they only contribute minimally to the genesis of EEG graphoelements. [Henderson CJ et al., 1975].

EEG activity can be classified in to four distinct rhythms: Alpha (8-13 Hz) Beta (14-30 Hz), Theta (4-7 Hz), and Delta (1-3 Hz). In general, the amplitude of EEG signal increases as the frequency decreases. Each of the four EEG frequencies is associated with a different level of arousal of the cerebral cortex. Alpha rhythm refers to the mature normal EEG frequency that falls in the alpha range of 8 to 13 cycles per second (Hz) and an amplitude of 15 to 45 microvolts [Niedermeyer E et al., 1997, Kozelka JW et al., 1990]. It dominates during relaxed wakefulness. It is enhanced by eye closure and physical relaxation or mental inactivity, and blocked by or attenuated by visual and mental effort. Beta rhythm is present in the awake mentally active state in adults and children. Its frequency ranges between 13-30 Hz is most prominent in the frontal cortex and is usually symmetric, having low amplitude (10-20 microvolts). Theta waves can be seen in the adult waking EEG and are symmetrically distributed. They predominance of theta frequency is considered normal for children as well as adolescents and they are also more prominently present during sleep [Nayak CS et al., 2020]. Delta waves, also often referred to as slow wave activity are most prominent during NREM sleep but they have also been correlated to cognitive and other integrative functions [Harmony T, 2013].

1.5 Acquisition and advanced analysis of biological signals

Significance of EEG in clinical practice and experimental research

Physiological brain function can be described as the end result of organized, continuous communication between neurons. The primary mode of intraneuronal communication is provided by synapses, junctions that convey signals from one neuron to another. Synaptic transmission is afforded by two structurally different arrangements: chemical or electrical synapses [Pereda AE 2014]. Capturing the electrical field oscillations produced during interneuronal communication is the goal of electrophysiology. In this way electrophysiology is one of the rare methods that can bring us closer to understanding processes that control overall body functions and behavior [Chorev E 2009]. Among multitude electrophysiological techniques, EEG is the one most commonly utilized in clinical practice.

In modern neurology, the EEG has become an essential test for clinical diagnosis and outcome prediction of various neurological conditions. At first used for confirming and classifying the diagnosis of epilepsy, it has gained importance in various other cases such as sleep disorders, encephalitis, Parkinson's and Alzheimer's disease, and even effects of pharmacological and toxicological agents [Freeborn DL 2015]. When it comes to scientific study, EEG is an essential tool used in various basic science and preclinical fields of study. The most common animal model, due to its low price and high availability combined with high capacity for generalization and advancement is the rodent model. Rodent models are now used as a proxy for many diseases associated with electroencephalographic changes and seizures such as epilepsy, stroke and traumatic brain injury [Leiser SC 2011; Yoo, Hyun-Joon et al., 2021].

The EEG is also important in analysis of physiological processes affected by different environmental and disease modifiers such as the sleep-wake cycle as well as dementia, autism, genetic syndromes associated with cognitive impairment etc. [Kent BA et al., 2018, 2021; Levenga J et al., 2018; Mouchati PR et al. 2019]. As opposed to human EEG recording which is largely noninvasive, EEG registration in rodents is an invasive procedure using highly precise surgical (stereotactic) methods to implant electrodes into brain areas of interest [Bertram EH et al., 1997]. The electrodes are then connected to an amplifier and computer system for recording, storing and further analysis by custom made or commercial software. The most common method of connecting electrodes to the amplifying/registering apparatus is via copper wires but we have recently seen a push towards wireless recording brought about by advances in miniaturization and the need for more stable signals with less motion artifact and related connection problems [Williams P et al., 2006]. Rodents being highly mobile animals, it is clear that motion artifacts are a significant challenge in EEG recording. This especially becomes significant for epilepsy research where the violent motion during generalized “grand mal” attacks can lead to complete loss of signal in less than air tight wired recordings [Medlej Y 2019]. When recording is adequately done, we arrive at the arguably most significant hurdle: analysis and interpretation of the EEG signal. This has been the driving force behind a lot of modern research that in concert with a significant increase in computing power and availability brought about novel analysis methods. Today, both complex novel and traditional as well as linear and nonlinear methods present a cornerstone of research [Jansen BH 1996; Khodabakhshi MB et al., 2020; Ma Yan et al., 2018].

Significance of ECG in clinical practice and experimental research

The electrocardiogram (ECG) can be defined as a time series representing the sum of action potentials on the membranes of myocardial fibers during the cardiac cycle [Narayanaswamy S 2002]. From its humble beginnings in 1924 when Willem Einthoven introduced the string galvanometer [Einthoven W et al 1902, Kligfield P. 2002] and until modern times the 12-lead electrocardiogram (ECG) has reached the status of the most frequently performed cardiovascular test. Not only it is an essential diagnostic tool in clinical cardiology, it is also critical for evidence-based management of patients with differing cardiovascular conditions.

ECG is used in virtually every instance of cardiological pathology, from acute myocardial infarction, chronic cardiac ischemia and heart failure to cardiac arrhythmias and implantable cardiac devices. As opposed to most other modern medical diagnostic techniques the ECG has multiple obvious strengths. Namely, ECG is cheap, compact, simple, and above all and increasingly so: universally available and mobile [Reichlin, T et al 2016]. The progress in computer science in both hardware and software, driving biomedical computing and signal processing advances, open new options for ECG analysis, including improved filtering, morphology feature analysis and a multitude of HRV methods [Surawicz B et al., 1997; Sharir T et al., 2012; Lee WK et al., 2016].

Besides its obvious significance in clinical work, the ECG is also invaluable in experimental studies on animal models of cardiovascular and other relevant pathology [Kumar P et al 2017]. There are various techniques for ECG registering available in laboratory practice with similarities to EEG and other biosignal recording methods. Firstly, ECG registering requires the use of electrodes weather invasively implanted or noninvasively applied, similarly to EEG recording. Secondly, it also must rely on a certain conduit to deliver the registered signal from the electrode to an amplifier/recorder device, and finally be analyzed through the use of custom built or commercial software [McCauley MD et al., 2010].

Available methods of ECG recording in small animals have several limitations that influence their usefulness in laboratory practice. These limitations arise mostly from problems with tightness of electrode adhesion and signal quality. To achieve high signal quality, most classical methods require anesthesia and/or use surgical procedures, what is essentially invasive electrode implantation and ECG registration. Methods that do not lean into surgical electrode placement compensate for the weaker bond by incapacitation of the laboratory animal. Both the use of anesthesia and surgical procedures may affect various ECG parameters such as morphology, heart rate and rhythm. [Deutschman CS et al., 1994; Kato M et al., 1992; Latson TW et al., 1992] Additionally, ECG recording with use of anesthetics is lacking validity for HR variability analysis [Fateev MM et al., 2012; Castiglioni P 2013].

In effort to create a technique for registering a stable, high quality ECG signal with ought the use of anesthesia various authors have developed specially designed boxes, stages, and jackets fitted with electrodes. [Pereira-Junior PP et al 2010, Kumar P QT al 2007] Additionally, the ideal technique, especially when it comes to registration of nuanced parameters reflecting neurocardiac control such as HRV is one that does not hinder the movement of rats.

When addressing the connection problem, it is clear that telemetry has many advantages over copper wire transmition and it is sometimes hailed as the gold standard for ECG recording in rats [Sgoifo A et al 1996], Besides being cost prohibitive, the most important downside to wireless connection when it comes to biosignal recording is in the lower sample rate which is especially important for HRV [Guild SJ et al., 2006]. For our study, it was important to use non-invasive electrode implantation without the use of anesthesia with overall high sampling rate, i.e. wired ECG recording in freely moving rats.

Advanced EEG signal analysis

Using complex algorithms and machine assisted analysis of the EEG signal in order to characterize and predict epileptic seizures has been theorized since 1970s, but the technology necessary for rigorous study of this possibility has only recently been developed [Viglione SS et al., 1975; Litt B et al., 2002]. Many EEG analysis methods rely on the fact that information processing in the brain is reflected in the EEG signal as a dynamic change of electrical activity in time, frequency, and space. Various linear and nonlinear methods have been used over time in an attempt further understanding of the mechanisms behind this information processing [Rosso OA et al., 2002; Osorio I et al., 2009]. The analysis of physiological signals and especially the EEG signal is challenging because of complexity inherent to the (neural) supstrate of the signal and biochemical processes involved in its generation [Acharya UR et al., 20012].

Techniques used in characterization and analysis of EEG can be divided into two categories: i) linear methods that are further subdivided in to a) time domain based, b) frequency domain based, c) time-frequency domain based, and ii) nonlinear methods.

Among the linear methods, the oldest and most commonly used method is Fourier transformation [Gotman J et al., 1997]. This frequency analysis method allows us to ascertain the frequency content of the EEG signal, and is also the basis for more advanced methods such as time-frequency analysis. Isolated, time or frequency domain based methods are good for whole signal analysis especially when it comes to stationary signals, (signals with little to no dynamic change in time). Since most biological signals including the EEG are non-stationary, there is necessarily a loss in information when standard frequency or time domain methods are used. In other words, the EEG signal analysis requires methods with both a temporal as well as frequency dimension. Examples that fulfill this requirement are time-frequency domain methods like the short time Fourier transform (STFT) and wavelet transform (WT) [Adeli H et al 2003; Khan YU et al 2003].

Methods of nonlinear dynamics are another set of tools that are increasingly used in EEG processing. When used with EEG, these measures help understand EEG dynamics in a different way than it is possible using other, more traditional methods. These methods have been proving themselves on various battlegrounds of neuroscience: one of the first instances was in Babloyantz et al., where it was shown that certain non-linear methods can be used to study slow wave sleep [Babloyantz A et al., 1985]. Since then applications of nonlinear methods in EEG have significantly increased in diverse research areas with new possible clinical applications being studied, such as in the prediction of epileptic seizures [Lehnertz K et al., 1988; Martinerie J et al., 1998], analysis of post anoxic encephalopathies [Stam CJ et al., 1999], characterization of sleep phenomena [Abou Jaoude M et al., 2020], and even surgical applications such as monitoring the depth of anesthesia [Gu Y et al., 2019; Hashimoto DA et al., 2020].

There are numerous nonlinear techniques each with a different take on EEG signal analysis. One frequently used approach is to quantify the degree of complexity in a time series using tools like fractal dimension (FD), correlation dimension, Hurst exponent, largest Lyapunov exponent, or entropy measures [Kannathal N et al., 2005]. Fractal dimension estimation is based on the concept of fractal geometry, that differs from Euclidian geometry in that the dimensions of fractal objects are non-integer forms. [Falconer KJ et al., 2003] As such they are not fully described by their topological dimension as two fractal objects of the identical topological dimension may "fill up" different amounts of space. This property is described by the fractal, non-integer, dimension that assumes the value between two adjacent topological dimensions. In essence, fractal objects have different characteristics based on the amount of space they fill, meaning two fractal objects of different densities have different fractal dimensions. FD represents a powerful method used in various neuroscientific studies [Smits FM et al., 2016; Gladun KV et al., 2020; Zappasodi F et al., 2014]. Also, the computational complexity of fractal dimension is comparatively lower when compared to other non-linear methods most of whom take up a lot of processing power. There are many algorithms used to determine the FD of a waveform, but two commonly used are the Higuchi method and the Katz method, since they produce accurate, consistent, and discriminating results for EEG analysis [Gladun KV et al., 2020; Anderson K et al., 2021].

Fractal dimension and other nonlinear parameters rely on the assumption that biological signals are nonlinear, and like other natural systems exhibit chaotic properties. Although this is basically true, it was shown that biological signals have mathematical characteristics which differentiate them from signals created by random processes (Brownian motion) as well as from those created by periodic and chaotic processes. These differences were characterized and subsequently collectively defined as Bios.

Bios is not exclusive to biological processes and can be found in recursive process equations that have bipolar feedback (mathematical bios) as well as temporal distribution of galaxies and economic fluctuations [Sabelli H at al., 2006; Kauffman L and Sabelli H 2003] Bipolar feedback being the cornerstone of regulation in biological organisms only further underlines the importance of Bios in characterization of biological signals. The defining characteristics of Biotic signals are: novelty, temporal (arrangement) complexity, diversification and isometry (especially low ratio of total vs consecutive isometry) as well as entropy [Sabelli H et al., 2005]. Biotic analysis of biological signals is a novel method that can open new possibilities for research and ultimately novel diagnostic and therapeutic approaches.

Advanced ECG signal analysis

Heart rate variability analysis (HRV) is a method for ECG signal analysis that goes beyond the clinically significant visual morphologic analysis that is used daily in MI, arrhythmia and other heart disease diagnosis. HRV non-invasively assesses the cardiac autonomic nervous system (ANS) by measuring the R-R interval fluctuations in the temporal plane [Shaffer and Ginsberg 2017].

Essentially, HRV is a surrogate marker for the total dynamic influence of sympathetic and parasympathetic branches of the ANS on the intrinsic cardiac nervous system, i.e. the neuro - cardiac axis (Clifford et al., 2006]. Multiple models attempt to explain HRV, but what has been consistently shown, is that low values of HRV indices relate to cardiac events, such as MI and heart failure [Huikuri et al., 1999; Laborde et al., 2017]. Beyond correlation to heart disease,

HRV parameters have been found to correlate to numerous other pathophysiological states such as acute and chronic stress [Murray 2012; Castaldo et al., 2015], depression and bipolar disorders [Bassett, 2015; Koenig et al., 2016], metabolic syndrome [Stuckey et al., 2014] etc. Furthermore, HRV parameters are sensitive to physiologic changes and can be used to increase understanding of various processes such as sports training and performance (Dong JG 2016; Gavrilova EA 2016), nuances of social interaction (Shahrestani S et al., 2015) as well as changes in emotional states (Choi KH et al., 2017).

The most important HRV analysis methods are: i) time domain methods: deviation, difference and geometric based approaches; ii) frequency domain methods: absolute and relative power; iii) time-frequency domain and iv) nonlinear domain methods.

Time-domain measures and frequency domain measures have no temporal resolution, they reflect total HR variability of the signal and are not able to quantify respective contributions of different underlying regulatory mechanisms. Deviation based metrics are standard deviation of NN intervals (SDNN) and its derivatives, standard deviation of average NN (SDANN) and standard deviation of NN interval index (SDNNI). SDNN is the square root of the total R-R (N-N) variance given in milliseconds (ms) over the entire signal. It encompasses both the high frequency and low frequency component of the HR signals, where the high frequency correlates to parasympathetic while the low frequency component is correlated to the mix of parasympathetic and sympathetic inputs [Shaffer F et al., 2017]. SDANN and SDNNI both add a certain temporal resolution to the analysis, SDNNI more so than SDANN, but as derived measures they do not achieve independent significance [Force T 1996].

The difference-based approach is derived from the difference between successive NN intervals. These measures include (but are not limited to): root mean square of successive difference (*RMSSD*), standard deviation of the successive difference (*SDSD*), proportion of successive NN intervals larger than a given threshold (for example 20 ms or 50 ms—*pNN20* and *pNN50*, respectively). Being derived from NN interval differences, these measures are primarily indicative of short-term variations in HR. Out of aforementioned indices that are highly intercorrelated, *RMSSD* stands out as generally preferred by researchers. This is generally due to better statistical properties [Ciccone AB et al., 2017]. As opposed to *SDNN*, *RMSSD* is more significantly influenced by parasympathetic activity. Therefore. RMSSD is often used to estimate vagally mediated fluctuations in HRV [Ciccone AB et al., 2017].

Geometric (i.e., graphical) methods rely on histogram and scatterplot representations of NN. Of note is the HRV triangular index (*HTI*) and triangular interpolation of NN histogram (*TTIN*) as well as other geometrical representations of NN intervals on scatter plots (e.g., Lorenz plots). The advantage of geometric methods is lower sensitivity to measurement errors [Malik M et al., 1993]. On the other hand, the number of NN intervals required for a reliable assessment is significant and requires at least 20 minutes for accurate assessment. This exceeds the time window of 5 minutes that is generally accepted as the norm in HRV recording [Force T 1996].

Frequency-domain analysis methods are successfully used for assessment of ANS contributions to HRV regulation and heart regulation in general. These methods reflect the power distribution across varying frequency bands in the ECG signal. The HRV power spectrum is classically divided into four bands: ultra-low frequency band (*ULF*; ≤0.003 Hz), very low frequency band (*VLF*; 0.0033–0.04 Hz), low frequency band (*LF*; 0.04–0.15 Hz) and high frequency band (*HF*; 0.15–0.4 Hz). The HF band is considered to be more under the influence of parasympathetic (vagal) modulation due to the higher dynamic of vagal as opposed to sympathetic signaling. Although this is still somewhat controversial, *HF* and *LF* are generally considered prominent reflections of parasympathetic and sympathetic activity and the ratio of

LF to HF power (*LF/HF*) is thus accepted as an index of sympathovagal balance [Acharya UR et al., 2006; Seyd PA et al., 2008].

Time-frequency analysis methods include, *STFT*, WT, and quadratic approaches such as the Wigner–Ville distribution (*WVD*). The advantages of time-frequency analysis methods are that they give us time resolution for spectral changes within the signal as opposed to isolated time, and frequency domain methods [Cohen L et al., 1989; Cohen L 1995].

Non-linear methods of HRV analysis have much the same strengths as in EEG analysis as well as much the same arguments for their use. HRV indices based on non-linear methods are necessary to adequately characterize the dynamical properties of ECG signal regulation that linear methods are unable to provide [Force T 1996]. The Poincare plot, is one of the most common nonlinear methods to asses HRV. Essentially, it represents a scatterplot of NN intervals plotted against the corresponding preceding interval, dispersed around the identity line and converging into an ellipsoid configuration [Brennan M et al., 2001]. Indices extracted from the Poincaré plot are SD1, reflecting short term variability (standard deviation of points perpendicular to the identity line), essentially equivalent to *RMSSD* [Ciccone AB et al., 2017] and *SD2* reflecting long-term NN variability (standard deviation of points parallel to the line of identity) equivalent to *SDNN*, representing long-term NN variability. SD1 can be used as surrogate for high frequency vagal activity whereas SD2 is more in line with sympathetic modulation. Putting SD1 and SD2 in opposition creates the *SD1/SD2 index*, inverse to LF/HF ratio and describing sympathovagal balance through relating short to long-term variations in NN interval fluctuation. [Hsu CH et al., 2012]. Another nonlinear method is signal entropy. Entropy can be calculated by numerous algorithms most commonly used of which are approximate entropy (*ApEn*), sample entropy (*SampEn*), and multiscale entropy (*MSE*) [Pincus SM 1991; Richman JS & Moorman JR 2000; Costa M et al., 2002].

Since HRV is also a result of underlying cellular electrical activity regulated through bipolar feedback as is the EEG it is logical to assume that it will exhibit biotic characteristics. Indeed, it was shown that HRV exhibits the defining characteristics of biotic signals and biotic signal analysis methods have also shown promise both in different physiological as well as pathological circumstances. [Sabelli H et al., 2010; Sabelli H et al., 2011]

1.6 Artificial neural networks

Artificial neural networks (ANN) are a classification method that deserves special mention. ANN systems focus on building models of pathologic and normal signal characteristics that are then used to classify a signal based on the models. The neural networks are thus trained on the known data set using a gold standard method as reference. This process serves to build a model based on characteristics extracted from the known, training, data set. Signal characteristics – features used for the model are then selected so that they capture the differences between the pathologic and normal signal (for example the epileptic and normal EEG). The training and model building process is a very important determinant of final classification performance when it comes to ANN models.

Neural network approaches have found many uses in EEG analysis in both physiologic and pathologic states. ANNs have successfully been used in automating determination of alertness level as well as discerning sleep stages [Kiymik MK et al., 2004; Schaltenbrand N et al., 2004]. More recently it has become possible to discern emotions using ANNs as well as determine cerebral workload [Siddiqui F et al., 2023; Phan TD et al., 2021]. When the role of

ANNs in pathologic EEG is concerned, advances have been made in recognizing the EEG signature of depression and bipolar disorder. [Akbari H et al., 2021; Gao Y et al.2020]

A very important field where advancements in using ANNs where made was in the classification and prediction of epileptic seizures [Yogarajan G et al., 2020]. The first paper to be published attempting to use ANNs in seizure detection on the EEG signal was published in 1996 and a recent literature review conducted in the field limited to only recent studies (five years between 2017 and 2022) examined a total of 91 papers [Petrosian AA et al., 1996; Nafea & Ismail, 2022].

ANN have shown promise in ECG signal analysis as well. One of the earliest uses of ANNs in ECG analysis was automation of ECG interpretation [Silipo & Marchesi 1998]. The possibilities of automatic ECG interpretation set to replace human visual pattern recognition have only improved over the years. Multiple algorithms for arrhythmias, AMI, and other pathognomonic ECG waveforms have been reported [Cho Y et al., 2020; Suzuki S et al., 2022; Ansari Y et al., 2023]. Besides the role in cardiologic morbidity ANN ECG interpretation especially in the field of HRV offers many possibilities. In physiological conditions ANN HRV algorithms have been used in detection of emotions, mental stress detection and even cognition [Castaldo R et al., 2019; Arakaki X et al., 2023; Chen YC et al., 2019].

When it comes to disease states, automatic detection and prediction of epileptic seizures based on HRV are also being extensively studied [Foo SY et al., 2002; Zambrana-Vinaroz D et al., 2022]. Both linear and nonlinear HRV features were used in a number of studies to varying effect [Behbahani S 2018; Mason F et al.,2024]. Since no currently available model has, so far been able to solve the problem of reliable and accurate seizure prediction based on the EEG signal and HRV is somewhat easier and more comfortable to record than EEG, HRV prediction of seizures remains an exciting field for research.

1.7 Biological signals as digital biomarkers

With the expansion of smartphone technologies, and more recently the wearable industry the signal registering and analysis technology has become much more mundane and accessible. [Kopetz H 2011: Montag & Diefenbach 2018] The technologies that have made this possible have also expanded the possible uses of signal analysis. Watches and rings that record pulse rates, oxygen saturation, galvanic skin response and increasingly advancing toward full-fledged ECG monitoring are now increasingly becoming available to the public bringing electrophysiology out of the laboratory [[Janković M et al., 2018; Ometov A et al., 2021].

This development has led to expansion in researching new, nontraditional, uses for the growing data stream of recorded signals as part of the “Big Data” revolution. The name that coined for physiological signals in this framework was digital biomarkers. There are multiple definitions of digital biomarkers. From very broad definitions such as that from Piau et al. that describe digital biomarkers as: “objective, quantifiable, physiological, and behavioral data that are collected and measured by means of digital devices, such as embedded environmental sensors, portables, wearables, implantables, or digestibles” [Piau A et al.,2019] to attempts at a more focused approach such as discussed in Montag, C et al. 2021.

Classical biological signals such as the EEG and ECG are at the forefront of research into digital biomarkers. Both EEG and ECG have their traditional roles in diagnosis and treatment of various disease states but we are now witnessing an expansion of their use into new venues.

The allure is especially in the possibility of continuous (especially ECG) registration and automatic signal analysis. The most extensive research in the field of automatic detection, for example, is being done on algorithms for automatic atrial fibrillation detection [Wesselius et al., 2021]. The ECG has also been studied as a biomarker for chronological age. It was found HRV has capabilities for independent prediction of all cause as well as cardiac mortality risk [Hirota N et al., 2021]. EEG, on the other side, is being investigated in early detection and classification of dementia [Al-Qazzaz et al., 2014] as well as Alzheimer's disease and even mild cognitive impairment [Poil SS et al., 2013; Schumacher J et al., 2020].

In order to extract all the information, the digital biomarkers can provide, it is of utmost importance to study the utility as well as robustness of each signal analysis technique. Also, expanding knowledge in to the interrelation of physiological systems such as is facilitated by the heart brain axis is essential to using biological signals in clinical practice. We believe our study addresses both problems and that it will serve to further advance the possibilities of EEG and/or ECG features as potential digital biomarkers.

2. STUDY GOALS

The goals of this research were to:

1. Determine the spectral, fractal and biotic characteristics of the medial PFC EEG signal as well as ECG signal characteristics in the period before and after Isoprenaline administration in the Isoprenaline induced AMI model in rats
2. Determine the spectral, fractal and biotic characteristics of the preictal, ictal and postictal EEG and ECG signal in the rat model of Lindane induced seizures.

3. MATERIALS AND METHODS

3.1 Experimental animals

All experiments were performed on adult male Wistar albino rats (200-230 g body weight, 2 months old). Experimental animals were obtained from the breeding laboratory of Military Medical Academy, Belgrade, Serbia. They were housed in transparent plastic cages with *ad labium* access to food and water. Controlled ambient conditions were used in animal housing and experimental facilities (22-23^{o}C, 50-60% relative humidity, 12/12 h light/dark cycle - light on at 8 a.m.). A sound-attenuated chamber was used and animals were habituated to handling. An acclimatization period of 7 days was used.

All experimental procedures were fully in compliance with the European Council Directive (2010/63/EU) and were approved by the Ethical Committee for Animal Welfare of Belgrade University Faculty of Medicine. Experimental procedures were also approved by the national ethical body for animal welfare (Permissions No 4455/2 and No 323-07-08097/1/2018-05).

3.2 EEG and ECG registration set-up and analysis

Electrode implantation

For EEG recordings, all animals were implanted with EEG registering electrode. Namely, a stereotaxic apparatus was used for electrode implantation with pentobarbital sodium (50 mg/kg, i.p.) used as anesthetic. One gold-plated recording electrode was implanted over the frontal cortex (coordianates according to Paxinos and Watson atlas: AP 3.5–3.8 mm, ML 0.5 mm, DV 3.5 mm). Dental acrylic cement was used to fix this system to the skull. Animals had a post implantation recovery period of one week prior to further experiments. A 24-h habituation to recording conditions was applied.

Dorsal thoracic region of each animal was carefully shaved one day before ECG recording. We developed a custom-made elastic cotton jacket to fit the rat's mean thoracic circumference. Using adhesive gel, the electrodes were attached on the skin of the rat for ECG recording, and each electrode was connected via cable to the acquisition system. The rat was then placed in the jacket fixing the electrodes in place. A 24-h habituation to recording conditions was also applied.

Data acquisition

An EEG apparatus (RIZ, Zagreb, Croatia) was used for simultaneous EEG and ECG data acquisition. The analog filters were set to 0.3 Hz and 100 Hz cutoff frequencies for the high-pass and low-pass filters, respectively and a notch filter was used at 50 Hz, for removing the ambient noise. A 16-bit NI-SCB-68 (National Instruments, Austin, Texas, USA) data acquisition card was used for signal digitization. Sampling frequency was set to 512 Hz. NeuroSciLaBG, custom made application developed in NI LabVIEW software package (National Instruments, Austin, Texas, USA), was used for continuous data acquisition, storage on computer hard disk and further signal processing.

ECG and EEG signal analysis: general aspects

EEG and ECG signals recorded during experiments (AMI induction and epilepsy induction, described in details further on) were first visually inspected and then processed with advanced signal analysis software techniques to extract relevant features.

Visual inspection comprised of:

1. Visual detection of changes in the EEG signal during epileptic activity as well as discerning the latency, amplitude, number and duration of seizure activity. Ictal period was defined as follow: i) paroxysmal spiking activity; ii) duration of at least 1s, iii) amplitude at least twice the background EEG activity
2. Visual detection of ST depression/elevation in the ECG signal during experimentally induced AMI.

Techniques of automatic signal processing comprised of:

1. Linear and nonlinear EEG/ECG signal analysis methods were used during both experiments to extract characteristic EEG and ECG features useful in differentiation and prediction.
2. A neural network was created for automatic detection/prediction of epileptic seizures based on extracted features of EEG and/or ECG signals.

EEG features extracted were:

1. Median of total signal power and signal power in delta, theta, alpha and beta frequency bands for each of the EEG epochs. Fast Fourier transform was used for calculations. Median frequency corresponding to maximal spectral density of power in delta, theta, alpha and beta frequency bands in all ECG epochs. Welch method was used to asses for spectral density signal power.
2. Fractal dimension (FD)
3. Biotic parameters:

   a) Isometry as measured by the difference in area under the curve (AUC) between the graph of consecutive and shuffled signal segments.
   b) Consecutive isometry as measured by the difference in area under the curve (AUC) of consecutive isometry between the graph of consecutive and shuffled signal segments.
   c) Originality graph AUC measurement
   d) Arrangement graph AUC measurement
   e) Standard deviation graph AUC for consecutive and shuffled signal segments.

HRV features were extracted from the ECG signal using *Kubios HRV Standard* 3.2.0 software (Kubios, Finland):

1. *General features:* PNS index – parasympathetic activity compared to values during normal activity. SNS index – sympathetic activity compared to values during normal activity. Stress index – square root of Baevsky's stress index that represents the geometric measure of heart rate variability reflecting cardiovascular stress. High values of stress index point to low HRV and high level of sympathetic activation.
2. *Time domain features:* mean length of RR interval (*MeanRR*), coefficient of RR interval variation (*CVRR=SDNN/MeanRR*), median heart rate frequency (*MeanHR*), standard deviation of heart rate (*STD HR*), minimum (*Min HR*) and maximum (*Max HR*) heart rate, *SDNN, RMSSD*, *NN20*, *pNN20*, *TINN*.

3. *Frequency domain features*: *VLF*, *LF* and HF power, the *LF/HF* relation as well as peak *VLF*, *LF* and *HF frequencies*. FFT and autoregressive (AR) method was used for spectral power analysis
4. *Nonlinear parameters*: SD1 and SD2 using *Poincare-s method*. SD2/SD1 relation, ApEn, *SampEn* as well as measures of signal regularity and complexity, detruded fluctuation analysis of short term (*DFA* $\alpha 1$) and long term fluctuations (*DFA* $\alpha 2$)

3.3. Experiment I: model of AMI

AMI induction and experimental design

Isoprenaline - induced experimental model of AMI has been used in this study, executed according to [Gupta et al., 2013]. We randomly divided animals (n=12) into two equal groups: experimental and control group (n=6/per group). For AMI induction in the experimental group we used intraperitoneal administration of isoprenaline (isoproterenol hydrochloride, Sigma Aldrich, USA). The dose used was 150 mg/kg diluted (n=6). The control group was injected with saline.

EEG and ECG signals were registered during five hours on the first day (one hour before and four hours after AMI induction) and on the second day for one hour (24 hours after AMI induction). Further details explained later in Details on data processing and Fig. 3.3.1.

Heart tissue sampling and histopathological evaluation

Twenty-four hours after isoprenaline/saline injection, rats were anesthetized using pentobarbital sodium (50 mg/kg, i.p.). An inverted T incision was used for accessing the thorax and the heart released by cutting the great vessels of the corona cordis. Hearts were subsequently removed from the rat body, fixed with 10% buffered formalin solution, dehydrated in ethanol, cleared by xylene, and embedded in paraffin. Routine staining with hematoxylin and eosin (HE) was used on the five μm thick sections which were then examined under the OlympusBX41 light microscope with an OlympusC5060A-ADU digital camera.

Data recording and processing details

During the first day ECG and EEG were recorded during a five-hour recording session in freely moving rats (one hour before and four hours after infarction induction). In the second day ECG and ECG tracings were recorded for one hour (24h after isoprenaline administration) This is illustrated in Fig. 3.3.1 with denominated periods referred to in the rest of the thesis. Signal traces were visually inspected and analyzed during subsequent offline analysis.

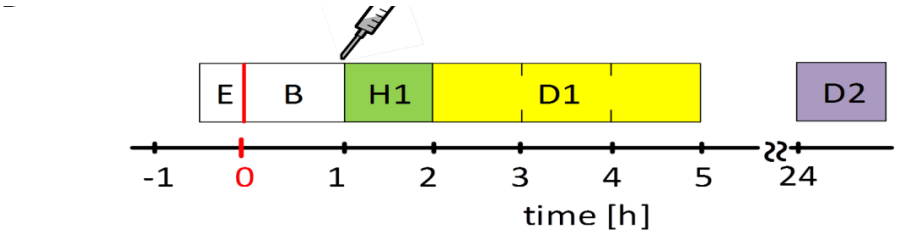

Fig. 3.3.1 Data acquisition timeline in experiment related to AMI

ECG electrodes montage and adaptation -E, baseline recordings - B, 1st h of data acquisition upon isoprenaline injection –H1, 2nd to 4th h of data acquisition upon isoprenaline injection –D1, 1h of data acquisition in the 2nd day (i.e.24h upon isoprenaline administration) – D2.

Recorded EEG traces were fragmented into consecutive epochs of 60 s. These isolated epochs were screened automatically for noise contamination. Rejected from further analysis were all epoch with voltage above 500 μV. Additionally, in order to get as clear data as possible, additional visual inspection were applied to the epochs and manual exclusions were done. Transformation was used to generate power spectrograms for visual inspection. Following parameters were used to generate spectrogram: 2 s window duration, 0.5 s window overlap and Hann window function.

We used these following definitions of four classically-reported EEG frequency bands: i) delta with range of 0.5 to 4 Hz, ii) theta with range of 4 to 7 Hz, iii) alpha with range of 7-13 Hz and iv) beta with range of 13 to 35 Hz. For each rat, band –power curves were computed.

EEG recordings were split for further analysis into four predefined time frames as follow: B, H1, D1, D2 (see Fig. 2.3.1.). For each rat, time frame and frequency band median value of band power were computed.

In addition, for each EEG frequency band (i.e. delta, theta, alfa, beta) peak frequency was determined. Peak frequency was determined as frequency value (Hz) that had maximum value of the Power spectral density estimated within the frequency band limits as defined previously.

We applied Welch algorithm on raw EEG epochs lasting 1 s to compute the power spectral density of the epoch. For each animal and time window (B, H1, D1 and D2) Median peak frequency was evaluated for each rat and time frame.

3.4 Experiment II: model of epilepsy

Epilepsy induction and registration

Epilepsy induction was performed using intraperitoneal lindane administration (n=8, 8mg/kg; Sigma Aldrich Co, SAD) (Vucević D et al 2008). The control group was injected with 2ml/kg of isotonic saline (n=8). EEG and ECG tracings were obtained during a 30-minute long monitoring period upon the administration of lindane/saline. Details on EEG and ECG registration are given in section 2.2.

Analysis of spectral ictal EEG data

Epoch containing ictal activity were extracted from registered EEG traces. Ictal activity has been defined by applying the previously adopted and described criteria (i.e. amplitude at least double compared to background activity lasting for more than 1 s). Such epochs were further subjected to the FFT in order to compute total spectral power and relative spectral power in predefined frequency bands (delta, theta, alpha and beta). We recorded and analyzed also duration of each ictal period. Amplitude Histogram of EEG spikes was created by applying NeuroSciLaBG functions for classification based on amplitude beans. We defined 22 beans of 50μV over the interval of -550 and +550 μV.

HRV based seizure prediction using neural networks

During classification system creation, there often arise feature vectors with large dimensions. These vectors can often include correlated, or even repeated information. When this is the case, it is necessary to apply dimension reduction, i.e. reduce the number of features included in every class sample. The method often used for dimension reduction, and the one we used is PCA (*Principal Component Analysis*) method, also known as the *Karhunen-Loeve (KL)* expansion.

In this work, before the feature reduction and classification, 51 HRV features (described in section 3.2 were standardized in the interval [-1, 1] (the difference between feature value and mean value was divided by the standard deviation of the feature value). Feature reduction (from 51 to 20 features) was performed using the PCA to select 95% of the variance.

Based on HRV features extracted during one minute before seizure commencement and application of PCA dimension reduction we devised a two-category classification: First class (class 1) was the normal state, i.e. the period when there is no danger of seizure onset. Second class (class 2) was the preictal state, when there is a danger of seizure onset.

The classification was performed in the Python programming language using the *sklearn* library for the classificator implementation. The reduced feature data set was divided into 6 folds, in the manner that each fold consists of only data from one rat (both healthy and epileptic). For the training and testing of the classificators, one-fold was used for testing and the rest for training. In order to balance the classes in the training set (originally healthy: epileptic ratio 1:2), each instance of the healthy class was repeated two times. Logistic regression (LR) and back propagation neural network (NN) were used for the classification.

The classification metrics used were Accuracy, Precision, Sensitivity, Specificity, and F1 score:

$$\text{Accuracy}=(TP+TN)/(TP+TN+FP+FN) \quad (1)$$

$$\text{Precision} = TP/TP+FP \quad (2)$$

$$\text{Sensitivity} = TP / FN+TP \quad (3)$$

$$\text{Specificity} = TN/FP+TN \quad (4)$$

$$\text{F1 score} = 2 * (\text{Precision} * \text{Sensitivity})/ (\text{Precision} + \text{Sensitivity}) \quad (5)$$

TP (true positive) represents the number of elements that were correctly classified as class 1, TN (true negative) represents the number of elements that were correctly classified as class 2, FP (false positive) represents the number of elements that were classified as class 2 and in fact belong in class 1, FN (false negative) represents the number of elements that were classified as class 1, in fact belong in class 2.

Biotic EEG based seizure detection using neural networks

Biotic parameters on EEG segments with a time window of 15 seconds and a moving frame of 5 seconds where extracted as neural network features. The following six biotic characteristics where used for each EEG signal segment: isometry, consecutive isometry, arrangement, originality and local diversification. The biotic characteristics where calculated using the Bios Analyser software [H. Sabelli et al 2005]. Previous research has shown that EEG signals indeed satisfy the criteria for biotic signals [M. Vorkapić et al 2017].

Isomety is a parameter that quantifies recurrent measurements of same length vectors. Vector length is calculated by determining the Euclidean norm (the square root of the sum of the squares of its terms). Two vectors are considered isometric if the absolute value of the difference in their Euclidian norms is lower than the border radius determined by the user [L. H. Kauffman et al 1999]. Fig 3.4.1 shows the isometry curve for an EEG segment with and without ictal activity.

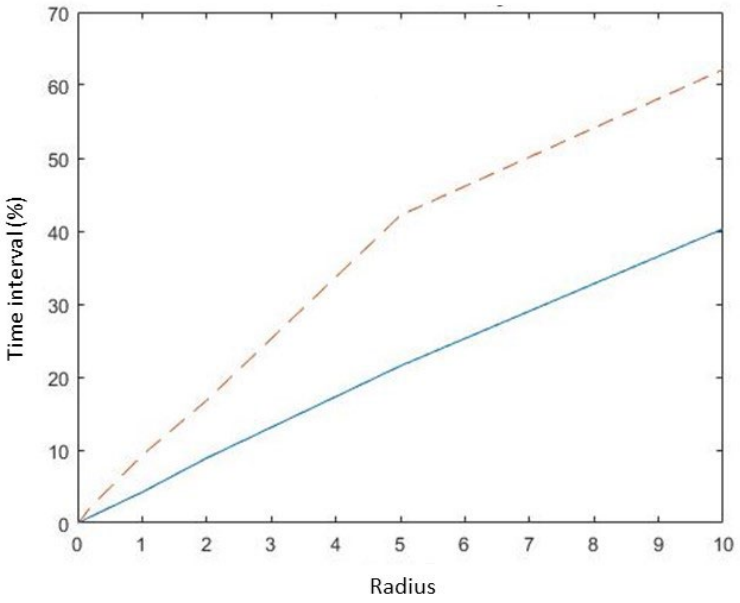

Fig. 3.4.1. Isometry ploted with radius (X axis) as percentage of time interval (Y axis) for ECOG signal with ictal activity (blue solid line) and without ictal activity (red dashed line)

Consecutive Isometry represents isometry for two consecutive vectors. Fig 3.4.2 shows the consecutive isometry curve for ictal and non ictal EEG segments. Biotic processes are characterized by consecutive isometry curves that have a swift initial upstroke followed by a smaller increase thereafter, with the increase of time series embedding. In Fig 3.4.2 it can be appreciated that both ictal and non ictal EEG signal curves show the feature of causality with the curve having a slightly less significant upstroke in the non ictal segment.

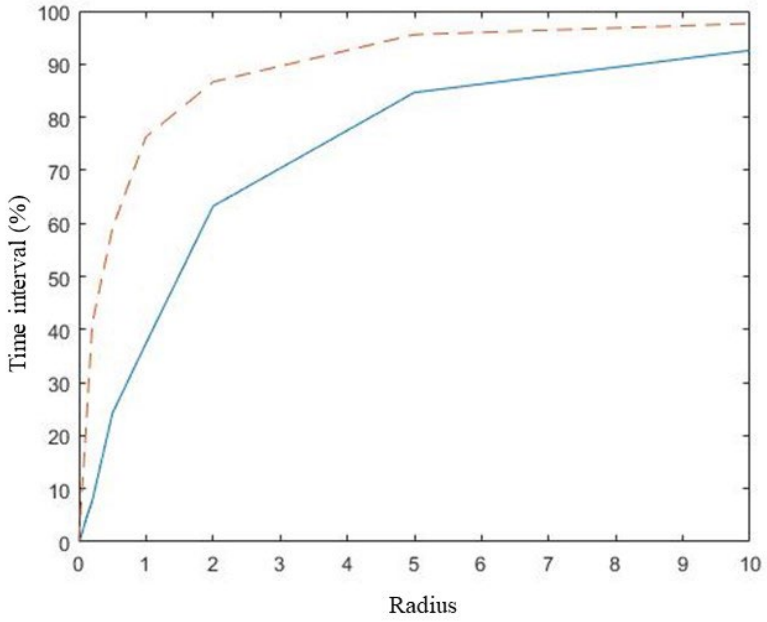

Fig. 3.4.2. Consecutive isometry plotted with radius (X axis) as percentage of time interval (Y axis) for ECOG signal with ictal activity (blue solid line) and without ictal activity (red dashed line)

The Arrangement feature for the ictal and non ical segments of EEG signal for 100 consecutive time series vectors is given in Fig 3.4.3. Arrangement in ictal vs non ictal EEG time series grows more significantly with increased embedding.

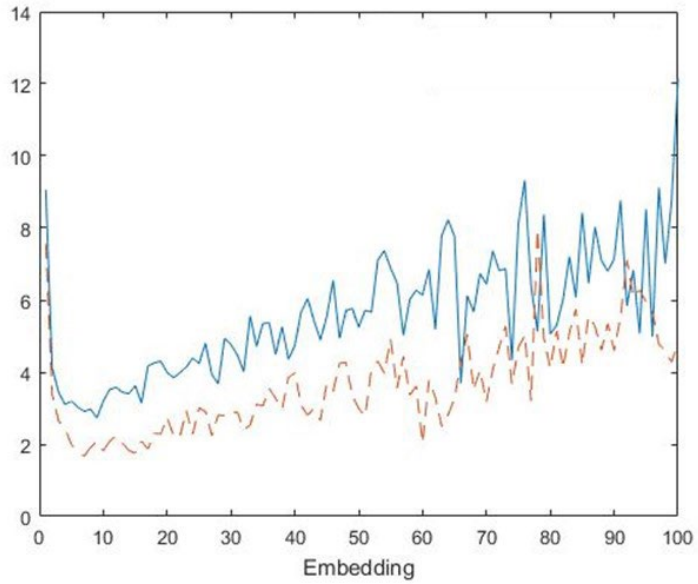

Fig. 3.4.3. Arrangement graph plotted for ECOG signal with ictal activity (blue solid line) and withought ictal activity (red dashed line)

Originallity is represented by a relation of isometry and its “shuffled“ copy (dividing the signal in to smaller intervals, them shuffling them) in a signal segment. The graph in Fig. 3.4.4 shows originality in ictal and non ictal EEG segments. The graph shows that originality for an

EEG segment grows further with increased embedding values for the ictal vs the non ictal segment.

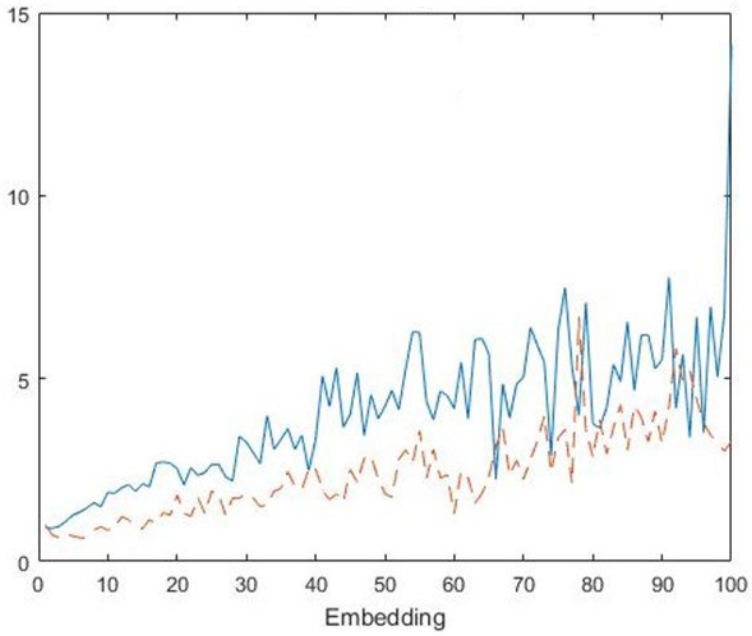

Fig. 3.4.4. Originality graph plotted for ECOG signal with ictal activity (blue solid line) and without ictal activity (red dashed line)

Local diversification (standard deviation of consecutive and "shuffled" vectors for signal segment observed) is given in Fig 3.4.5 The standard deviation has a much larger value in the ictal EEG for both consecutive and shuffled segments.

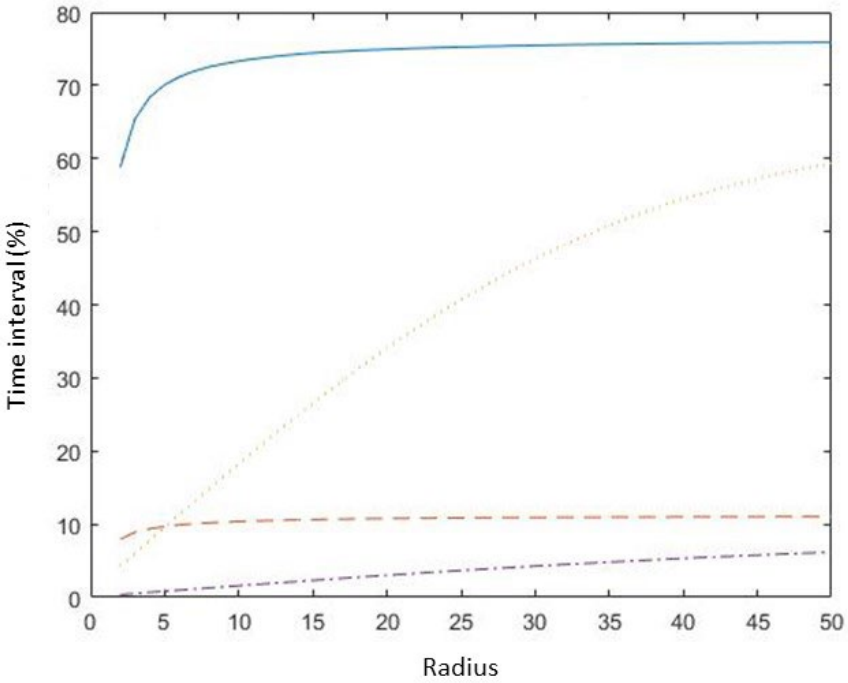

Fig. 3.4.5. Local diversification plotted with radius (X axis) as a percentage of time interval (Y axis) for consecutive ECOG signal segments with ictal activity (blue solid line) and without ictal activity (red dashed line) as well as shuffled ECOG signal segments segments with ictal activity (blue dotted line) and without ictal activity (black dash dotted line)

Neural network output consists of two columns, representing ictal and non-ictal segments. The signal segment was initially classified visually. Creating, training and testing of the neural network was done using *Neural Network Pattern Recognition Tool* in *Matlab 2016b* (Mathworks, USA) software. The algorithm used to train the network is the *scaled conjugate gradient backpropagation* activated by calling Matlabs built in function *trainscg*. A dual layer neural network with six hidden layers was used.

3.5 Statistical analysis

Normal distribution of data has been determined by Shapiro-Wilks test. The statistical significance of the difference in the registered, observed or calculated parameters with normal data distribution were evaluated by t test of one-way ANOVA with LSD post hoc test for independent samples. Kruskal-Wallis ANOVA and Mann-Whitney U were used for non-parametric data comparisons. For determination of statistical significance of differences among measurements done in different time points, repeated – measures ANOVA with LSD post hoc test was used for multiple comparisons when data showed normal distribution and Friedman's test with non-parametric data. Pairwise comparisons were done by Wilcoxon's signed rank test. Data are expressed as mean ± standard deviation/standard error (SD/SE) or median as a non-parametric measure of central tendency with 25th and 75th percentiles as corresponding measures of variation. A criteria for statistical significance *$p < 0.05$, **$p < 0.01$ and ***$p < 0.001$ were applied.

4. RESULTS

4.1 Isoprenaline induced acute myocardial infarction model

4.1.1 Isoprenaline - induced ECG and histological changes

No abnormalities in ECG wave morphology and dynamics were recorded in baseline measurements of the control, as well as in the experimental group. The same holds true for control group in all subsequent traces. However, as fast as upon 14 min upon isoprenaline administration, first ST elevation was recorded in the experimental group. ST elevation was present in ECG during all recordings done within the first day (Fig 4.1.1). ST elevation indicates development of AMI upon isoprenaline administration.

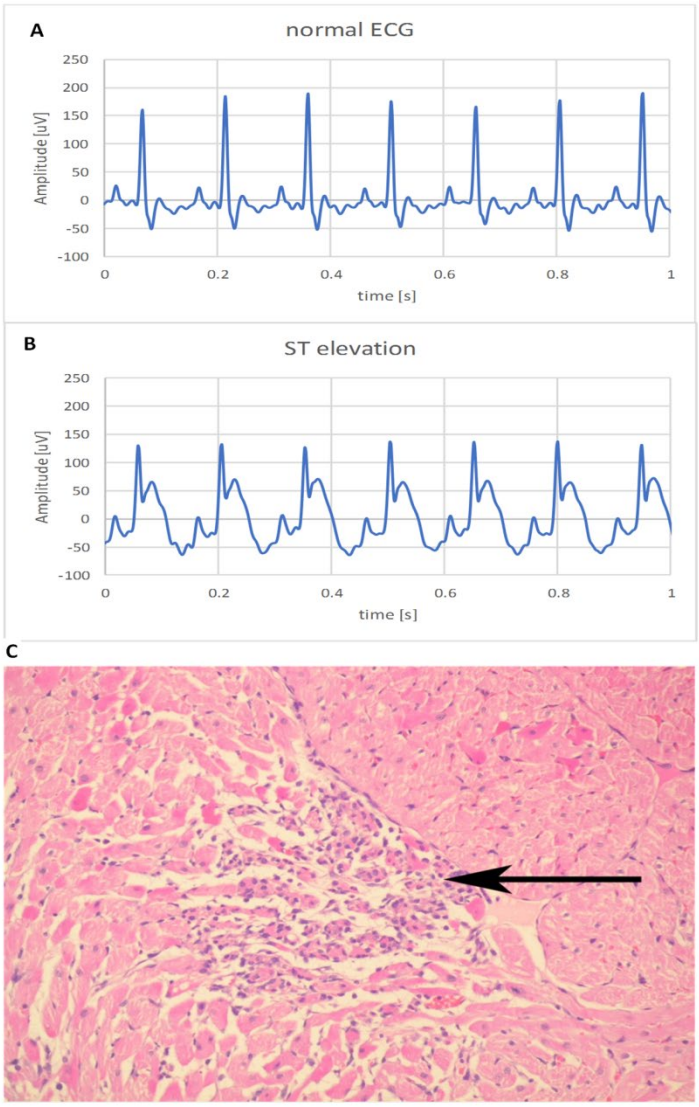

Fig. 4.1.1 Representative ECG traces and histological verification of AMI

(A) *Baseline ECG trace,* ***(B)*** *ECG upon isoprenaline administration with present ST elevation,* ***(C)*** *Histological alterations found 24h upon isoprenaline administration in the myocardial wall. Arrow*

indicates necrotic cells with hyper-eosinophilia, pyknotic nuclei, and inflammatory cell infiltration (H/E staining, 200x)

Histological analysis of myocardial wall was performed 24h upon isoprenaline/saline administration in experimental/control group of rats. This evaluation showed presence of ischemic injury in the myocardial wall of rats from experimental group receiving isoprenaline. This ischemic injury was featured by presence of necrotic myocardium with an interface of inflammation and necrotic area were characterized additionally with hyper-eosinophilia, pyknotic nuclei, and inflammatory cells infiltration. On the other hand, no histomorphological alterations were find in myocardial wall slices from the control rats receiving saline (Fig. 4.1.1.C)

4.1.2 Medial prefrontal cortex EEG signal characteristics during AMI

EEG power spectrum analysis

The representative EEG strip as well as representative frequency bands after decomposition can be seen in Fig 4.1.2 and 4.1.3 consecutively. The results of median power distribution represented by 4 time-windows in the experimental group are presented by Fig 4.1.4. Statistically significant differences ($p<0.05$) over all animals were found in median band-power of alpha, beta and theta frequency bands. For the theta band power, the statistically significant difference was detected between baseline (B) and 1h (H1) upon isoprenaline injection ($p<0.05$, Fig. 4.1.4B). As for alpha band power, the significant difference was between B and measurement done 2-4h upon isoprenaline injection (D1) ($p<0.05$, Fig. 4.1.4C); and for beta band power it was between B and H1 as well as between B and D1 ($p<0.05$, Fig. 4.1.4D). There was no statistically significant difference between baseline and activity in D2 for any of the frequency bands, indicating that the differences detected in time-windows of day 1 were immediate effects associated with isoprenaline induced AMI.

Band peak-frequency analysis results for the 4 time-windows showed differences of theta band peak frequency that were statistically significant. The band peak-frequency analysis results for theta band are given in Fig. 4.1.4F where we can observe a significant increase of median theta peak frequency in the first hour after isoprenaline administration as compared to the baseline. This effect is not present during the rest of the day 1 and day 2 windows in which the theta peak frequency did not differ significantly from the baseline ($p>0.05$). No differences were found in peak frequency analysis in the remaining frequency bands. No differences in median band power were found in any of the observed time-windows in the control group Fig. 4.1.5 ($p>0.05$).

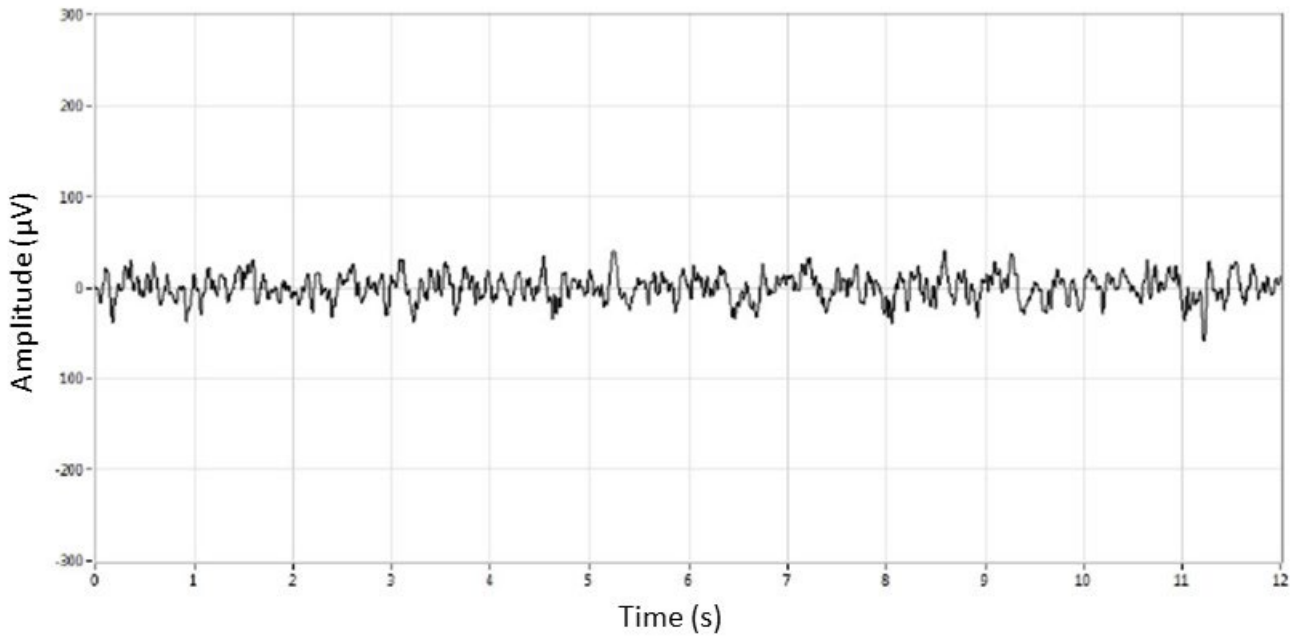

Fig. 4.1.2 Representative EEG strip.

Delta	Theta	Alpha	Beta
0.5-4Hz	4-7Hz	7-15Hz	15-30Hz

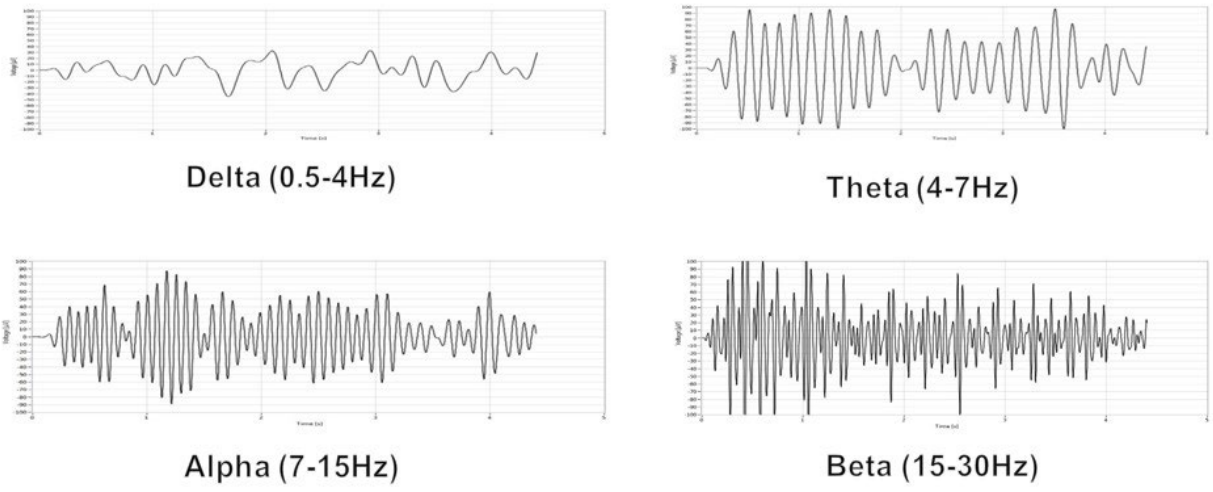

Fig. 4.1.3 Representative EEG frequency bands and their respective frequences

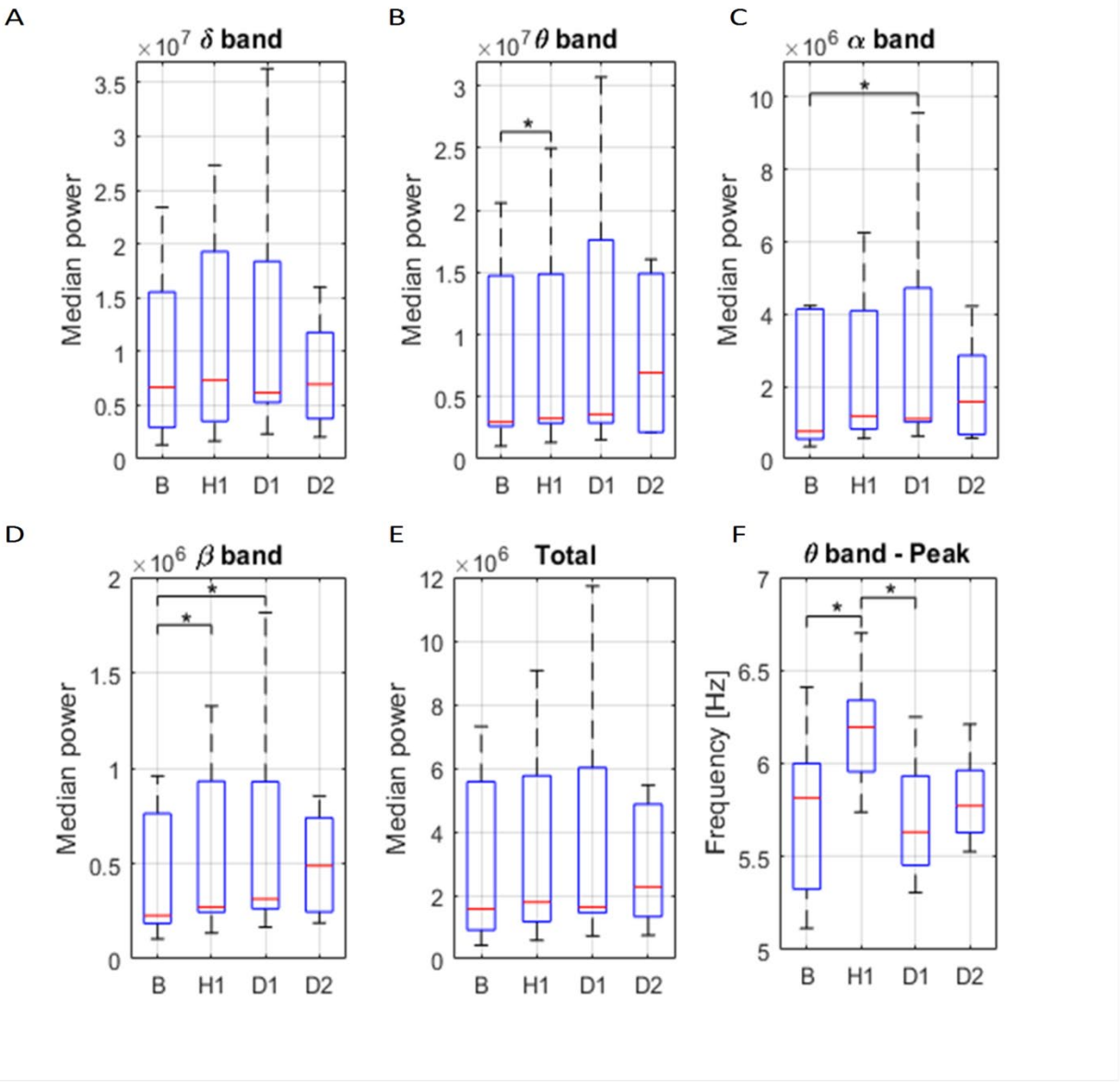

Fig. 4.1.4 Median power changes per frequency band for the experimental group before and after isoprenaline administration

*Median power of delta (A), theta (B), alpha (C) and beta band (D) and total median power (E). Peak frequency for theta band (F). *p<0.05 B–baseline, H1 –1h, D1 –2-4h, D2 –24h upon isoprenaline injection.*

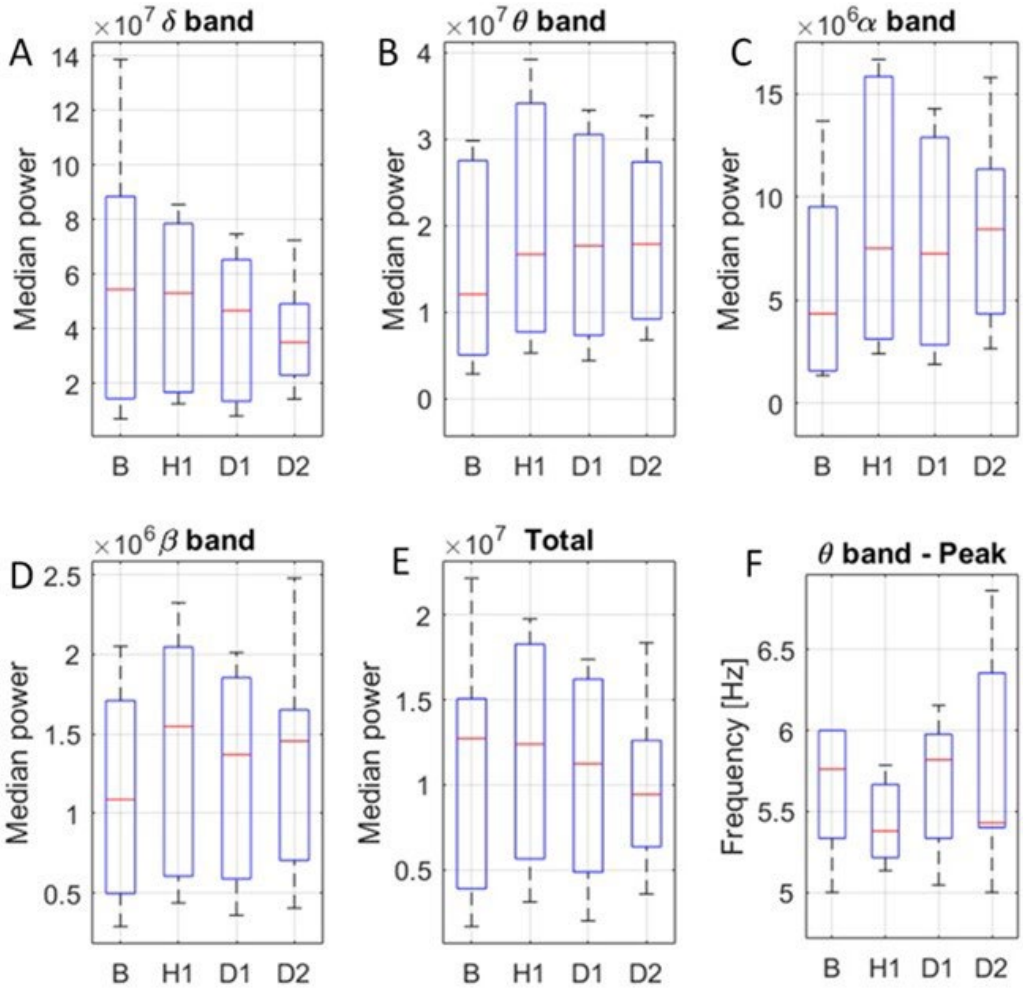

Fig. 4.1.5 Median power changes per frequency band for the control group before and after saline administration.

*Median power of delta (A), theta (B), alpha (C) and beta band (D) and total median power (E). Peak frequency for theta band (F). *p<0.05 For details see caption to Figs 3.3.1 and 4.1.4*

Correlation analysis of EEG frequency band relative power and ST elevation

We used the Pearson correlation coefficient in order to investigate the relationship between ST elevation amplitude and relative change of total and each EEG frequency band (delta, theta, alpha and beta) median power in time windows 1h (H1), 2-4h (D1) and 24h (D2) upon isoprenaline in relation to baseline (B). Fig 4.1.6 depicts scatterplots of statistically significant outcomes.

We detected a statistically significant strong positive correlation between ST elevation amplitude and relative change in power of the alpha band in D1 ($r = 0.85$, $p<0.05$, Fig 4.1.6A). There was also a significant relative change in power of the beta band in H1 ($r = 0.86$, $p<0.05$, Fig 4.1.6B) and D1 ($r = 0.90$, $p<0.05$, Fig 4.1.6C) that strongly correlated with ST elevation. The relative change in power of other frequency bands as well as total power in relation to B were not statistically significantly correlated with ST elevation in any of the time windows (r in range from 0.31 to 0.62, $p>0.05$).

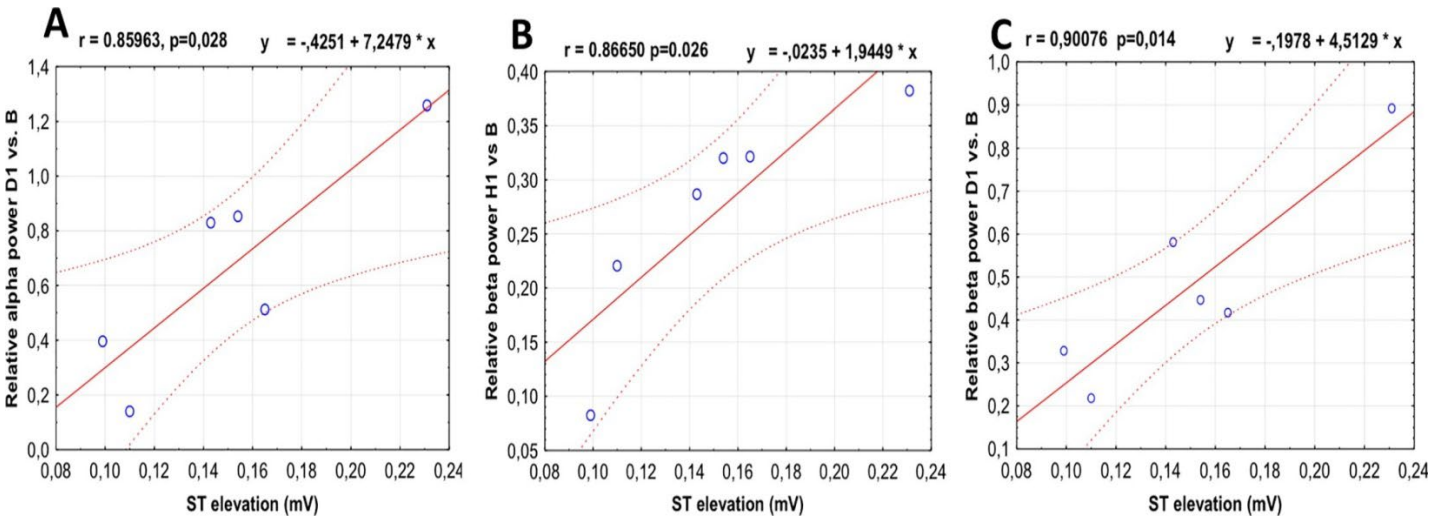

Fig. 4.1.6. Correlation plots of ST elevation and relative EEG power.

Pearson correlation demonstrates a strong positive relation between the degree of ST elevation and relative change in power of the alpha band in D1 (A); beta band power in H1 (B) and D1 (C) as opposed to B time window. For details see caption to *Figs 3.3.1 and 4.1.4*

4.1.3 ECG characteristics during AMI

Time domain HRV features

Mean RR interval duration showed a significant decrease in 1h ($p<0.001$), 2h ($p<0.001$), 3h ($p<0.001$) and 4h ($p<0.001$) compared to baseline values and compared to 24h upon isoprenaline administration (Fig 4.1.7 A). Standard deviation of RR interval graph showed no statistically significant change in any time point upon isoprenaline administration. Also, there were no significant differences in standard deviation of RR interval measured in baseline condition and 24h upon isoprenaline administration (Fig. 4.1.7 B).

Mean HR was significantly increased when measured in 1h ($p<0.001$), 2h ($p<0.001$), 3h ($p<0.001$) and 4h ($p<0.001$) upon isoprenalin administration compared to baseline values and compared to 24h upon isoprenaline administration (Fig 4.1.8 A). Standard deviation of HR showed no statistically significant change in any time point upon isoprenaline administration and there were no significant differences in Mean HR measured in baseline condition and 24h upon isoprenaline administration (Fig. 4.1.8 B).

Max HR was significantly increased when measured in 2h ($p<0.01$) and 3h ($p<0.05$) upon isoprenalin administration compared to baseline values and compared to 24h upon isoprenaline administration (Fig. 4.1.9 A). Min HR showed no statistically significant change in any time point upon isoprenaline administration and there were no significant differences in Min HR measured in baseline condition and 24h upon isoprenaline administration (Fig. 4.1.9 B).

RMSSD, TRI RR index and TNN measurement showed no statistically significant change in any time point upon isoprenaline administration and there were no significant differences measured between baseline condition and 24h upon isoprenaline administration (Fig. 4.1.10 A-C).

NN50 beats and pNN50 measurement showed no statistically significant change in any time point upon administration and there were no significant differences measured between baseline condition and 24h upon isoprenaline administration (Fig. 4.1.11 A and B).

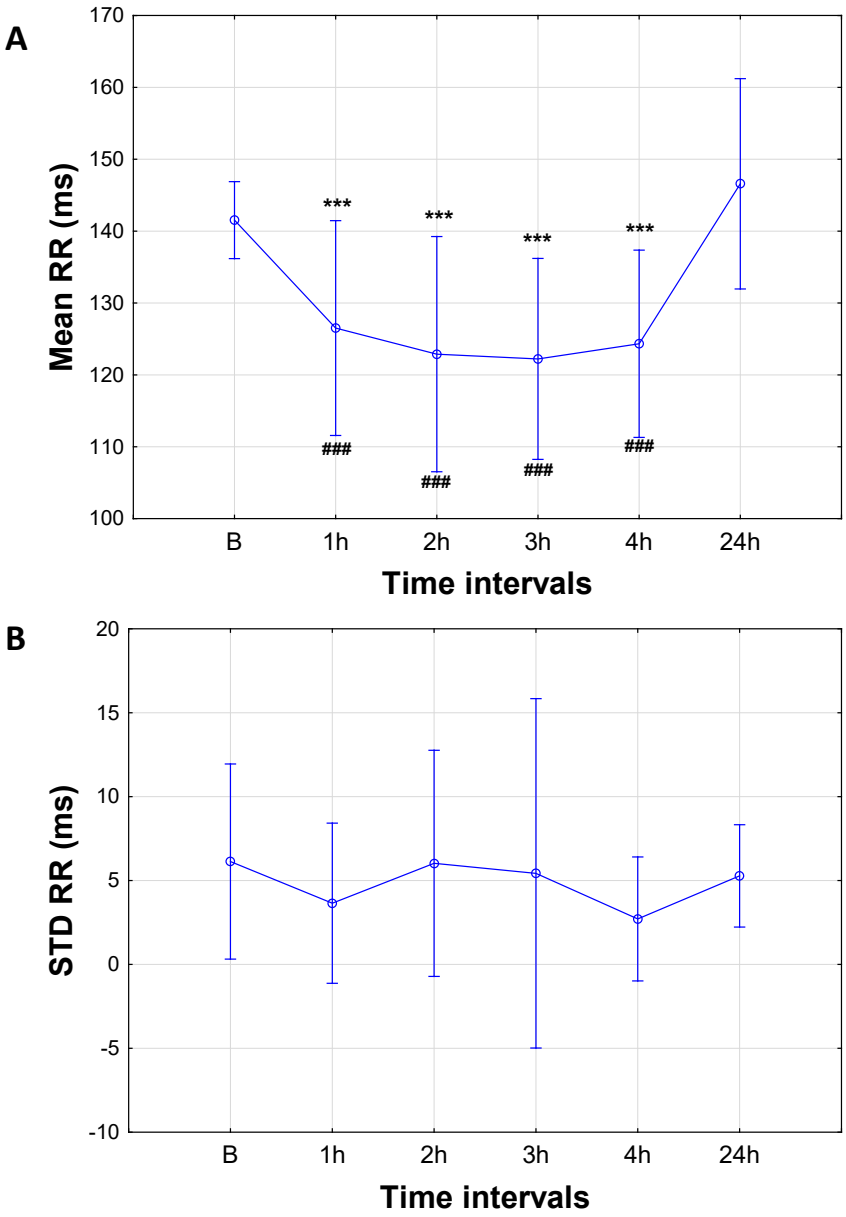

Fig. 4.1.7 Time course of changes in Mean RR interval (A) and STD of RR intervals (B).

*Values are means ± SE, *p<0.05, **p<0.01, ***p<0.001 vs B; #p<0.05 vs. 24h. Time intervals before (B) and after (1-24h) isoprenaline administration*

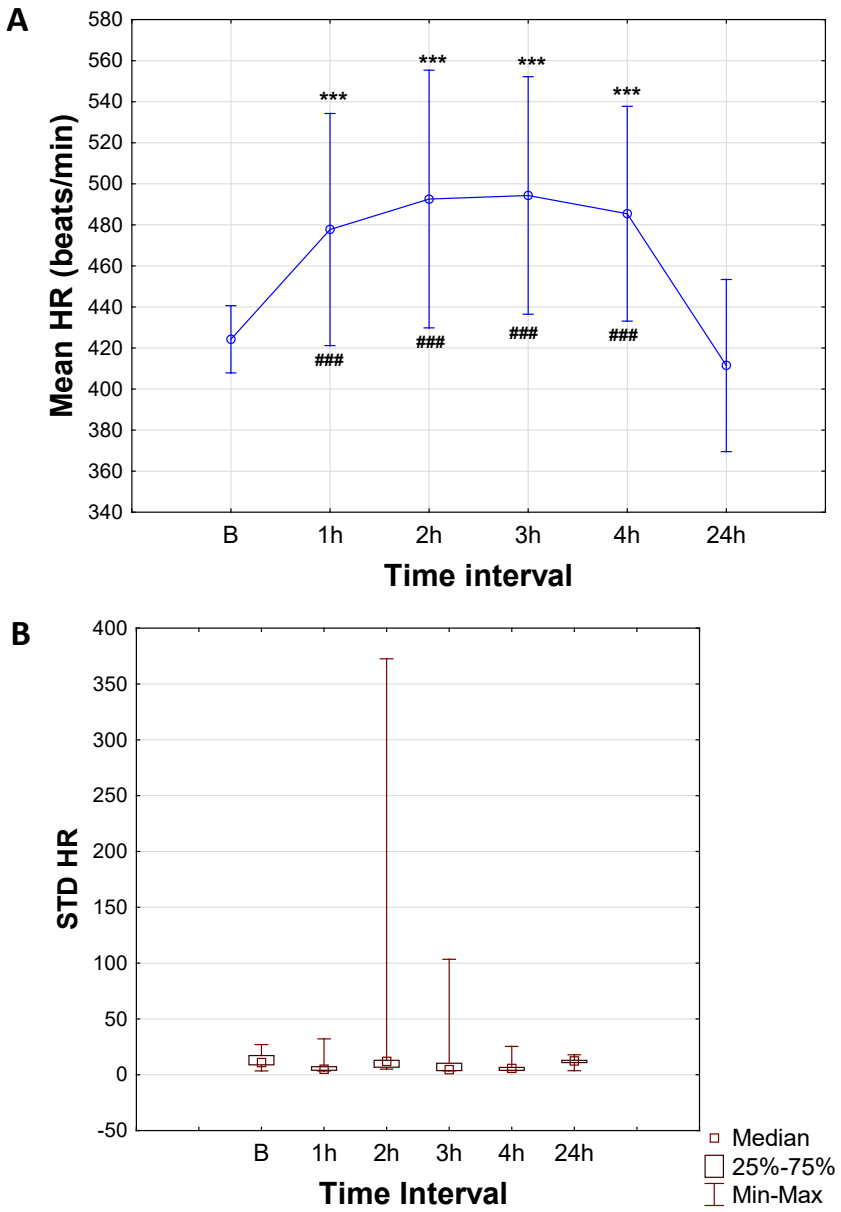

Fig. 4.1.8 Time course of changes in Mean HR (A) and HR STD (B), measurement.

*Values are means ± SE, *p<0.05, **p<0.01, ***p<0.001 vs B; #p<0.05 vs. 24h. For details see Fig. 4.1.7*

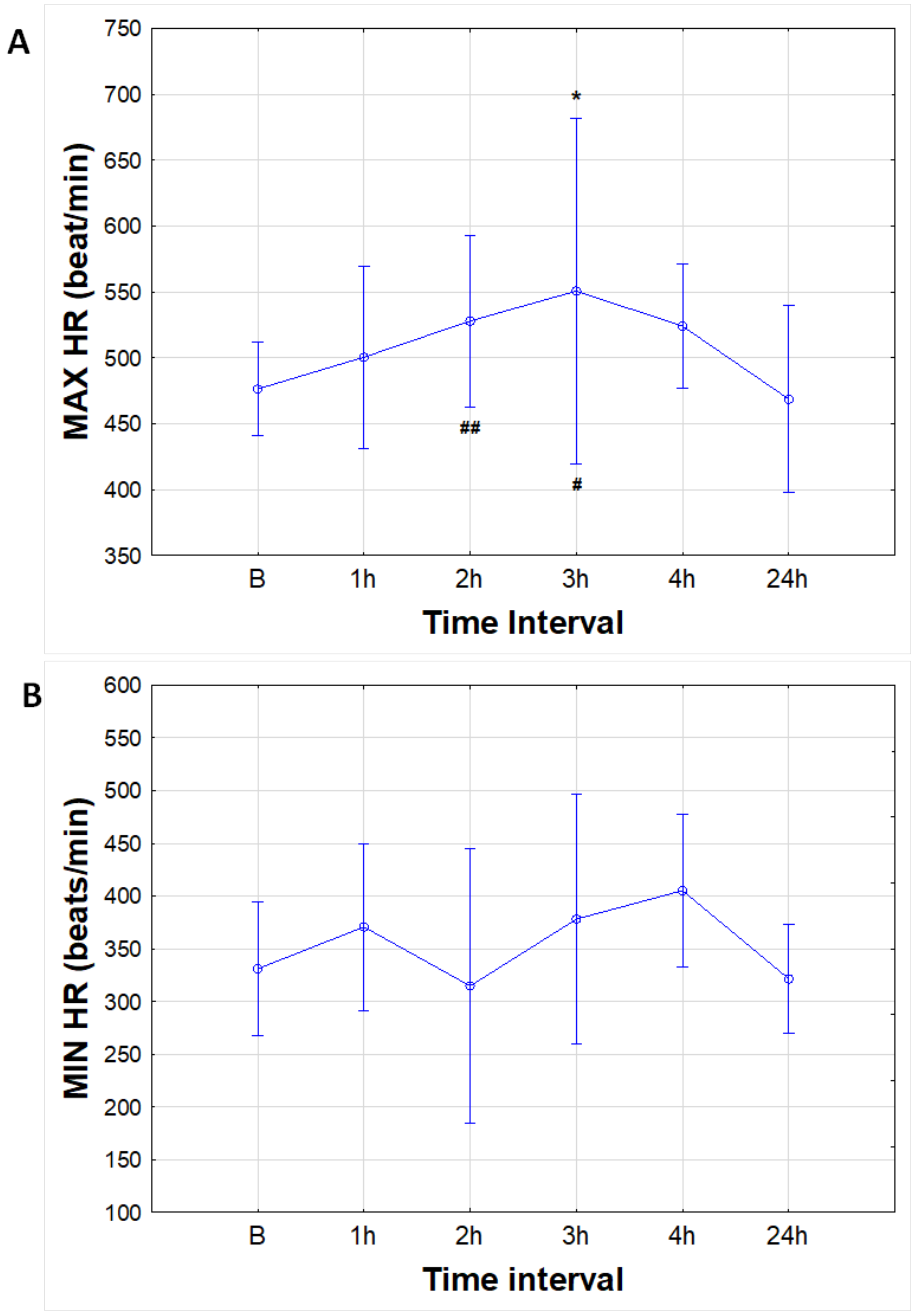

Fig. 4.1.9 Time course of changes in MAX HR (A) and MIN HR (B) measurement.

*Values are means ± SE, *p<0.05, **p<0.01, ***p<0.001 vs B; #p<0.05 vs. 24h. For details see Fig. 4.3.1*

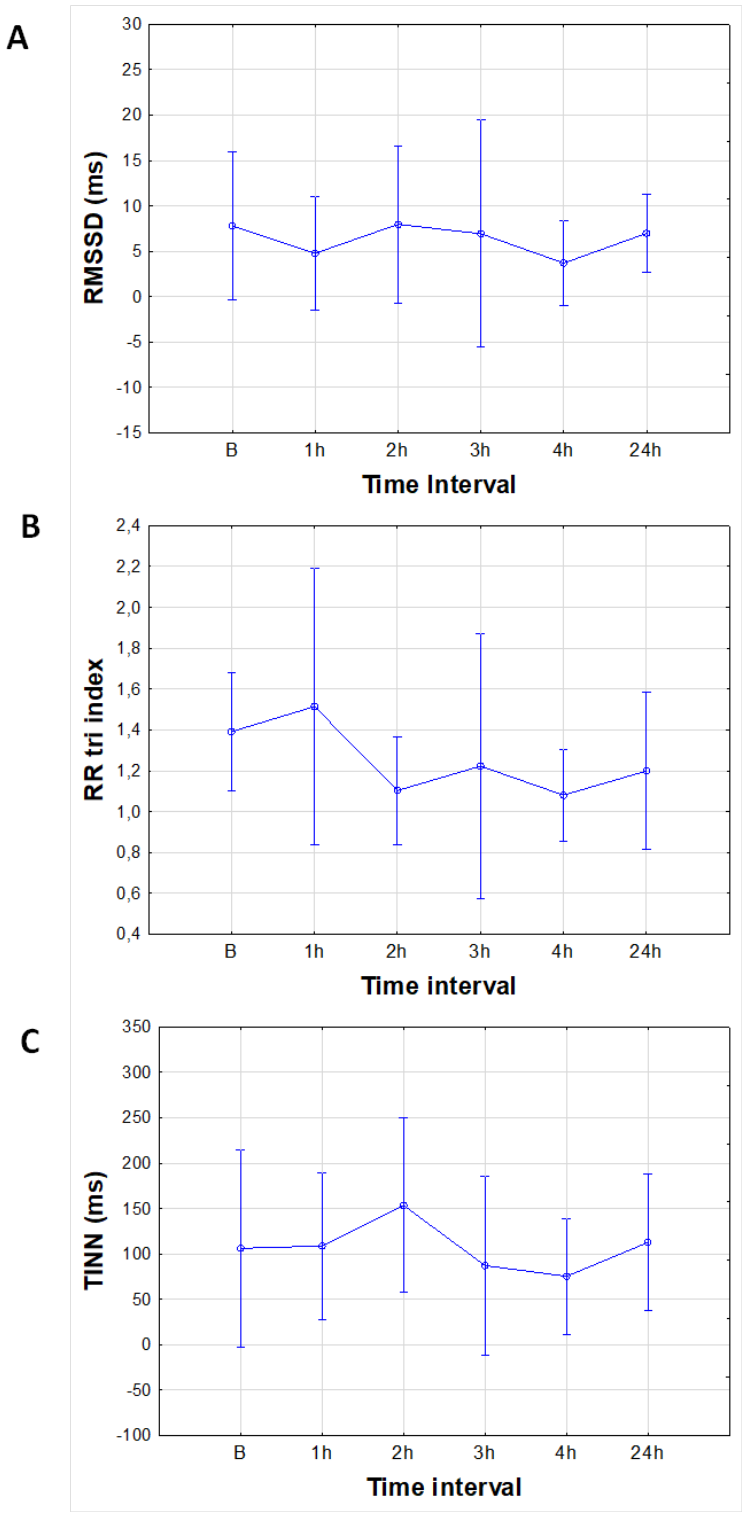

Fig. 4.1.10 Time course of changes of RMSSD (A), RR tri-index (B) and TINN (C) measurement.

*Values are means ± SE, *p<0.05, **p<0.01, ***p<0.001 vs B; #p<0.05 vs. 24h. For details see Fig. 4.1.7*

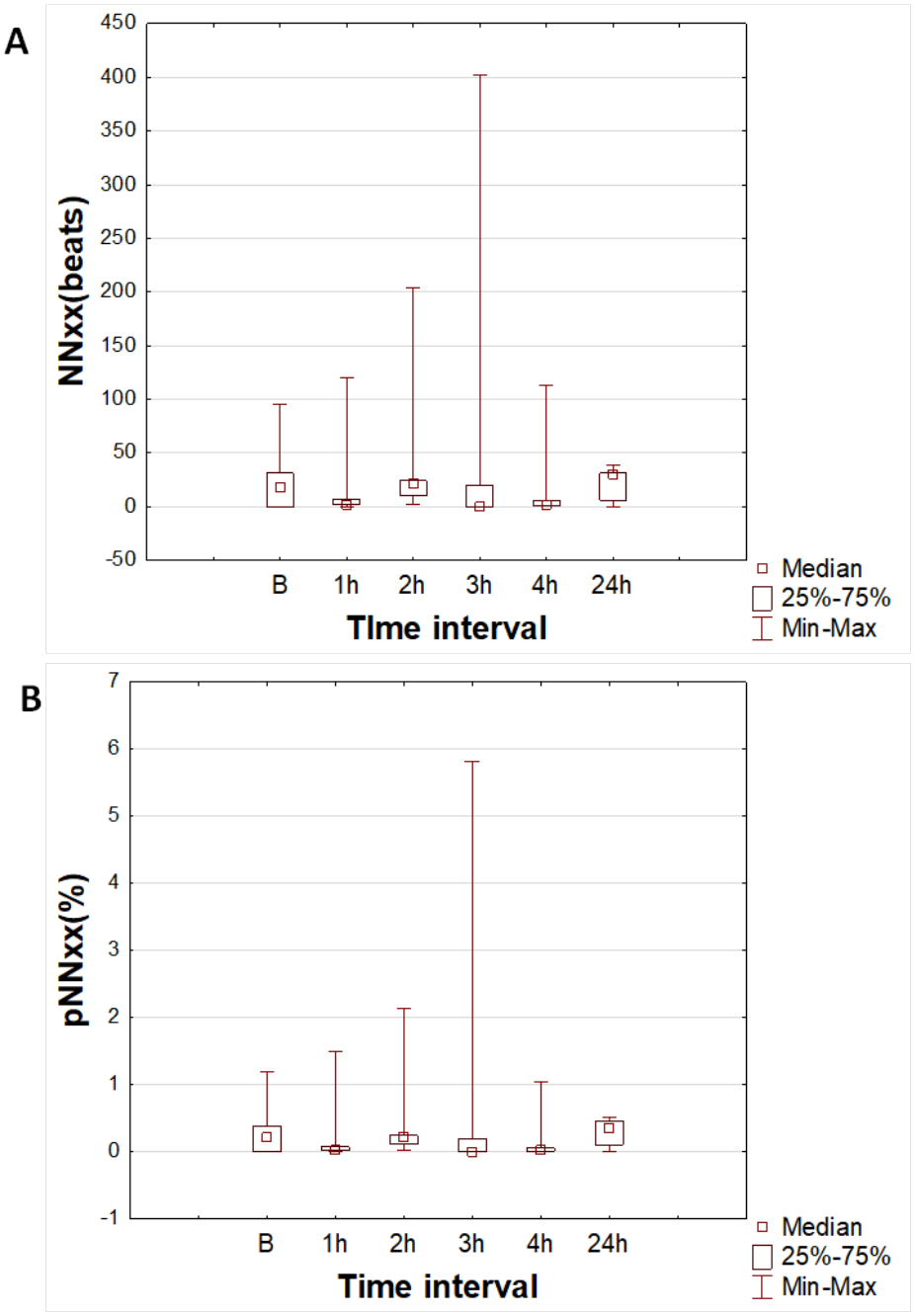

Fig. 4.1.11 Time course of changes of pNN50 (A) and pNN50 (B) measurement.

*Values are means ± SE, *p<0.05, **p<0.01, ***p<0.001 vs B; #p<0.05 vs. 24h. For details see Fig. 4.1.7*

Frequency domain HRV features

The log graph of VLF shows a decrease in VLF power during 1-4h upon isoprenaline administration especially pronounced in the 4h of recording, but fails to reach statistical significance (Fig. 4.1.12 A). The log graphs of LF and HF distribution in the ECG have the same overall pattern but also show no statistically significant change in any time point upon isoprenaline administration (Fig. 4.1.12 B-C). There was no significant difference measured between baseline condition and 24h upon isoprenaline administration in any of the frequency domain log graphs (Fig. 4.1.12 A-C).

The percentage of VLF an LF power showed no statistically significant differences in any time point upon isoprenaline administration (Fig. 4.1.13-B). The HF power distribution percentage graph in the ECG showed a moderate increase in the 1h and 2h upon isoprenaline administration but also fails to reach statistical significance in any time point upon isoprenaline administration. (Fig. 4.1.13 C). There was no significant difference measured between baseline condition and 24h upon isoprenaline administration in any of the frequency band percentage (Fig. 4.3.13 A-C).

Total spectral power of the ECG RR intervals showed no statistically significant change in any time point upon isoprenaline administration and there were no significant differences in this parameter measured between baseline condition and 24h upon isoprenaline administration (Fig. 4.1.14 A). The LF/HF ratio showed a slump in the 1h and 2h that failed to reach statistically significance. No statistically significant changes were seen between baseline condition and 24h upon isoprenaline administration as well (Fig. 4.1.14 B).

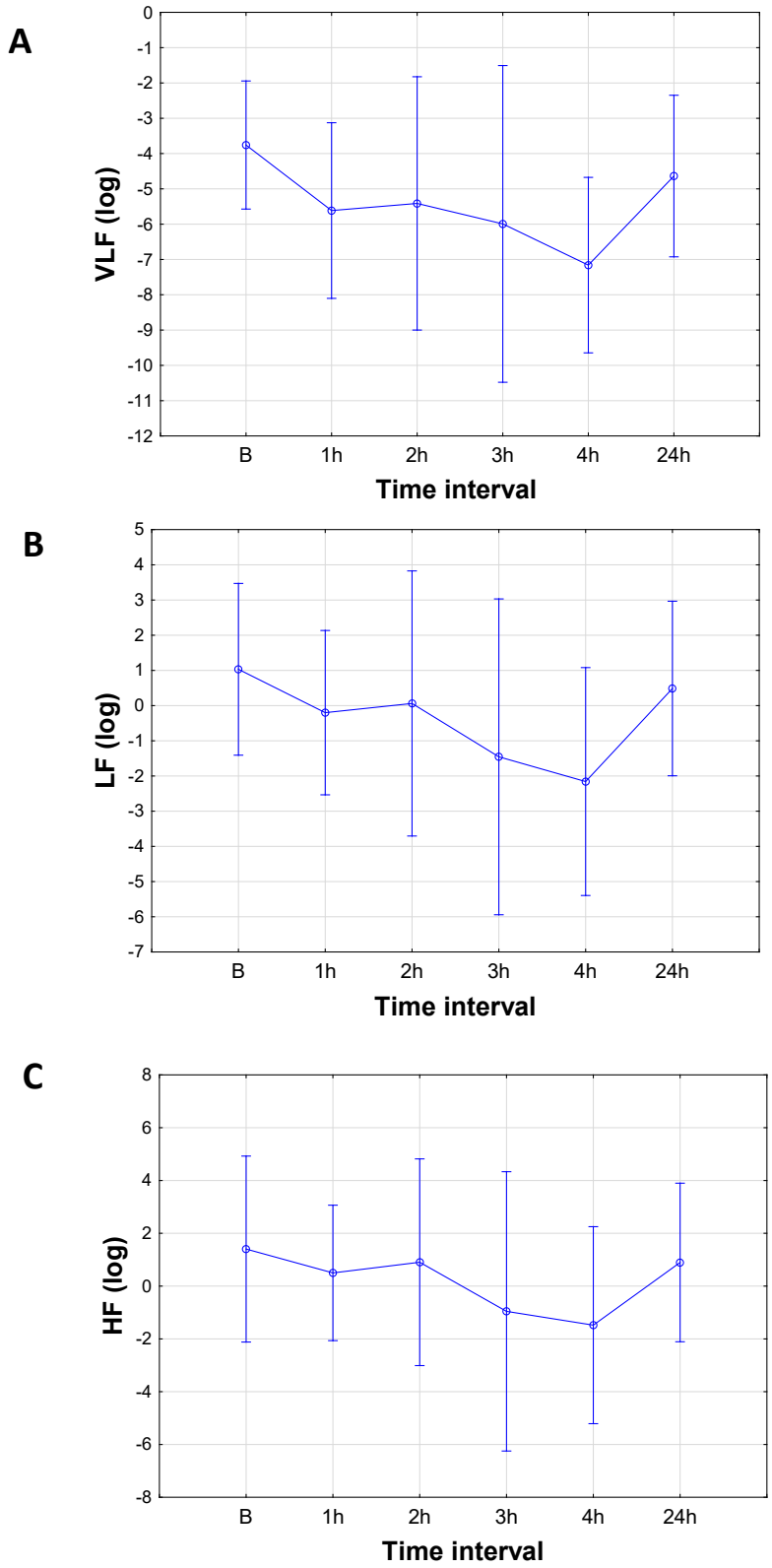

Fig. 4.1.12. Time course of changes in frequency distribution VLF (A), LF (B) and HF (C) on logarithmic scale (log).

*Values are means ± SE, *p<0.05, **p<0.01, ***p<0.001 vs B; #p<0.05 vs. 24h. For details see Fig. 4.1.7*

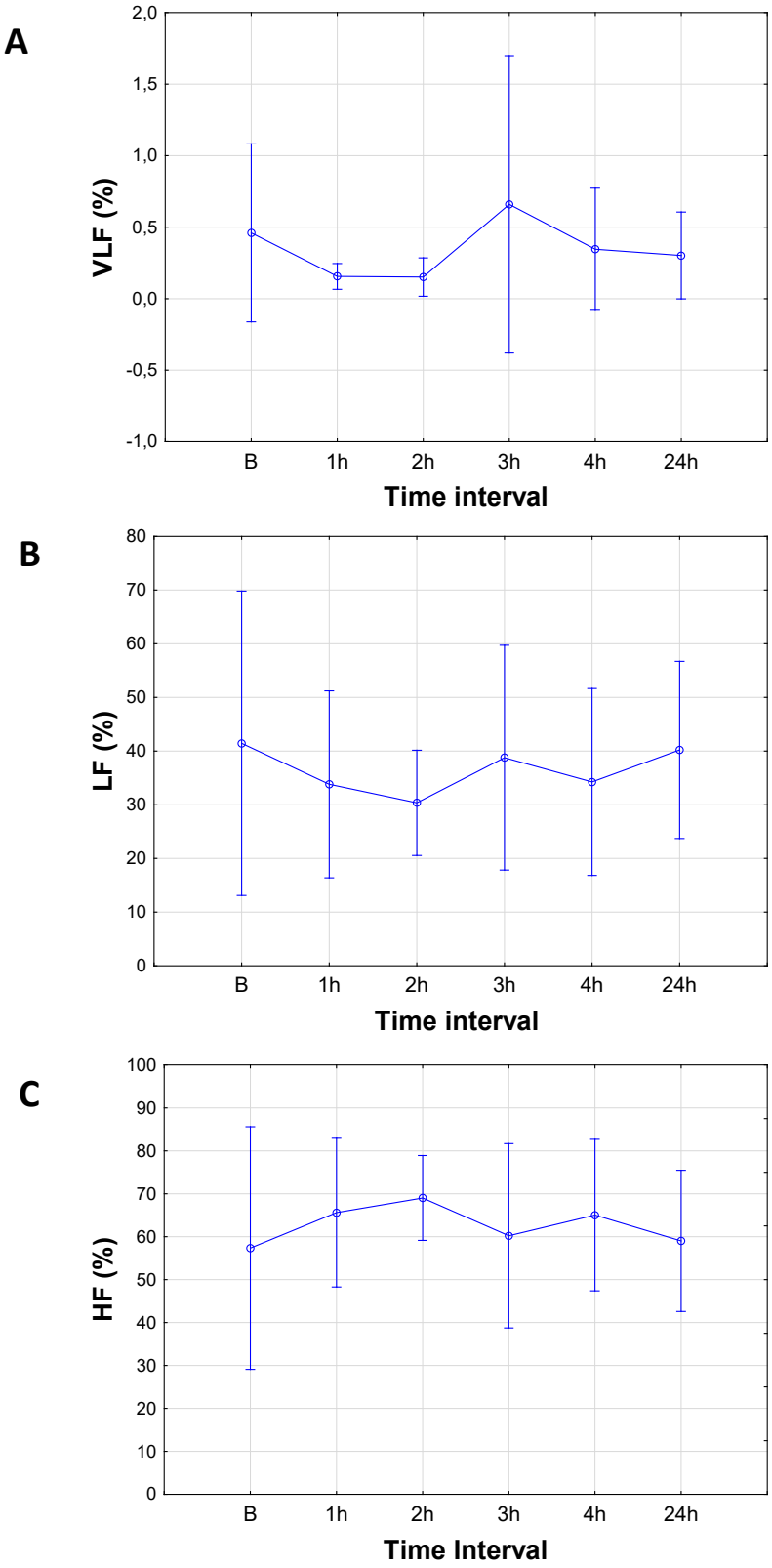

Fig. 4.1.12. Time course of changes in VLF (A), LF (B) and HF (C) on percentage scale (%).

*Values are means ± SE, *p<0.05, **p<0.01, ***p<0.001 vs B; #p<0.05 vs. 24h. For details see Fig. 4.1.7*

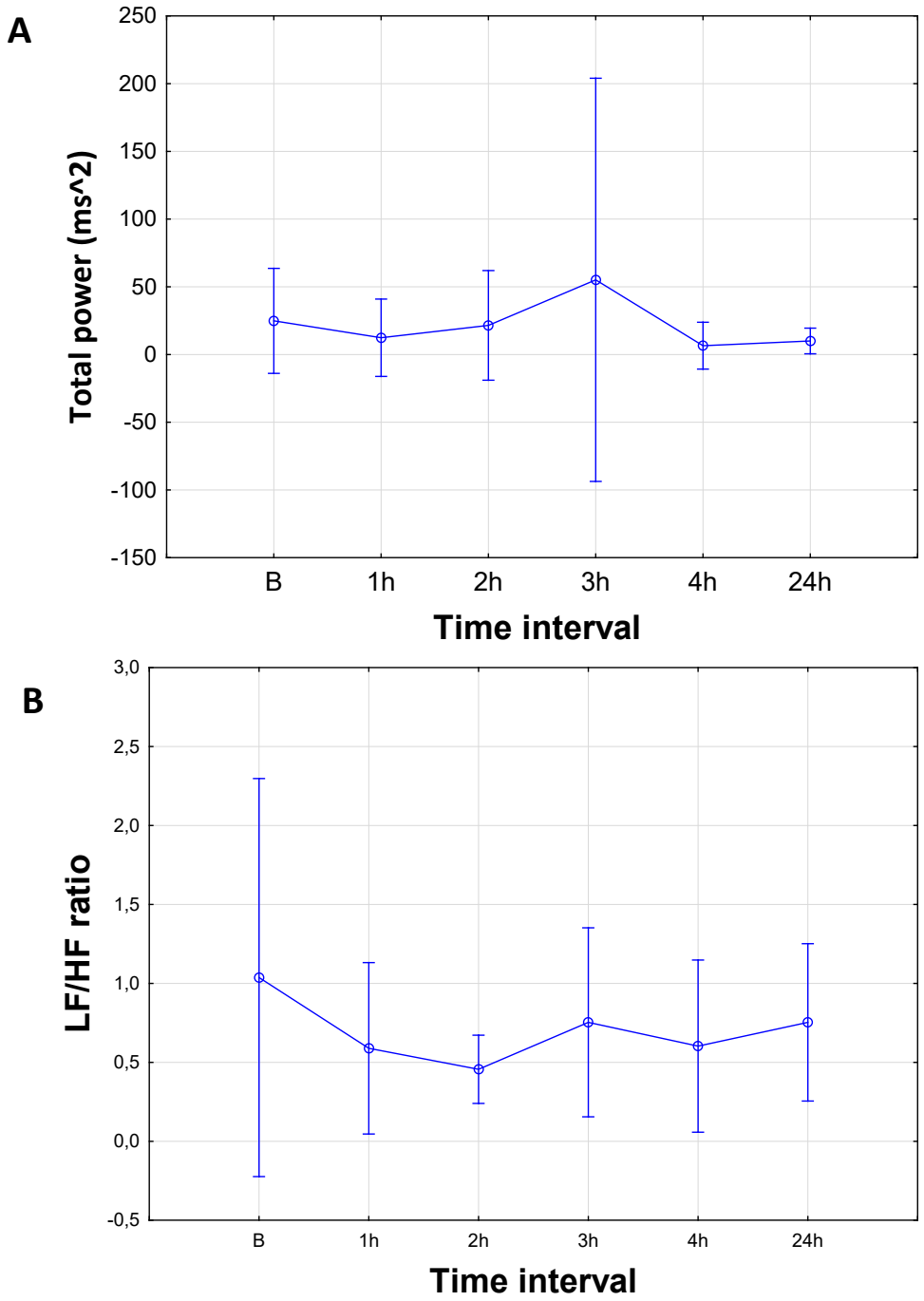

Fig. 4.1.14. Time course of changes in Total power (A) as well as LF/HF ratio measurement.

*Values are means ± SE, *p<0.05, **p<0.01, ***p<0.001 vs B; #p<0.05 vs. 24h. For details see Fig. 4.1.7*

Nonlinear HRV features

Fractal dimension was significantly increased in 1h ($p<0.05$), 2h ($p<0.01$), 3h ($p<0.01$) and 4h ($p<0.001$) upon isoprenaline administration compared to baseline values. Fractal dimension values were significantly higher in 3h and 4h compared to 24h upon isoprenaline administration ($p<0.05$). On the other hand, there was no significant difference in fractal dimension measured in baseline condition and 24h upon isoprenaline administration (Fig. 4.1.15)

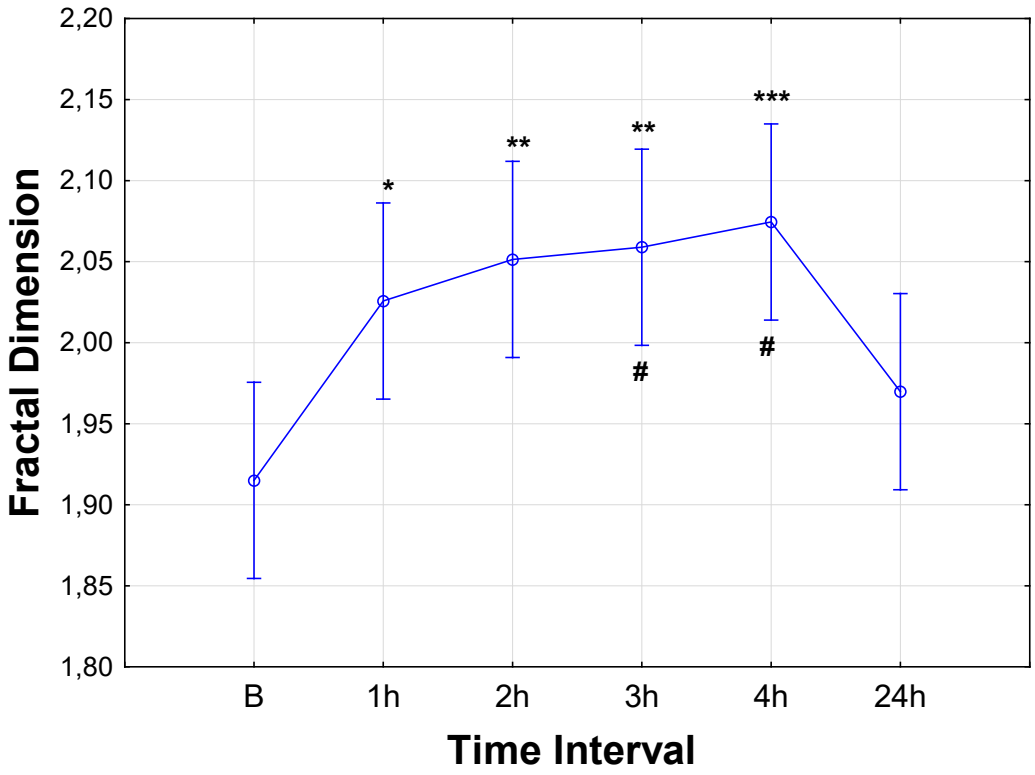

Fig. 4.1.15. Time course of Fractal Dimension measurement.
*Values are means ± SE, *p<0.05, **p<0.01, ***p<0.001 vs B; #p<0.05 vs. 24h. For details see Fig. 4.1.7*

Entropy as measured by the algorithm used in BIOS analyzer was significantly decreased in 1h ($p<0.001$), 2h ($p<0.001$), 3h ($p<0.001$) and 4h ($p<0.001$) upon isoprenaline administration compared to baseline values. Entropy values were significantly lower in 1h ($p<0.05$), 2h ($p<0.01$), 3h ($p<0.01$) and 4h ($p<0.01$) compared to 24h upon isoprenaline administration ($p<0.05$). On the other hand, there was no significant difference in entropy measured in baseline condition and 24h upon isoprenaline administration (Fig. 4.1.16 A). The same time course was observed in entropy bins measurement (Fig 4.1.16 B)

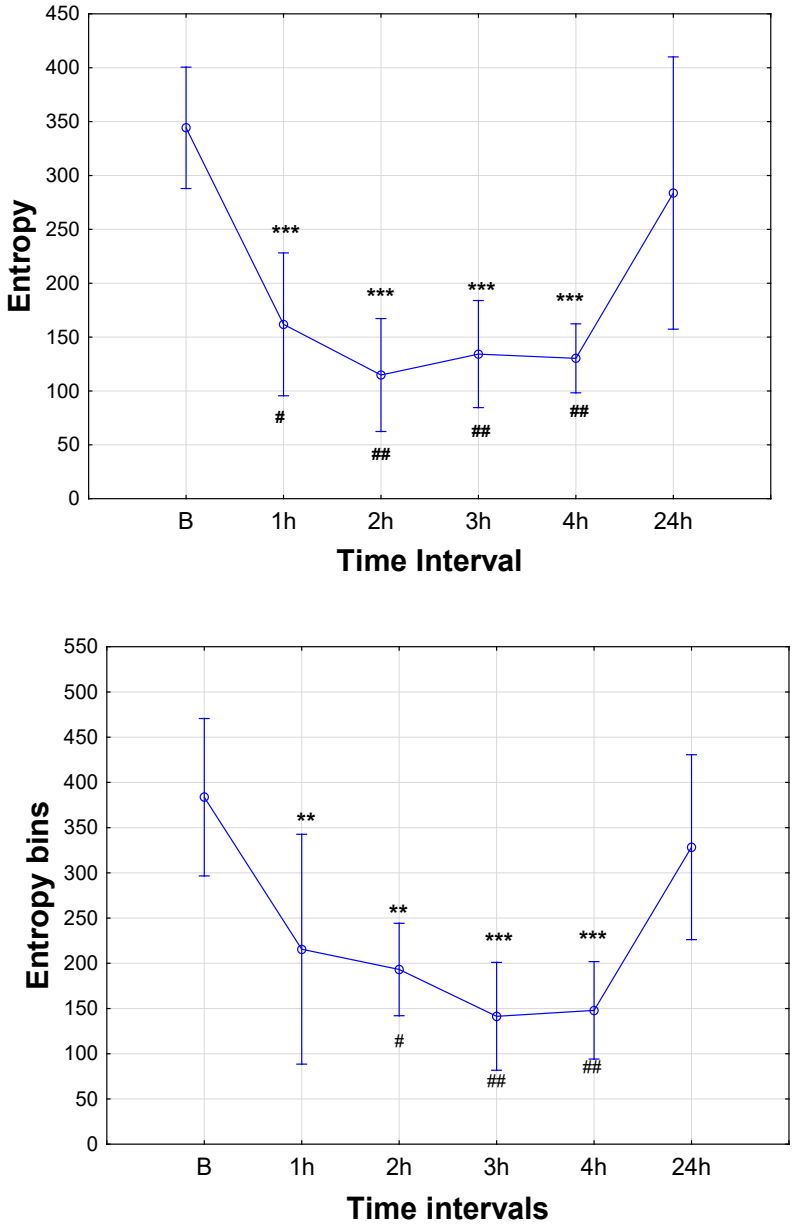

Fig. 4.1.16. Time course of changes in entropy measurement.
Values are means ± SE, *p<0.05, **p<0.01, ***p<0.001 vs B; #p<0.05 vs. 24h. For details see Fig. 4.1.7

The two entropy measures calculated by Kubios software are approximate entropy and sample entropy. Approximate entropy was decreased in 1-4h upon isoprenaline administration compared to baseline values, but the differences failed to achieve statistical significance (Fig. 4.1.17 A). On the other hand, sample entropy values were significantly lower in 1h ($p<0.05$), 2h ($p<0.001$), 3h ($p<0.001$) and 4h ($p<0.001$) compared to baseline and there was no significant difference in entropy measured in baseline condition and 24h upon isoprenaline administration (Fig. 4.1.17 B)

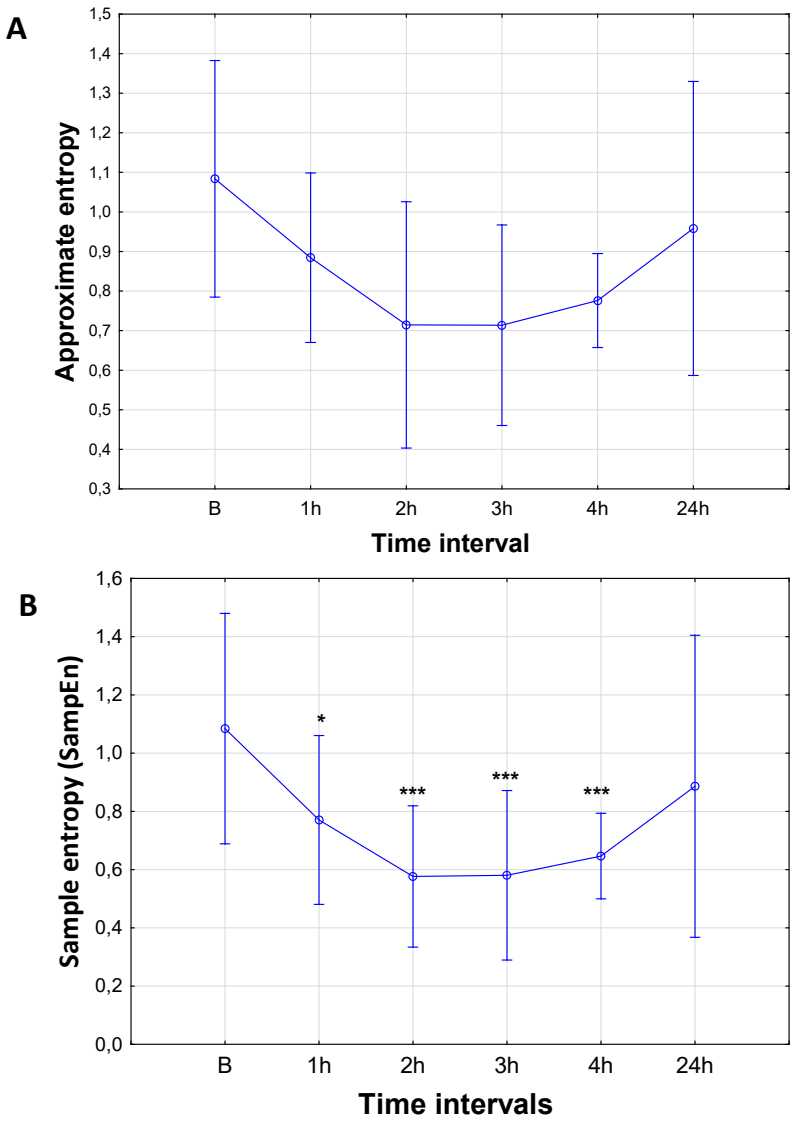

Fig. 4.1.17. Time course of changes in sample entropy (A), and approximate entropy (B) measurements.

*Values are means ± SE, *p<0.05, **p<0.01, ***p<0.001 vs B; #p<0.05 vs. 24h. For details see Fig. 4.1.7*

Serial isometry was significantly increased in 2h ($p<0.05$), 3h ($p<0.05$) and even more signifcantly in the 4h ($p<0.001$ upon isoprenaline administration compared to baseline values and compared to 24h upon isoprenaline administration. On the other hand, there was no significant difference in isometry measured in baseline condition and 24h upon isoprenaline administration (Fig. 4.1.18 A). Shuffled consecutive isometry showed the opposite pattern being significantly decreased in 1h ($p<0.01$), 2h ($p<0.001$), 3h ($p<0.01$) and 4h ($p<0.001$) upon isoprenaline administration compared to baseline values and compared to 24h upon isoprenaline administration (Fig. 4.1.18 B). A similar pattern is present in shuffled isometry where there is statistically significant decrease only in 1h ($p<0.05$) and 2h ($p<0.05$) which disappears afterwards in the 3h and 4h as well 24 hours after isoprenaline administration (Fig. 4.1.18 C).

Radial Isometry was significantly increased in 1h ($p<0.05$) and even more so in 2h ($p<0.01$), 3h ($p<0.001$) and 4h ($p<0.001$) upon isoprenaline administration compared to baseline values and compared to 24h upon isoprenaline administration. On the other hand, there was no significant difference in isometry measured in baseline condition and 24h upon isoprenaline administration (Fig 4.1.19 C). Radial consecutive isometry exibits the same pattern as Radial isometry but gains statistical significance only in the 3h ($p<0.05$) and 4h ($p<0.01$) hour upon isoprenaline administration with no significant decrease after 24h compared to baseline (Fig. 4.1.19 B). Isometry radius shows an opposite pattern being significantly decreased in the 1h ($p<0.001$), 2h ($p<0.001$), 3h ($p<0.001$) and 4h ($p<0.001$) upon isoprenaline administration (Fig. 4.1.19 A).

Series Isometry was significantly increased in 3h ($p<0.001$) and 4h ($p<0.01$) upon isoprenaline administration compared to baseline values and compared to 24h upon isoprenaline administration (Fig. 4.1.20 A). Series consecutive isometry was also significantly increased only in the 3h ($p<0.05$) and 4h ($p<0.05$) (Fig. 4.1.20 B). In both cases there was no significant difference in series isometry measured in baseline condition and 24h upon isoprenaline administration (Fig. 4.1.20 A-B)

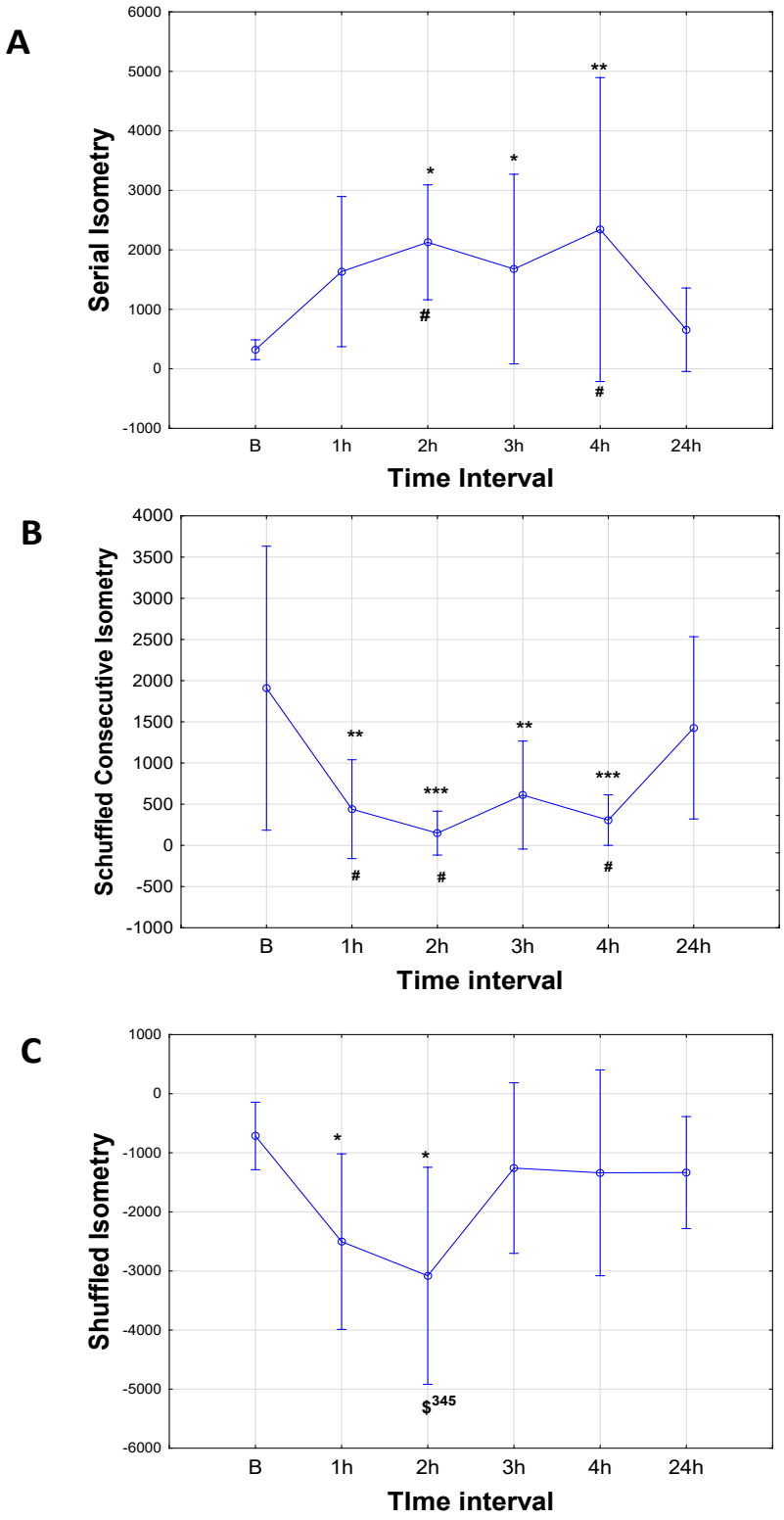

Fig. 4.1.18. Time course of changes in Serial Isometry (A), Consecutive Isometry (B) and Shuffled Isometry (C) measurements.

*Values are means ± SE, *p<0.05, **p<0.01, ***p<0.001 vs B; #p<0.05 vs. 24h. For details see Fig. 4.1.7*

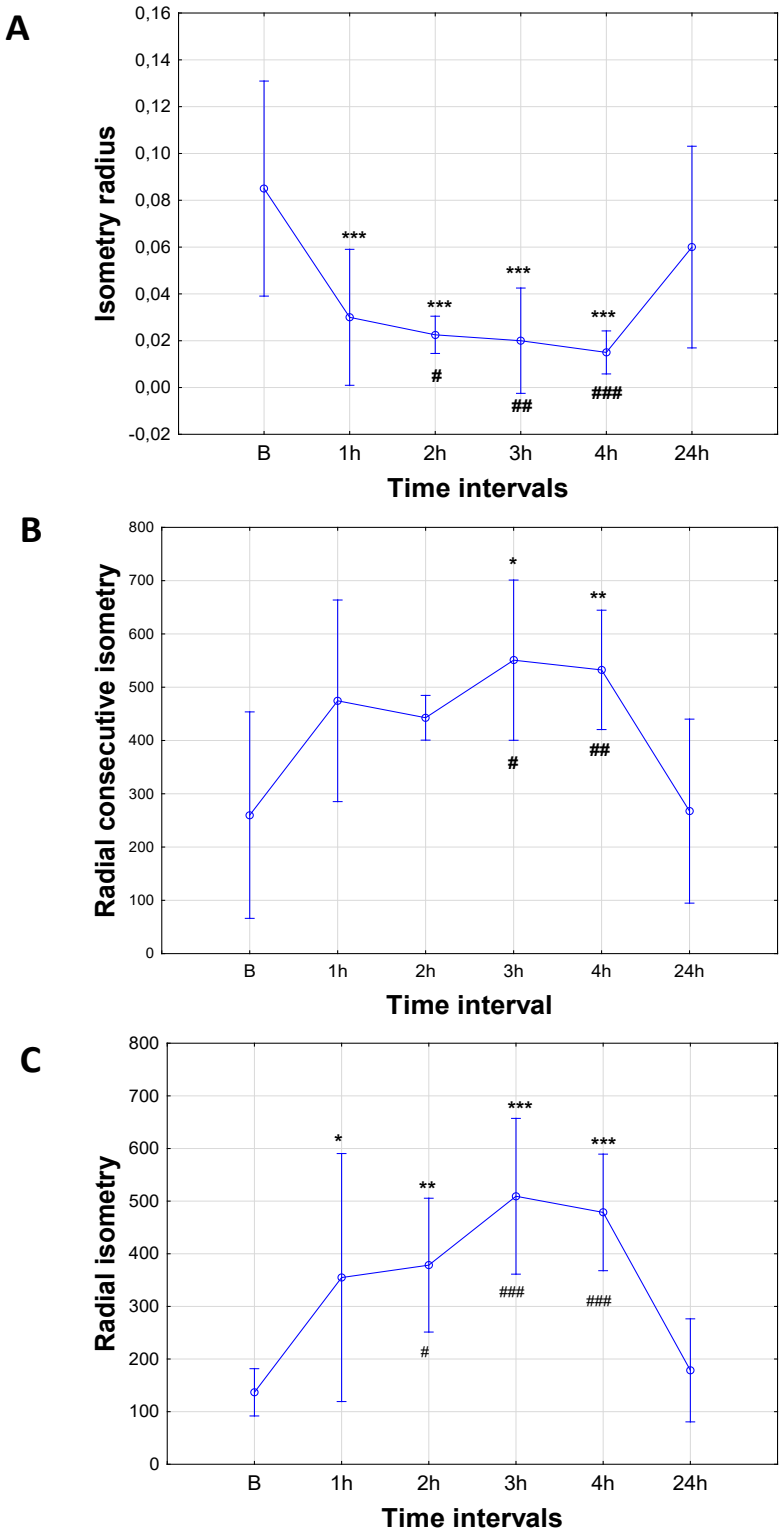

Fig. 4.1.19. Time course of changes in Isometry radius (A), Radial consecutive Isometry (B) and Radial isometry measurements

*Values are means ± SE, *p<0.05, **p<0.01, ***p<0.001 vs B; #p<0.05 vs. 24h. For details see Fig. 4.1.7*

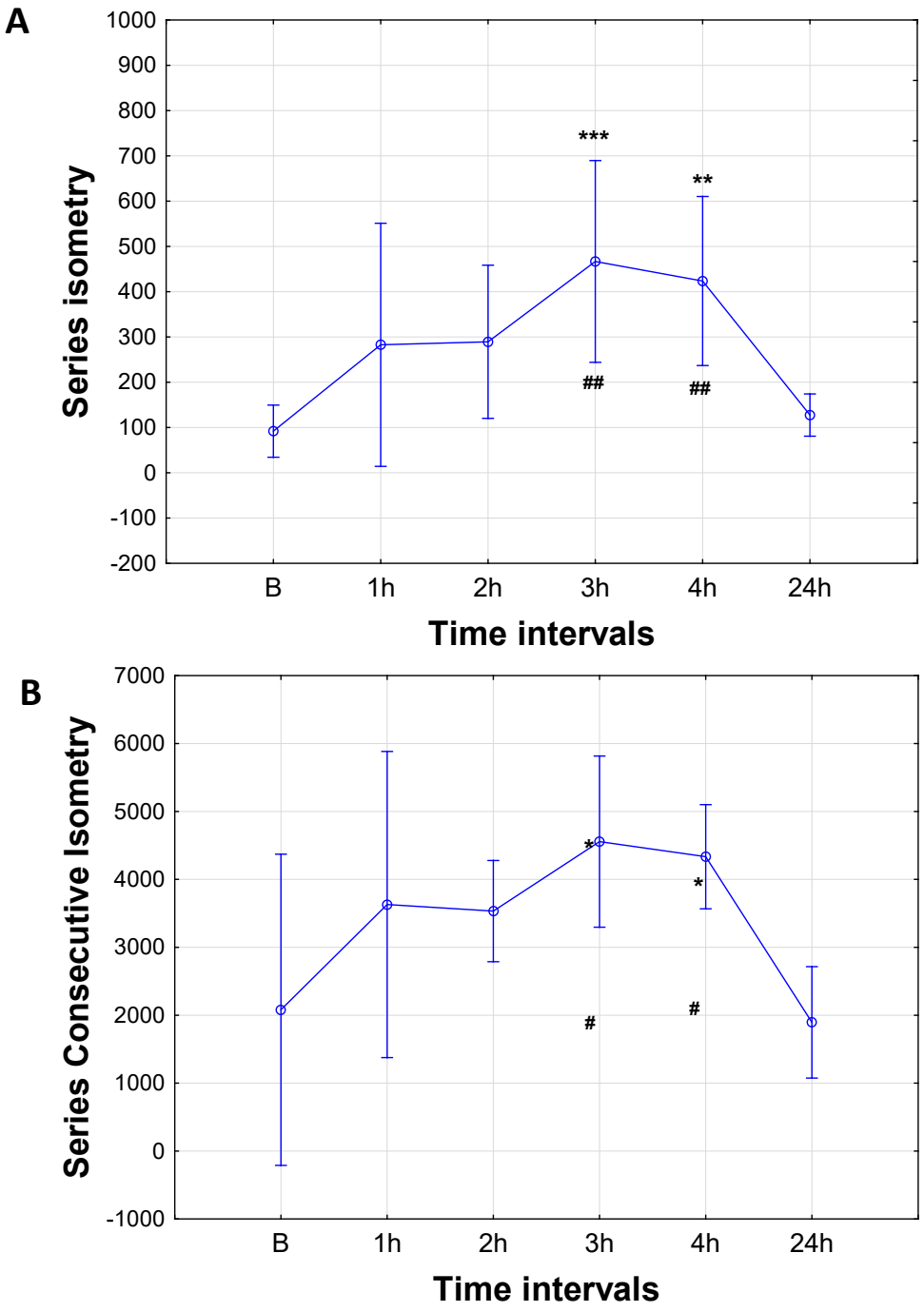

Fig. 4.1.20 Time course of changes in Series Isometry (A), and Series consecutive isometry (B) measurements.

*Values are means ± SE, *p<0.05, **p<0.01, ***p<0.001 vs B; #p<0.05 vs. 24h. For details see Fig. 4.1.7*

Series local diversification was significantly decreased in the 3h ($p<0.05$) and 4h ($p<0.05$) upon isoprenaline administration compared to baseline values and compared to 24h upon isoprenaline administration (Fig. 4.1.21 A). Shuffled local diversification was also significantly decreased in the 3h ($p<0.01$) and 4h ($p<0.01$) but also in the 2h ($p<0.05$) compared to baseline values and to 24h upon isoprenaline administration (Fig. 4.1.21 B) In both cases there was no significant difference measured in baseline condition and 24h upon isoprenaline administration (Fig. 4.1.21 A-B)

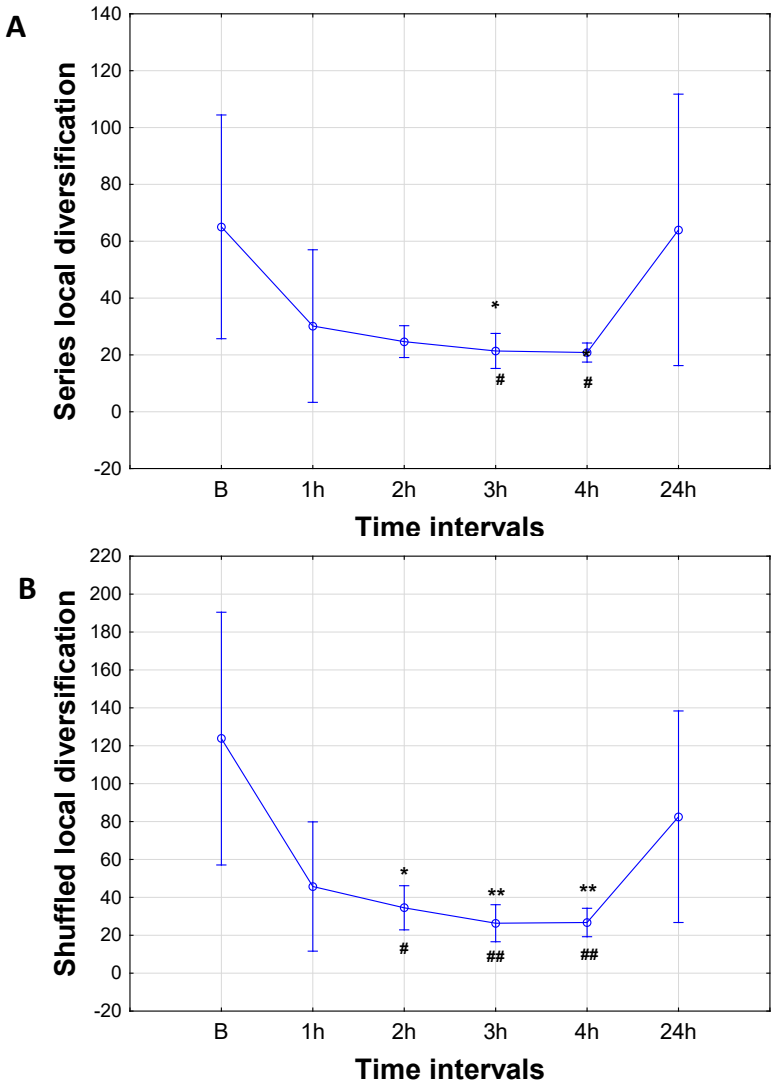

Fig. 4.1.21 Time course of changes in Series local diversification (A), and Shuffled local diversification (B) measurements.

Values are means ± SE, *p<0.05, **p<0.01, ***p<0.001 vs B; #p<0.05 vs. 24h. For details see Fig. 4.1.7

The novelty showed a significant decrease in 2h ($p<0.05$), 3h ($p<0.01$) and 4h ($p<0.05$) upon isoprenaline administration compared to baseline values and compared to 24h upon isoprenaline administration (Fig. 4.1.22 A). The Arrangement showed a highly significant decrease in all hours after isoprenaline administration: 1h ($p<0.001$), 2h($p<0.001$), 3h ($p<0.001$) and 4h ($p<0.001$) (Fig. 4.1.22 B) In both cases, there was no significant difference measured in baseline condition and 24h upon isoprenaline administration (Fig. 4.1.22 A-B)

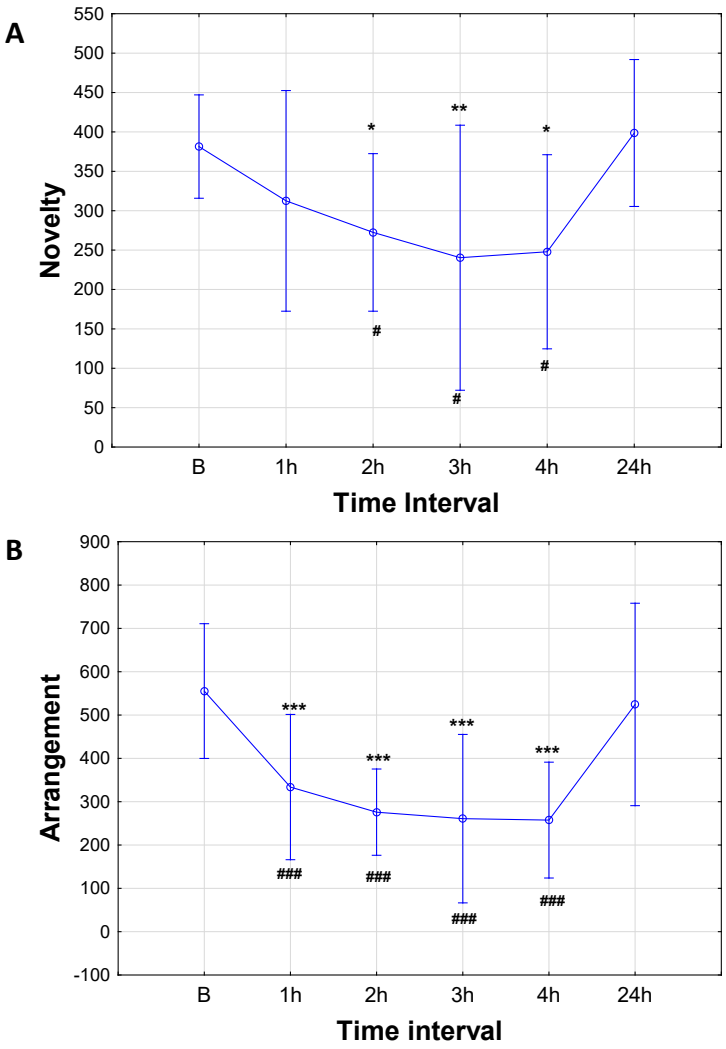

Fig. 4.1.22. Time course of changes in Novelty (A) and Arrangement (B) measurements

*Values are means ± SE, *p<0.05, **p<0.01, ***p<0.001 vs B; #p<0.05 vs. 24h. For details see Fig. 4.1.7*

Poincare plots (SD1 and SD2) measure of the ECG RR intervals showed no statistically significant change in any of the time points upon isoprenaline administration and there was no significant difference measured between baseline condition and 24h upon isoprenaline administration (Fig. 4.1.23 A and B). The SD2/SD1 ratio showed no statistically significant changes as well (4.1.23 C).

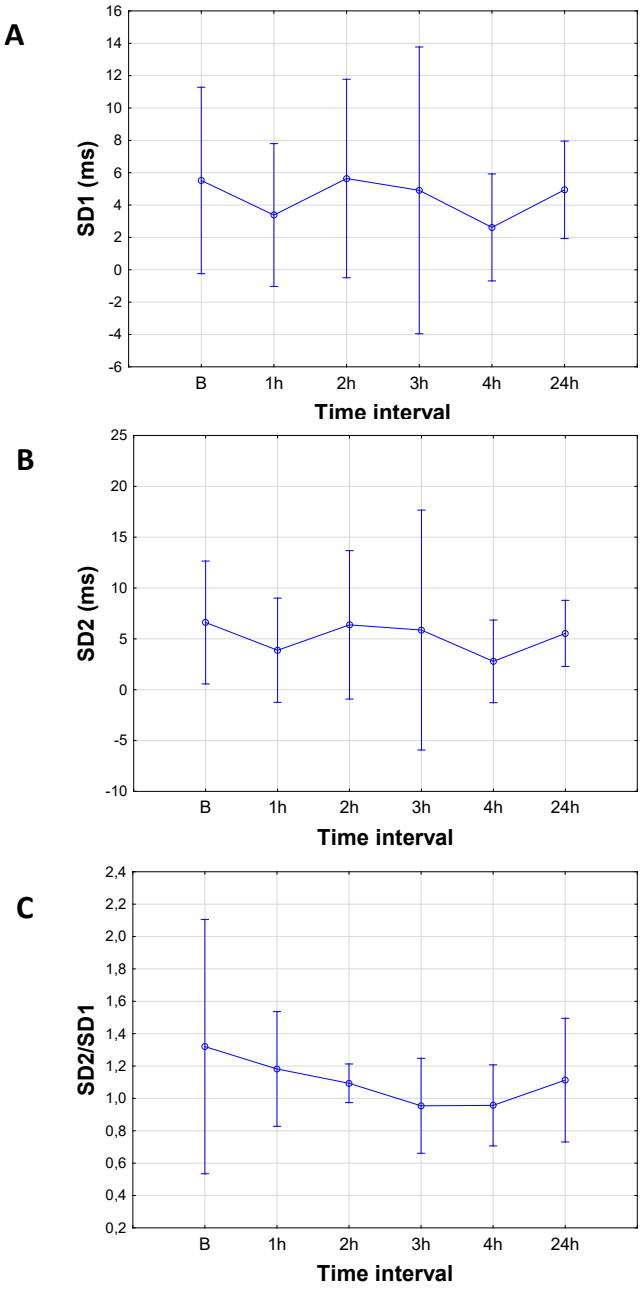

Fig. 4.1.23 Time course of changes in Poincare plot parameters SD1 (A), SD2 (B) and SD2/SD1 measurements.

*Values are means ± SE, *p<0.05, **p<0.01, ***p<0.001 vs B; #p<0.05 vs. 24h. For details see Fig. 4.1.7*

Alpha 1 measure of DFA was decreased in 1-4h upon isoprenaline administration compared to baseline values, but the difference failed to achieve statistical significance (Fig. 4.1.24 A). On the other hand, alpha 2 values were significantly lower in 2h ($p<0.001$), 3h ($p<0.001$), and 4h ($p<0.05$) compared to baseline. (Fig. 4.1.24 B). There was no significant difference in alpha 1 or alpha 2 measured in baseline condition and 24h upon isoprenaline administration (Fig. 4.1.24 A and B).

There were no statistically significant differences in time course of any of the examined linear and nonlinear ECG-derived HRV parameters in the control group upon saline administration.

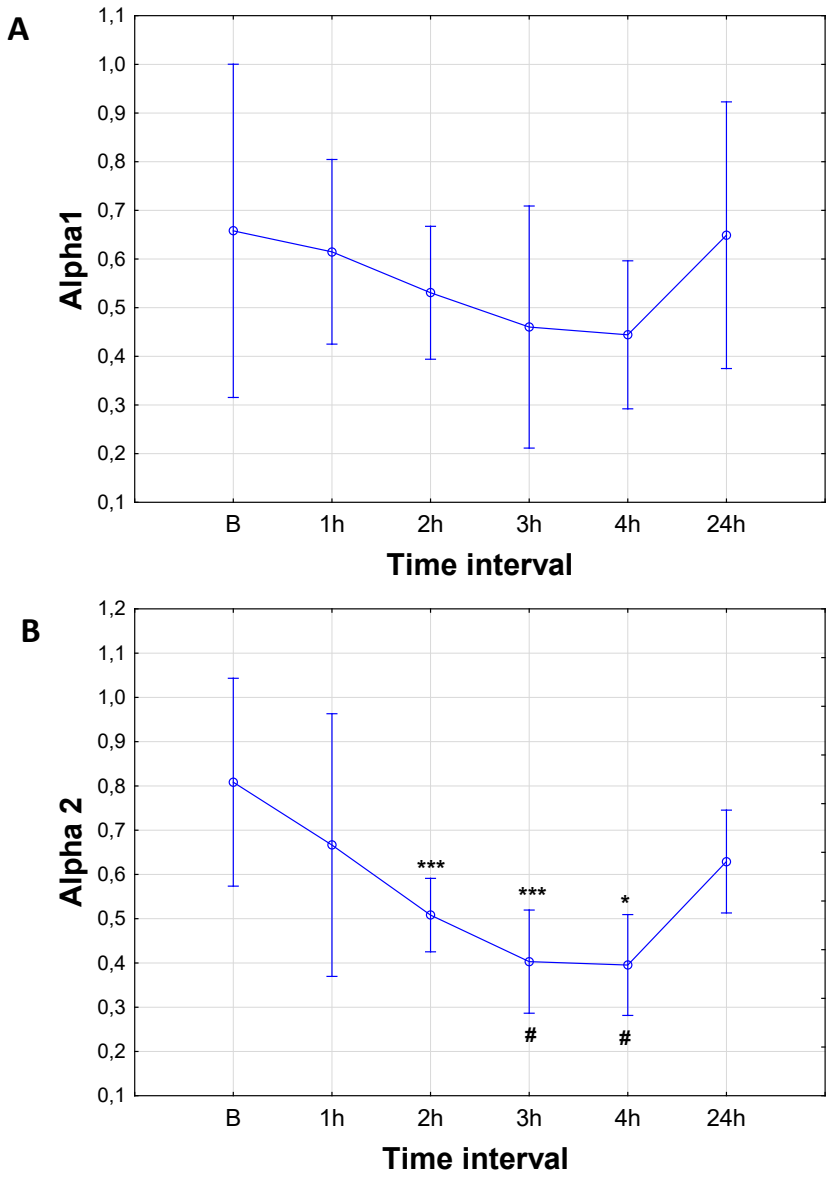

Fig. 4.1.24 Time course of changes in Detrended fluctuation analysis (DFA) alpha 1 (A) and alpha 2 (B) measurements

*Values are means ± SE, *p<0.05, **p<0.01, ***p<0.001 vs B; #p<0.05 vs. 24h. For details see Fig. 4.1.7*

4.2. Lindane induced epilepsy model

The control (saline administered) group exhibited no behavioral changes. In the experimental group, all rats developed grand mal tonic clonic seizures 30 minutes after Lindane administration with characteristic EEG spike wave complexes (as seen in Fig 4.2.1). Mean duration of an ictal period was 7.34 ± 1.56 s, while the peak frequency was 5.12 ± 0.18 Hz. Total density of spectral power in these epochs was 6042.41 + 674.42 $\mu V^2/Hz$.

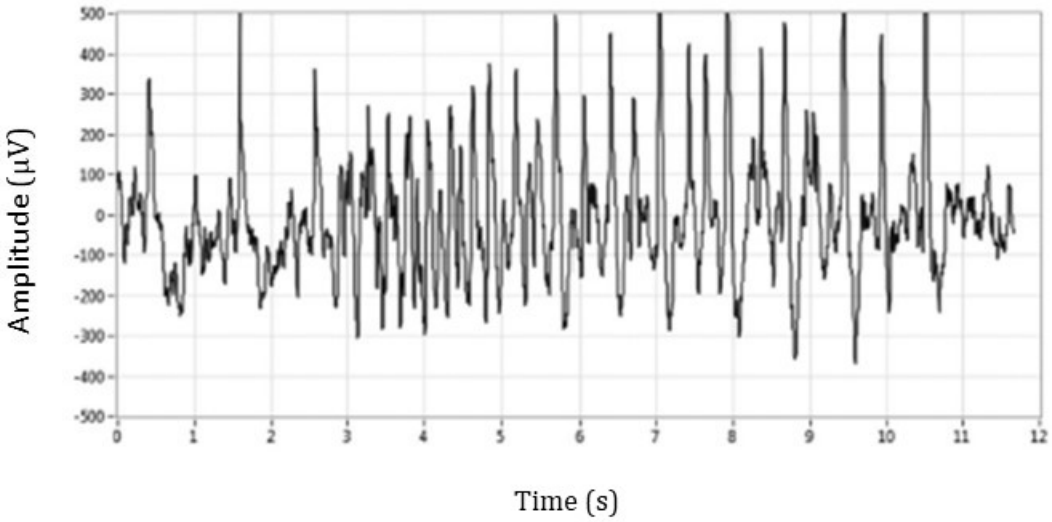

Fig. 4.2.1 Representative ictal EEG

4.2.1 Linear EEG signal characteristics during lindane induced epilepsy model

FFT analysis results show that, theta rhythm dominates during ictal EEG activity. Furthermore, statistical significance was obtained between each of the four standard frequency bands (delta, theta, alpha, beta), compared to all other rhythm pattern, reflecting the significant stratification of EEG activity during the ictal periods (see also statistical report matrix table to Figure 4.2.2).

Statistical significances of variation in PSD were determined by one-way ANOVA followed by Fischer's LSD test and results are presented in statistical matrix table. An amplitude histogram (Figure 4.2.3) was used to represent analysis of the 50 μV-bean intervals between 100 and 500 μV. We can perceive that most of the spikes were in lower amplitude ranges (especially 100-150 μV and 150-200 μV intervals), while 350-400 μV interval and above were infrequently observed. Comparison between individual intervals with statistical analyses is also shown in Table 4.2.1.

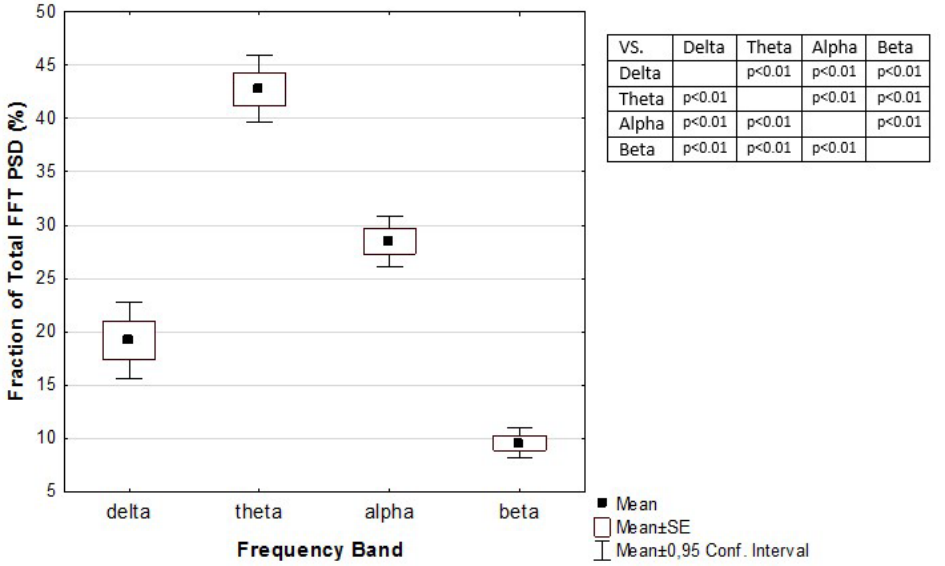

VS.	Delta	Theta	Alpha	Beta
Delta		p<0.01	p<0.01	p<0.01
Theta	p<0.01		p<0.01	p<0.01
Alpha	p<0.01	p<0.01		p<0.01
Beta	p<0.01	p<0.01	p<0.01	

Fig. 4.2.2. Individual frequency band spectral power densities (relative, PSD, %) in ictal periods as a percent of total. ().

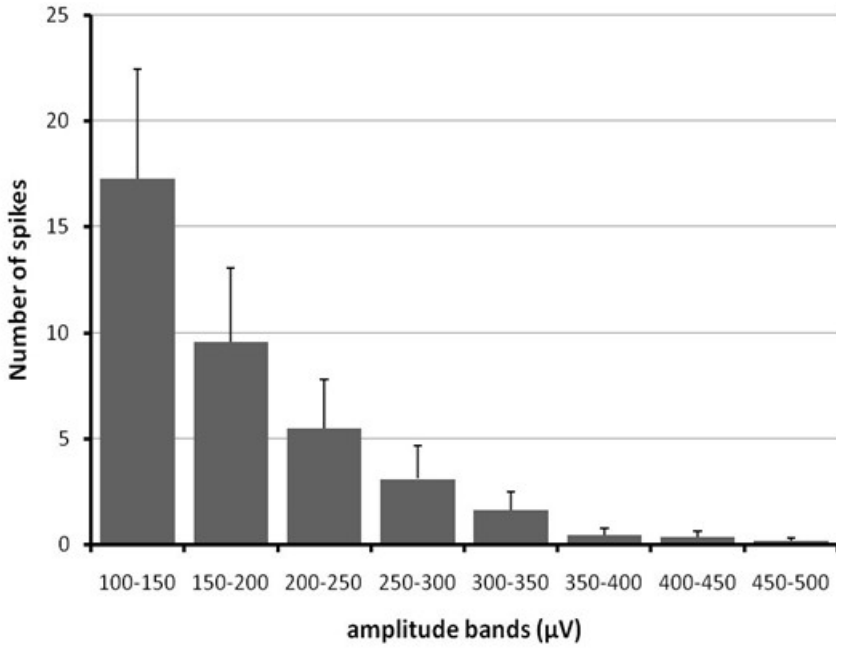

Fig. 4.2.3. Number of spikes in lindane induced ictal periods represented as 50 µV-size amplitude bins. Spikes from the extracted EEG epochs were differentiated in 50 µV-bin intervals using NeuroSciLaBG program Amplitude Histogram Feature Function. Only spikes of voltage 100 µV and higher were analyzed.

Table 4.2.1 Statistical analysis and comparison of individual intervals illustrated in Fig 4.4.3.

vs.	100-150 µV	150-200 µV	200-250 µV	250-300 µV	300-350 µV	350-400 µV	400-450 µV	450-500 µV
100-150 µV		p = 0.02	***p = 0.04**	****p < 0.01**	****p < 0.01**	****p < 0.01**	****p < 0.01**	****p < 0.01**
150-200 µV	p = 0.21		p = 0.33	p = 0.09	***p = 0.03**	****p = 0.01**	****p < 0.01**	****p < 0.01**
200-250 µV	***p = 0.04**	p = 0.33		p = 0.4	p = 0.12	***p = 0.03**	***p = 0.03**	***p = 0.03**
250-300 µV	****p < 0.01**	p = 0.09	p = 0.4		p = 0.41	p = 0.1	p = 0.09	p = 0.07
300-350 µV	****p < 0.01**	***p = 0.03**	p = 0.13	p = 0.41		p = 0.19	p = 0.15	p = 0.09
350-400 µV	****p < 0.01**	****p = 0.01**	***p = 0.04**	p = 0.1	p = 0.19		p = 0.85	p = 0.43
400-450 µV	****p < 0.01**	****p < 0.01**	***p = 0.03**	p = 0.09	p = 0.15	p = 0.85		p = 0.51
450-500 µV	****p < 0.01**	****p < 0.01**	***p = 0.03**	p = 0.07	p = 0.09	p = 0.43	p = 0.51	

4.2.2 Seizure recognition using neural networks in lindane induced epilepsy model.

The results of the HRV based seizure prediction algorithm were expressed as NN and LR values of accuracy, precision, sensitivity and specificity. For LR, metrics were as follows: Accuracy was 86.81±8.87%; Precision was 96.3±8.28%, Sensitivity was 94.44± 12.42& and F1-score was 89.42±7.05%. The results of NN values were as follows: Accuracy was 66.3±22.97; Precision was 77.86±17.83; Sensitivity was 69.92±23.79; Specificity was 56.67±36.26; and F1-score was 72.55±19.02. The comparison of HRV-based seizure prediction results using LR and NN are presented in Table 4.2.2

Table 4.2.2. Classification results using NN and LR.

Classifier	Accuracy [%]	Precision [%]	Sensitivity [%]	Specificity [%]	F1-score [%]
LR	86.81±8.87	96.3±8.28	83.95±8.69	94.44±12.42	89.42±7.05
NN	66.3±22.97	77.86±17.83	69.92±23.79	56.67±36.26	72.55±19.02

The results of EEG biotic feature based seizure detection algorithm obtained after neural network training are as follows: during the training there was a total of 4.2% missclasiffied signal segments. For the training set data the eror was 5.2% while for the testing set the error was 5.6% and in the validation set it was 2.8 %. The Confusion matrix constructed is presented in Fig. 4.2.4. The best performance was achieved in the epoch 21. The total performance of the neural network was 92.9%. The neural network performance is represented by Fig 4.2.5.

Fig. 4.2.4 Confusion matrix constructed during neural network training

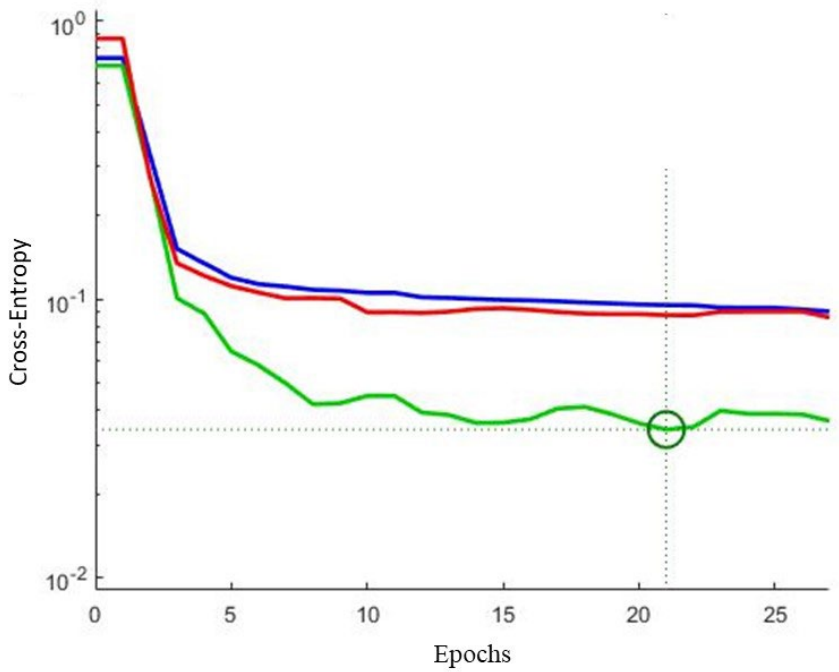

Fig. 4.2.5. Neural network perfomance during training: blue line-training set, green line-validation set, red line- testing set. Black circle represents the epoch with best detection probability.

5. DISCUSSION

We used the Isoprenaline intraperitoneal injection to model myocardial infarction. The onset of myocardial infarction was confirmed by visual analysis of ECG (ST segment elevation). The method used to confirm necrosis of the heart muscle and development of infarction was histopathology with HE staining. The isoprenaline model of acute myocardial infarction is a robust and reproducible model that has excellent construct validity. [Filho L et al 2011].

We recorded cortical EEG signals in the mPFC before and after isoprenaline administration and demonstrated following results: 1) Spectral power in the beta band was significantly increased during the first hour (H1) recording as well as in the second to fourth hours (D1); 2) Spectral power in the theta band was significantly increased during the first hour (H1); 3) Spectral power in the alpha band was significantly increased between the second and fourth recording hours; 4) Spectral power changes in all bands reversed to baseline levels in the recording made after 24 hours.

The medial PFC plays an important role among executive cortical areas in charge of regulating emotion, cognition and executive function [Miller EK, 2006; Miller EK et al 2001 Kane MJ et al 2002; Etkin A et al 2011]. Indeed, studies in rodents have pointed to the medial PFC as a key region for regulation of the stress response as well as development of anxiety states [Padilla-Coreano N et al 2016].

Furthermore, the medial PFC lies at the crux of neural pathways involved in visceral function regulation and has even earned the moniker "visceral motor cortex" [Neafsey EJ, 1990]. Detailed studies involving lesioning/stimulating of sub regions in the medial PFC have gone far in working out the finer points in autonomic regulation evoked from this region: both cardiovascular (arterial pressure and heart rate) and metabolic rate as well as respiratory frequency (aka phrenic nerve discharge frequency) are areas significantly affected by medial PFC manipulation. The aforementioned studies go far in positioning the medial PFC as an integrative “command” center connecting affective and emotional states with autonomic control and executive functions [Owens NC & Verberne AJ, 2001: Resstel LB & Correa FM, 2006: Hassan SF et al 2013].

Epidemiological studies have further shown that even a mild decrease in cardiac output can lead to deterioration of executive functions and that atherosclerosis, atrial fibrillation and heart failure worsen the risk profile of patients for development of dementia [Ritz K et al, 2013: Jefferson AL et al, 2013].

Given the tentative position of the medial PFC at the core of multiple physiological control systems presented in aforementioned studies we posit that the spectral power changes shown in our study might further elucidate the influence medial PFC function has at least when it comes to the heart-brain axis.

During states of arousal, higher frequency activity, such as beta frequency, dominates the EEG spectrum [Foster PS & Harrisson DW, 2001; Vazquez Marrufo M et al, 2002]. Furthermore, increases in beta power are also perceived in states of impaired emotional control and increased anxiety [Adhikari A et al 2017; Li H et al 2017]. It was shown that behavioral patterns akin to anxiety with a heightened stress response can be elicited in a model of AMI and that pathohistological studies show structural remodeling of neuronal networks in the medial PFC in a rodent model of induced stress [Banozic A et al, 2014]. When it comes to structural effects, histopathological studies of medial PFC have demonstrated remodeling of cortical networks affected by stress [Holmes A & Wellman CL, 2009].

Our results show that there is an increase in beta band power during the first hour (H1) that extended during the entire four hours (D1) after isoprenaline administration. Taking into account the demonstrated correlations between behavioral changes (anxiety and stress response), AMI and structural changes in medial PFC innervation, we can hypothesize that the increase in beta frequency power detected in our study could be the signature of psychological and behavioral effects of necrosis/pain that occurs during AMI.

Several studies in rodents have focused on pain related EEG changes. For example, it was shown that acute neuropathic and inflammatory forms of pain have a significant effect on PFC EEG signal [LeBlanc BW et al, 2016]. In fact, an increase in EEG spectral power was noted over the PFC in all forms of pain studied [LeBlanc BW et al, 2014] while, acute somatosensory pain led to an increase in theta band EEG power. There is also a report of a significant increase in PFC theta band power on a rat model of chronic neuropathic pain where the rats were also exposed to anxiogenic stimuli [Sang K et al, 2018]. Importantly cardiac pain, such as occurs during AMI is a form of acute visceral pain known to produce high levels of anxiety.

While there is a significant number of studies implicating visceral pain in causing anxiety states [Finn DP, Leonard BE, 2015] The EEG signal changes caused by visceral pain remain underexplored. The increase of theta band power we recorded could thus be the electroencephalographic representation of pain perception and anxiety whose development has already been demonstrated in AMI. This explanation is further supported by the existence of heart afferents creating the structural connection to the PFC and providing the pathway to facilitate EEG changes in theta band power as well as other EEG power spectrum changes observed. Thus, our results may imply a connection between EEG spectral changes and the perception of visceral pain, and together with increased beta power, increased anxiety occurring during isoprenaline induced AMI.

Increases in cortical alpha power were correlated in previous studies with cognitive effort as well as mental states of focused internal attention [Benedek M et al, 2014]. Basic (attention, memory) as well as more complex cognitive functions (divergent and convergent and thinking) have been associated with heightened alpha activity [Klimesch W, 2012; Fink A, Benedek M, 2013; Benedek M et al, 2011]. The D1 period was marked by an increase of alpha band power that may represent cognitive activation and higher levels of focus. We can hypothesize that neural signaling from intrinsic myocardial afferents stimulated by necrosis during isoprenaline-induced AMI is leading to an increase in focused attention- an advantageous state for mounting a response to imminent danger.

The changes in power spectrum we observed also correlate with peak ST- segment elevation. Necrosis associated with AMI leads to loss of cell membrane function in the ischemic myocardium that creates a potential difference between the ischemic and non-ischemic myocardial segments. This process is represented by ST elevation in the ECG. [Etkin A et al, 2011].

Because of its correlation to the degree of myocardial necrosis, magnitude of ST elevation is used as a marker for the extent of myocardial infarction [Kane MJ & Engle RW 2002]. We posit that there are two main mechanisms that can possibly account for the correlation of ST segment elevation amplitude and spectral power changes we observed: neural and humoral mechanisms. Neural mechanisms are the favored mechanism due to the velocity of EEG power spectrum changes we observed following ischemia onset but humoral factors cannot be excluded.

An important consideration lies in the knowledge that afferent inputs from cardiac neural circuits have been known to modulate CNS functions even under physiologic conditions

[Armour JA; 2008]. When physiologic and especially pathologic stimuli arise in the myocardium weather in the form of hormonal or mechanical stimuli, the information is transformed into nerve impulses. This takes place within sensory neurons of the heart [McCraty R, 2011] Information is further transported to the mPFC via the vagus nerve and dorsal columns [Siddiqui MA et al, 2016].

Thus the correlation of ST elevation with EEG changes found in our study can be explained by the connection of myocardial infarction size with ST elevation magnitude as well as the number of myocardial sensory neurons involved in afferent signaling. The anatomical connections described constitute a possible direct heart-brain axis neural link potentially explaining the EEG changes we observed.

In our study we observed an increase in Mean HR after isoprenaline administration as compared to the baseline with a concomitant decrease in mean RR interval length (these parameters are inversely correlated). An increase in Max HR was also noted albeit not with the same robustness. The statistical time domain parameters: standard deviation of RR intervals, standard deviation of HR, root mean square of the successive difference in RR intervals, RR triangular index and NNx50and pNN50 showed no significant changes.

Therefore, our results demonstrate that Isoprenaline administration has significant effects on heart rate that begins immediately after administration, extends at least four hours after administration, and subsides in the measurement after 24 hours. The instantaneous effect we observed is in line with previous studies into isoprenaline effects on heart beta receptors [Overgaard & Dzavík 2008; Ali A et al., 2020]. On the other hand, as Isoprenaline metabolism is very fast, practically instantaneous, and the effects on heart rate we observed have extended through the fourth hour after isoprenaline administration we can conclude that the effects on heart rate increase we observed cannot be explained only by direct effects of Isoprenaline. The extended tachycardia is rather, more probably, explained by AMI development.

There was no significant change in distribution of VLFH, LFH or HF before and after isoprenaline administration. Additionally, total power and LF/HF ratio were also not significantly different before and after isoprenaline administration. Taking into account the high correlation between RMSSD, pNN50and HF changes it makes sense that statistical time domain and frequency domain parameters concomitantly demonstrate lack of significance in our study [Shaffer and Ginsberg 2017]. This finding is unusual in that Isoprenaline being a sympathomimetic and AMI being a state of increased sympathetic stimulation we would expect a lowering in HF and increase in LF/HF ratio as well as lowering of RMSSD.

Fractal dimension showed a robust statistically significant increase compared to baseline in all four hours after isoprenaline administration with a tendency of rising significance and level during hours 1-4 and reverting to baseline after 24 hours. Previously, studies have posited that fractal dimension may be positively correlated with parasympathetic activity, represented by correlation with the classic HRV parameters such as HF and RMSSD [Butler GC et al., 1994]. Newer studies have reported that patients with chronic heart failure have increased FD during the day as well as in nighttime [Beckers F et al., 2006].

Entropy, on the other hand, has shown a decisive and statistically highly significant decrease after isoprenaline administration that also spans the entire four-hour interval and reverts to normal after 24h. Entropy is essentially a measure of irregularity within the signal, and our results would imply an increase in signal regularity post isoprenaline administration. When it comes to biological signal it has been postulated that increased regularity is a sign of pathology [Henriques T et al., 2020]. Indeed, it was shown that HRV entropy decreases in

various pathologic states such as chronic obstructive disease (COPD), sleep apnea, and coronary artery disease [Jin Y et al., 2017; Liang X et al., 2021; Acharya UR et al., 2018].

Biotic parameters are designed to be analyzed in their totality in order to give precise insight in to the nature of a signal. Here, we will summarize our and offer our interpretation. Isometry parameters showed a statistically significant decrease in shuffled consecutive as well as shuffled isometry with an increase in series isometry. Furthermore, isometry radius was increased while radial isometry and radial consecutive isometry were statistically significantly decreased. Diversification and shuffled diversification were both statistically significantly decreased as were novelty and arrangement, with arrangement exhibiting a higher level of significance. Bios was developed as a method of measuring and describing system complexity. The first signals that bios was developed and used on were ECG HRV time series [Sabelli & Lawandow 2010]. It was further shown that physiologic biological signals exhibit a high level of nonrandom complexity, diversification and autocorrelation as a result of bipolar feedback. Also, one of the hallmarks of pathological states is loss or suppression of these inherent biological signal characteristics [Sabelli H et al., 2011]. It has been shown that pathologic states such as psychosis and depression are marked by less diversification, less novelty and more consecutive isometry. Although AMI represents a much different pathology, the results of biotic parameters in our study are in line with previous findings in other pathological states and show promise as a possible avenue of further research in heart disease.

Poincare plot parameters, both in SD1, SD2 as well as SD1/SD2 showed no statistically significant changes after isoprenaline administration compared to baseline as well as after 24 hours. Previous studies have shown a connection between Poincare plot parameters and autonomic regulation especially when it comes to sympathetic nervous system cardiac control [Naranjo Orellana J et al., 2015; Toichi M et al., 1997; Tulppo MP et al., 1996]. In fact, different Poincare parameters have been associated with different autonomic control aspects: SD1 as a measure parasympathetic activity and SD2 with SD1/SD2 as a proxy of sympathetic activity [Kamen PW et al., 1996; Tulppo MP et al., 1996]. Since significant correlations were also found between Poincare plot parameters and time and frequency domain parameters especially RMSSD [Carrasco S et al., 2001; Guzik P et al., 2007; Hoshi RA et al., 2013] our findings are consistent in that neither parameter shows statistically significant differences.

Detrended fluctuation analysis showed a decline in both alpha 1 and alpha 2 parameters after isoprenaline administration compared to baseline with only alpha 2 reaching statistical significance. The effects in alpha 1 reverted to baseline after 24h while the alpha 2 parameter remained depressed albeit not significantly. Detrended fluctuation analysis alpha 1 represents aspects of beat-to-beat fractal correlation over short time frames while alpha 2 represents the same correlation properties over longer time frames although there is naturally cross reference between the two [Peng CK et al., 1995]. DFA has shown superior predictive power to traditional HRV parameters in many cardiovascular pathologies [Ho YL et al., 2011, Tsai CH et al 2020]. Furthermore, it was reported that alpha 2 is significantly decreased after inferior myocardial infarction which is in line with our results but the depressed alpha 2 was also present during long term follow up. [Tang SY et al., 2023].

Considering that increased spectral energy correlates with increased spectral density, spectral density values could provide significant information in to severity and extent of pathological brain functioning, the mechanistic basis of epileptic activity. Major drawback of FFT in this respect is a lack of time resolution.

Although FFT provides important detail about signal frequencies, the inability to precisely determine the moment when a specific series occurs in the EEG, emphasizes the need to complete other quantitative analysis algorithms. FFT analysis relies on the assumption of

signal stationarity whereas biological signals such as the EEG, are inherently non-stationary. Nevertheless, as many linear analysis methods have the same problem this is most commonly overcome via study design.

Importantly, FFT is described as a bidirectional analysis. Bidirectionality is a term denoting the ability to restore the original signal ideally with no loss of data during the process. Further, the mean duration of ictal epoch we used was of 7.34 ± 1.56 s which helps alleviate the problem of temporal resolution sufficiently to enable the application of FFT, which previous research has confirmed (Stam CJ, 2005; Campbell, 2009).

Our results show that there was significant slowing of EEG signal frequency spectrum during ictal periods. This led to an increase of power in theta and delta band spectrums compared to alpha and beta waves. FFT derived spectral densities calculated showed that theta band was the dominant frequency while beta frequency was least represented.

There have previously been three distinct patterns of ictal EEG spectral signatures reported: 1) high frequency waves arising before clinically apparent ictal behavior, 2) low frequency wave activity and 3) desynchronized of electrical discharges Honda R et al 2015). This representation is in line with our results, which show a significant increase in low frequency waves during ictal periods.

Delta waves on the other hand, are usually understood to be a manifestation of neural plasticity and NREM sleep –related memory consolidation [Tononi G, 2012; Assenza G, 2015]. Brain plasticity is often pronounced during and after structural brain damage. Delta wave activity is both correlated to the size of the organic lesion, as well as the recovery chances [Assenza G et al 2009; Finnigan SP et al 2015]. Delta wave spectral power shown by the FFT in this study could be a predictor of epileptic activity in terms of it extent and severity, although more research is needed to derive definitive conclusions.

Theta waves in the human brain are normally found in two locations: the hippocampus (known as hippocampal oscillatory rhythm), and the cortex (known as cortical theta rhythm). Theta wave function is not completely explored. However, it is usually elaborated as important player in arousal (Green JD et al, 1954) and memory creation (Greenberg JA et al 2015). As the latter study shows, the single most consistent alteration during memory formation is drop in theta power. As theta waves were consistently the dominant fraction for the majority, if not all of the ictal periods analyzed in our study, it can be argued that the rise in spectral power of theta waves is an EEG signature of impairment in consciousness. This impairment is correlated with a degree of amnesia regarding the seizure itself, as is generally known with patients suffering from seizures.

Relatively lower power in high-frequency part of the spectrum can be a contributing aspect in the development of memory associated problems (Scholz S et al 2017). Studies that focus on spectral power in EEG, as well as individual frequency density bands are also a part of Azheimer's disease and generalized anxiety disorder research (Dadashi M et al 2015; Wang R et al 2015).

Alzheimer's disease research has showed an amplification of low frequency band power with a concomitant decrease of high-frequency power, which is in accordance with results of our study. The explanation for the changes in power spectrum we observed is not straightforward. An adequate explanation may be that lower power in the high-frequency band results in a momentary perturbation in connection between cortical areas, while increased low-frequency power may arise from a perturbation in cholinergic signaling from subcortical

regions. This have already been studies presenting similar theories on Alzheimer's disease patients [Jeong J, 2004; Moretti DV et al 2009].

The importance of ictal period characterization in the frequency domain may be in the potential to exploit these characteristics through advanced signal analysis. This may further enable the creation of systems for automated seizure detection as well as prediction. We also made a categorization of spike EEG activity using voltage as the main criterion. The 100 to 200 μV category contained the greatest number of spikes while the 200 to 350 μV category contained a lower number and the 350 to 500 μV category had very few. It is not yet clear whether or not the characterization and sorting of spikes in to categories based on voltage has merit as an estimate of seizure severity, or if it may be of use as a variable in therapeutic approaches to epilepsy.

The holy grail of epilepsy research has always been automatic seizure detection or prediction. Recently there have been many systems developed in attempt to reach this goal. An attractive solution would involve integration of seizure detection and prediction algorithms into a warning device that could allow for minimization of injuries and also lower anxiety levels connected to lack of control and unpredictability of epileptic seizures [Ramgopal, S. et al 2014]. Ideally, these systems would have automated communication systems to alert emergency services before seizure onset, ensuring prompt reaction and treatment.

Although all patients would benefit from such development, patients suffering from drug-resistant (or medically intractable) epilepsy (DRE) are at the highest risk. DRE, as of today, cannot be controlled using conventional treatments. Knowing that these patients represent about 30% [Li S et al 2012; Bou Assi E et al 2017; Kuhlmann L et al 2017] of all patients with epilepsy only serves to stress how necessary for us it is to focus on creating new seizure-controlling methodologies.

In our study, we used bios analyzer software to extract nonlinear, biotic features of preictal and postictal EEG signals in order to train an ANN. The goal was to create an automated ANN system for ictal EEG detection. We reached a total performance in seizure detection of 92.9%.

The research into EEG based automatic seizure detection is very extensive with the first studies being published in the 1990s [Petrosian AA et al., 1996]. A multitude of linear and non-linear analysis techniques have previously been used. In fact, only listing and describing all the possible algorithms that have been studied to this effect would far surpass the scope of this thesis and an excellent review such as Nafea & Ismail, 2022 can offer the reader necessary overview of the field. We should note that nonlinear techniques have proven to be superior to linear analysis methods and many have been developed over the years. Some of the nonlinear techniques include fractal-based measures (fractal dimension, Hurst exponent etc), various entropy measures, discreet wavelet transform (DWT) and detrended fluctuation analysis [Silalahi DK et al.,2020; Kumar Y et al 2014; Yuan Q et al., 2011]. Non-linear mode decomposition (NMD) is another nonlinear method which was, along with Recurrence plots (a graphical nonlinear method) successfully used in seizure detection [Li M et al., 2020; Ravi S et al., 2022].

Despite multitudes of nonlinear techniques developed, the biotic features we used are a nonlinear analysis method that has, to our knowledge, never been attempted in seizure detection until now. Since our results are comparable to the results other studies have reported using nonlinear analysis techniques it can be concluded that biotic methods can successfully be used for automatic detection of seizure EEG signal and contribute to further improvements to this field of research.

In our study, we used *Kubios HRV Standard software* to extract linear and nonlinear HRV features that were then used to train an ANN. We reached the accuracy (86.81±8.87) and precision (96.3±8.2896.3±8.28) with high sensitivity (83.95±8.69) and specificity (94.44±12.42).

When it comes to seizure prediction, EEG based studies represent the overwhelming majority of research [Ren Z et al.,2022]. On the other hand, the use of HRV in seizure detection has more recently gained ground although studies in to algorithms using HRV for seizure prediction are still limited. An example of successfully applying HRV for seizure prediction can be found in a study by Fujiwara K et al. [Fujiwara K et al 2016] which proposed an HRV-based seizure prediction algorithm based on technology using multivariate statistical process control. Multiple HRV features were extracted from the interictal and preictal RR periods. Applying their method to clinical data has shown the possibility of seizure detection at least 1 minute before seizure occurrence, which strengthened the probability of realizing a successful HRV-based seizure prediction algorithm. A study by Behbahani et al. [Behbahani S et al 2016] used time and frequency domain HRV features. The features were extracted for consecutive time windows and an adaptive decision threshold method was applied. The algorithm achieved a sensitivity of 78.59% which was statistically significant.

Multiple studies have used data classification and machine learning techniques, especially Support Vector Machines (SVMs) as well as ANNs for the detection and prediction of epileptic seizures, on EEG data [Park Y et al., 2011; Moghim N et al., 2016; Costa RP et al., 2008; Kharbouch A et al., 2011]. SVMs [Cortes C et al 1995] are classification tools that implement learning algorithms and analyze data in order to determine important patterns through the solution of non-convex optimization problems. An example of using SVMs and HRV for seizure prediction can be found in Pavei et al [Pavei J et al., 2017]. Using SVMs they achieved a sensitivity of 94.1%.

There are even approaches that correlate wearable ECG based HRV recording to photoplethysmography (PPG) recording in attempt to predict seizure activity [Vandecasteele K et al 2017]. This algorithm classified seizures using HRV feature of HR increase. Respectively the sensitivity of the wearable ECG device and wearable PPG device was 70% and 32%. The underperformance of the PPG device underscored the value of conventional ECG monitoring.

Ultimately, the detection of preictal HRV patterns may provide adequate and reliable data for seizure prediction. The capability of seizure prediction may also lead to development of new avenues for therapeutic intervention, weather as on demand automated drug administration or closed-loop electrical stimulation. Our study results represent one more step in this direction and we hope that further research will enable us to reach the difficult goal of reliable and accurate seizure prediction.

.

6. CONCLUSIONS

1. EEG power registered during AMI development was s significantly increased in alpha, beta and theta bands four hours upon isoprenaline administration as compared to baseline values. These power spectrum changes reverted to baseline after 24 hours.

2. ECG registration during AMI development showed that there were significant alterations in nonlinear, biotic and time domain HRV parameters in the first four hours upon isoprenaline administration. Time domain parameters showed a significant shortening of the RR interval and increase in heart rate. Nonlinear, entropy measures showed a significant drop in system iregullarity. Detrended fluctuation analysis alpha 2 has a significant drop and there is a significant increase in fractal dimension. When it comes to biotic parameters: novelty, arrangement, diversification and shuffled isometry measures all showed a significant drop while radial isometry, series and serial isometry measures have a significant increase.

3. FFT analysis of the power spectrum was significantly increased in alpha, beta and gamma EEG bands during lindane-induced seizure activity with significant spike wave activity.

4. Neural network trained on biotic parameters in the EEG signal reported favorable sensitivity and specificity in detecting ictal activity while the logistic regression trained on HRV parameters showed a significant result in seizure prediction.

7. LITERATURE

A

Abou Jaoude M, Sun H, Pellerin KR, Pavlova M, Sarkis RA, Cash SS, Westover MB, Lam AD. Expert-level automated sleep staging of long-term scalp electroencephalography recordings using deep learning. Sleep. 2020 Nov 12;43(11):112.

Acharya UR et al. Entropies for automated detection of coronary artery disease using ECG signals: A review. Biocybernetics and Biomedical Engineering 2018,38(2):373–384.

Acharya UR, Joseph KP, Kannathal N, Lim CM, Suri JS. Heart rate variability: A review. Med Biol. Eng. Comput. 2006;44:1031–1051.

Acharya UR, Sree SV, Ang PCA, Yanti R, Suri JS. Application of non-linear and wavelet based features for the automated identification of epileptic EEG signals. Int J Neural Syst 2012;22(2):1250002

Adeli H, Zhou Z, Dadmehr N. Analysis of EEG records in an epileptic patient using wavelet transform. Journal of Neuroscience Methods 2003;123: 69–87.

Adhikari A, Topiwala MA, Gordon JA. Single units in the medial prefrontal cortex with anxiety-related firing patterns are preferentially influenced by ventral hippocampal activity. Neuron. 2011;71(5): 898-910. Adhikari A et al 2011; Li H et al 2017

Aitman TJ, Critser JK, Cuppen E, Dominiczak AF, Fernandez XM, Flint J, Gauguier D, Geurts AM, Gould M, Harris PC, Holmdahl R, Huebner N, Iszvak Z, Jacob H, Kuramoto T, Kwitek AE, Marrone A, Mashimo T, Moreno-Quinn C, Mullins J, Mullins LJ, Olsson T, Riley L, Saar K, Serikawa T, Shul JD, Szpirer C, Twigger SN, Voigt B, Worley K. Progress and prospects in rat genetics: a community view. Nat Genet 2008;40:516–522

Akbari H, Sadiq MT, Rehman AU. Classification of normal and depressed EEG signals based on centered correntropy of rhythms in empirical wavelet transform domain. Health Inf Sci Syst. 2021 Feb 6;9(1):9.

Ali A, Redfors B, Lundgren J, Alkhoury J, Oras J, Gan LM, Omerovic E. The importance of heart rate in isoprenaline-induced takotsubo-like cardiac dysfunction in rats. ESC Heart Fail. 2020 Oct;7(5):2690-2699.

Al-Qazzaz, Noor K et al. Role of EEG as biomarker in the early detection and classification of dementia. The Scientific World Journal 2014;l2014: 906038.

Anand M, Agrawa AK, and Rehmani, BNH. Role of GABA receptor complex in low dose lindane (HCH) induced neurotoxicity: Neurobehavioural, neurochemical and electrophysiological studies. Drug Chem. Toxicol. 1998;21:35–46.

Anderson K, Chirion C, Fraser M, Purcell M, Stein S, Vuckovic A. Markers of Central Neuropathic Pain in Higuchi Fractal Analysis of EEG Signals From People With Spinal Cord Injury. Front Neurosci. 2021 Aug 26;15:705652.

Ansari Y, Mourad O, Qaraqe K, Serpedin E. Deep learning for ECG Arrhythmia detection and classification: an overview of progress for period 2017-2023. Front Physiol. 2023 Sep 15;14:1246746.

Arakaki X, Arechavala RJ, Choy EH, Bautista J, Bliss B, Molloy C, Wu DA, Shimojo S, Jiang Y, Kleinman MT, Kloner RA. The connection between heart rate variability (HRV),

neurological health, and cognition: A literature review. Front Neurosci. 2023 Mar 1;17:1055445.

Ardell JL, Andresen MC, Armour JA, Billman GE, Chen P, Foreman RD, Herring N, O'Leary DS, Sabbah HN. Schultz HD, et al. Translational neurocardiology: Preclinical models and cardio neural integrative aspects. J. Physiol. 2016;594:3877–3909.

Ardell JL, Armour JA. Comprehensive Physiology. Wiley; Hoboken, NJ, USA: Neurocardiology: Structure-Based Function; 2016;1635–1653.

Armour JA. Cardiac neuronal hierarchy in health and disease. Am. J. Physiol. 2004;287:R262–R271.

Armour JA. Potential clinical relevance of the 'little brain' on the mammalian heart. Exp. Physiol. 2008;93:165–176.

Assenza G, Di Lazzaro V. A useful electroencephalography (EEG) marker of brain plasticity: delta waves. Neural Regen Res. 2015;10(8):1216-7.

Assenza G, Zappasodi F, Squitti R, et al. Neuronal functionality assessed by magnetoencephalography is related to oxidative stress system in acute ischemic stroke. Neuroimage 2009;44:1267-73.

B

Babloyantz AC, Nicolis JM. Evidence of chaotic dynamics of brain activity during the sleep cycle, Phys. Lett. 1985;111A:152—157.

Barkmeier DT, Loeb JA. An animal model to study the clinical significance of interictal spiking. Clin EEG Neurosci. 2009;40(4):234–238.

Beckers F, Verheyden B, Couckuyt K, Aubert AE. Fractal dimension in health and heart failure. Biomed Tech (Berl). 2006 Oct;51(4):194-7.

Behbahani S, Dabanloo NJ, Nasrabadi AM, Dourado A. Prediction of epileptic seizures based on heart rate variability. Technol Health Care 2016;24:795–810.

Behbahani S. A review of significant research on epileptic seizure detection and prediction using heart rate variability. Turk Kardiyol Dern Ars. 2018 Jul;46(5):414-421.

Benedek M, Bergner S, Könen T, Fink A, Neubauer AC. EEG alpha synchronization is related to top-down processing in convergent and divergent thinking. Neuropsychologia. 2011;49:3505–3511

Benedek M, Schickel RJ, Jauk E, Fink A, Neubauer AC. Alpha power increases in right parietal cortex reflects focused internal attention. *Neuropsychologia*. 2014;56(100):393-400.

Bennet DH. Bennett 's cardiac arrhythmias: practical notes on interpretation and treatment. 1st ed. Oxford: Wiley-Blackwell; 2013.

Bertram EH, Williamson JM, Cornett JF, Spradlin S, Chen ZF. Design and construction of a long-term continuous video-EEG monitoring unit for simultaneous recording of multiple small animals. Brain Res Protoc. 1997;2(1):85–97.

Boateng S, Sanborn T. Acute myocardial infarction. Dis Mon. 2013;59(3):83-96.

Bou Assi E, Nguyen DK, Rihana S, Sawan M. Towards accurate prediction of epileptic seizures: a review. *Biomed. Signal Process. Control* 2017;**34**:144–157

Brennan M, Palaniswami M, Kamen P. Do existing measures of Poincaré plot geometry reflect nonlinear features of heart rate variability? IEEE Trans Biomed Eng. 2001 Nov;48(11):1342-7.

Briggs F. Organizing principles of cortical layer 6. Front Neural Circuits. 2010;4:3.

Brooks WW and Conrad CH. Isoproterenol-induced myocardial injury and diastolic dysfunction in mice: structural and functional correlates. Comp. Med. 2009;59:339.

Butler GC, Yamamoto Y, Hughson RL. Heart rate variability to monitor autonomic nervous system activity during orthostatic stress. J Clin Pharmacol. 1994 Jun;34(6):558-62.

C

Campbell IG. EEG recording and analysis for sleep research. Curr Protoc Neurosci. 2009; 49(1):10-2.

Carrasco S, Gaitán MJ, González R, Yánez O. Correlation among Poincaré plot indexes and time and frequency domain measures of heart rate variability. J Med Eng Technol. 2001 Nov-Dec;25(6):240-8.

Castaldo R, Melillo P, Bracale U, Caserta M, Triassi M, Pecchia L. Acute mental stress assessment via short term HRV analysis in healthy adults: a systematic review with meta-analysis. Biomed. Signal Process. Control 2015;18:370–377.

Castaldo R, Montesinos L, Melillo P, James C, Pecchia L. Ultra-short term HRV features as surrogates of short term HRV: a case study on mental stress detection in real life. BMC Med Inform Decis Mak. 2019 Jan 17;19(1):12.

Castiglioni P, Di Rienzo M, Radaelli A. Effects of autonomic ganglion blockade on fractal and spectral components of blood pressure and heart rate variability in free-moving rats. Auton Neurosci Basic Clin. 2013;178:44–9.

Cerqueira JJ, Almeida OFX, Sousa N. The stressed prefrontal cortex. Left? Right! Brain Behav Immun 2008;22: 630–638.

Chapman AR, Adamson PD, Mills NL. Assessment and classification of patients with myocardial injury and infarction in clinical practice. Heart. 2017 Jan 1;103(1):10-18.

Chen YC, Hsiao CC, Zheng WD, Lee RG, Lin R. Artificial neural networks-based classification of emotions using wristband heart rate monitor data. Medicine (Baltimore). 2019 Aug;98(33):e16863.

Cho Y, Kwon JM, Kim KH, Medina-Inojosa JR, Jeon KH, Cho S, Lee SY, Park J, Oh BH. Artificial intelligence algorithm for detecting myocardial infarction using six-lead electrocardiography. Sci Rep. 2020 Nov 24;10(1):20495.

Choi KH, Kim J, Kwon OS, Kim MJ, Ryu YH, Park JE. Is heart rate variability (HRV) an adequate tool for evaluating human emotions? - A focus on the use of the International Affective Picture System (IAPS). Psychiatry Res. 2017 May;251:192-196.

Chorev E, Epsztein J, Houweling AR, Lee AK, Brecht M. Electrophysiological recordings from behaving animals--going beyond spikes. Curr Opin Neurobiol. 2009;19(5):513–519.

Ciccone AB, Siedlik JA, Wecht JM, Deckert JA, Nguyen ND, Weir JP. Reminder: RMSSD and SD1 are identical heart rate variability metrics. Muscle Nerve. 2017;56:674–678.

Clifford G, Azuaje F, McSharry PE. Advanced Methods and Tools for ECG Data Analysis. Norwood, MA: Artech House. 2016.

Cohen L. Proceedings of the IEEE. Volume 77. Institute of Electrical and Electronics Engineers (IEEE); Piscataway, NJ, USA: 1989. Time-frequency distributions-a review; pp. 941–981.

Cohen L. Time-Frequency Analysis. Volume 778 Prentice Hall; Englewood Cliffs, NJ, USA: 1995.

Cortes C, Vapnik V. Support-vector networks. Mach Learn. 1995;20: 273.

Costa M, Goldberger AL, Peng CK. Multiscale entropy analysis of complex physiologic time series. Phys Rev Lett. 2002 Aug 5;89(6):068102.

Costa RP, Oliveira P, Rodrigues G, Leitao B, Dourado A. Epileptic seizure classification using neural networks with 14 features, In: Lovrek I, Howlett RJ, Jain LC, editors. Knowledge-Based Intelligent Information and Engineering Systems. Berlin, Heidelberg: Lecture Notes in Computer Science, 2008. p. 5178.

D

Dadashi M, Birashk B, Taremian F, Asgarnejad AA, Momtazi S. Effects of Increase in Amplitude of Occipital Alpha & Theta Brain Waves on Global Functioning Level of Patients with GAD. Basic Clin Neurosci. 2015;6(1):14-20.

Detweiler DK. Electrocardiography in toxicology studies. In: Sipes IG, McQueen CA, Gandolf IJ, editors. Comprehensive toxicology, vol. 6. New York: Pergamon Press; 1997. p. 95–114.

Deutschman CS, Harris AP, Fleisher LA. Changes in heart rate variability under propofol anesthesia: A possible explanation for propofol-induced bradycardia. Anesth Analg. 1994;79:373–7.

Dong JG. The role of heart rate variability in sports physiology. Exp Ther Med. 2016 May;11(5):1531-1536.

E

Einthoven W, Jaffe AS, Venge P, Lindahl B. Galvanometrische registratie van het menschelijk electrocardiogram. In: Herinneringsbundel Professor S S Rosenstein Leiden, Netherlands: EdardIjdo 1902:101–7.

Etkin A, Egner T & Kalisch R. Emotional processing in anterior cingulate and medial prefrontal cortex. Trends Cogn Sci. 2011;15: 85–93.

F

Falconer KJ, Fractal Geometry: Mathematical Foundations and Applications, Wiley, 2003.

Farraj AK, Hazari MS, Cascio WE. The utility of the small rodent electrocardiogram in toxicology. Toxicol Sci. 2011;121(1):11–30.

Fateev MM, Sidorov AV, Grigor'eva MV, Rakov AA, Fateeva KM. Heart rate variability in conscious and anesthetized rats under the action of angiotensin converting enzyme inhibitors. Bull Exp Biol Med. 2012;152:590–4.

Fedele L, Brand T. The Intrinsic Cardiac Nervous System and Its Role in Cardiac Pacemaking and Conduction. Journal of Cardiovascular Development and Disease 2020; 7(4):54.

Filho L, Ferreira H, Sousa L, Carvalho RB, Lobo ER, Dantas PL, Glauco J Experimental model of myocardial infarction induced by isoproterenol in rats. Rev Bras Cir Cardiovasc, 2011;26: 469-476.

Fink A, Benedek M. The creative brain: Brain correlates underlying the generation of original ideas. In: Vartanian O., Bristol A.S., Kaufman J.C., editors. Neuroscience of creativity. MIT Press; Cambridge, MA: 2013. pp. 207–232.

Finn DP, Leonard BE: Pain in Psychiatric Disorders. Mod Trends Pharmacopsychiatry. Basel, Karger, 2015;30: 103-119

Finnigan SP, Rose SE, Chalk JB. Contralateral hemisphere delta EEG in acute stroke precedes worsening of symptoms and death. Clin Neurophysiol 2008;119:1690-4.

Foo SY, Stuart G, Harvey B, Meyer-Baese A. Neural network-based EKG pattern recognition. Engineering Applications of Artificial Intelligence 2002;15: 253–260.

Force T. Standards of Measurement, Physiological Interpretation and Clinical Use. Task Force of the European Society of Cardiology and the North American Society of Pacing and Electrophysiology. Circulation. 1996;93:1043–1065.

Foster PS, Harrisson DW. The relationship between magnitude of cerebral activation and intensity of emotional arousal. Int J Neurosci. 2002;112: 1463–1477.

Frasure-Smith N, Lespérance F. Depression and cardiac risk: present status and future directions. Postgrad Med J 2010;86: 193–196.

Freeborn DL, McDaniel KL, Moser VC, Herr DW. Use of electroencephalography (EEG) to assess CNS changes produced by pesticides with different modes of action: effects of permethrin, deltamethrin, fipronil, imidacloprid, carbaryl, and triadimefon. Toxicol Appl Pharmacol. 2015;282(2):184–194.

Friedman, B. H. An autonomic flexibility–neurovisceral integration model of anxiety and cardiac vagal tone. Biological Psychology 2017;74(2): 185–199.

Fujiwara K, Miyajima M, Yamakawa T, Abe E, Suzuki Y, Sawada Y, Kano M, Maehara T, Ohta K, Sasai-Sakuma T, Sasano T, Matsuura M, Matsushima E. Epileptic Seizure Prediction Based on Multivariate Statistical Process Control of Heart Rate Variability Features. IEEE Trans Biomed Eng. 2016 Jun;63(6):1321-32.

Furtado MA, Braga GK, Oliveira JA, Del Vecchio F, Garcia-Cairasco N. Behavioral, morphologic, and electroencephalographic evaluation of seizures induced by intrahippocampal microinjection of pilocarpine. Epilepsia. 2002;43(5):37–39.

G

Gao Y, Gao B, Chen Q, Liu J, Zhang Y. Deep Convolutional Neural Network-Based Epileptic Electroencephalogram (EEG) Signal Classification. Front Neurol. 2020 May 22;11:375.

Gavrilova EA. [Heart Rate Variability and Sports.]. Fiziol Cheloveka. 2016 Sep;42(5):121-129.

Gladun KV. Higuchi Fractal Dimension as a Method for Assessing Response to Sound Stimuli in Patients with Diffuse Axonal Brain Injury. Sovrem Tekhnologii Med. 2021;12(4):63-70.

Goldman S, Raya TE. Rat infarct model of myocardial infarction and heart failure. J Card Fail. 1995 Mar;1(2):169-77.

Gorlin R, Fuster V, Ambrose JA. Anatomic-physiologic links between acute coronary syndromes. Circulation. 1986;74(1):6–9.

Gotman J, Flanagan D, Zhang J, Rosenblatt B. Automatic seizure detection in the newborn: methods and initial evaluation. Electroencephalogr Clin Neurophysiol. 1997 Sep;103(3):356-62.

Green JD, Arduini A. Hippocampal activity in arousal. J Neurophysiol. 1954;17(6): 533–57.

Greenberg JA, Burke JF, Haque R, Kahana MJ, Zaghloul KA. Decreases in theta and increases in high frequency activity underlie associative memory encoding. Neuroimage. 2015;114:257-63.

Gu Y, Liang Z, Hagihira S. Use of Multiple EEG Features and Artificial Neural Network to Monitor the Depth of Anesthesia. Sensors (Basel). 2019 May 31;19(11):2499.

Guild SJ, Barrett CJ, McBryde FD, Van Vliet BN, Malpas SC. Sampling of cardiovascular data; how often and how much? Am J Physiol Regul Integr Comp Physiol. 2008 Aug;295(2):R510-5.

Guzik P, Piskorski J, Krauze T, Schneider R, Wesseling KH, Wykretowicz A, Wysocki H. Correlations between the Poincaré plot and conventional heart rate variability parameters assessed during paced.

H

Haleagrahara N, Varkkey J and Chakravarthi S. Cardioprotective effects of glycyrrhizic acid against isoproterenol-induced myocardial ischemia in rats. Int. J. Mol. Sci. 2011;12:7100-7113

Hall JE. Rhythmical excitation of the heart. In: Guyton and Hall textbook of medical physiology. 14th ed. Philadelphia: Elsevier; 2020. p. 114–33.

Harmony T. The functional significance of delta oscillations in cognitive processing. Front Integr Neurosci. 2013;7:83.

Hashimoto DA, Witkowski E, Gao L, Meireles O, Rosman G. Artificial Intelligence in Anesthesiology: Current Techniques, Clinical Applications, and Limitations. Anesthesiology. 2020 Feb;132(2):379-394.

Hassan SF, Cornish JL, Goodchild AK. Respiratory, metabolic and cardiac functions are altered by disinhibition of subregions of the medial prefrontal cortex. The J of Phys. 2013;591(23): 6069-6088.

Henderson CJ, Butler SR, Glass A. The localization of equivalent dipoles of EEG sources by the application of electrical field theory. Electroencephalogr Clin Neurophysiol. 1975;39:117–30.

Henriques T, Ribeiro M, Teixeira A, Castro L, Antunes L, Costa-Santos C. Nonlinear Methods Most Applied to Heart-Rate Time Series: A Review. Entropy (Basel). 2020 Mar 9;22(3):309.

Hilz MJ, Devinsky O, Szczepanska H, Borod JC, Marthol H, Tutaj M. Right ventromedial prefrontal lesions result in paradoxical cardiovascular activation with emotional stimuli. Brain 2006;129:3343–55.

Hirota N, Suzuki S, Arita T et al. Prediction of biological age and all-cause mortality by 12-lead electrocardiogram in patients without structural heart disease. BMC Geriatr 2021;21:460.

Ho YL, Lin C, Lin YH, Lo MT. The prognostic value of non-linear analysis of heart rate variability in patients with congestive heart failure–a pilot study of multiscale entropy. *PLoS One.* 2011;**6**:e18699.

Holm TH, Lykke-Hartmann K. Insights into the pathology of the α3 Na+ /K+ -ATPase ion pump in neurological disorders; lessons from animal models. Front Physiol. 2016;7:209.

Holmes A & Wellman CL Stress-induced prefrontal reorganization and executive dysfunction in rodents. Neurosci Biobehav Rev. 2009;33: 773–783.

Holmes G & Khazipov R. Basic Neurophysiology and the Cortical Basis of EEG. 2007.

Honda R, Saito Y, Okumura A, et al. Characterization of ictal slow waves in epileptic spasms. Epileptic Disord. 2015;17(4):425-35.

Hoshi RA, Pastre CM, Vanderlei LC, Godoy MF. Poincaré plot indexes of heart rate variability: relationships with other nonlinear variables. Auton Neurosci. 2013 Oct;177(2):271-4.

Hrnčić D, Rašić-Marković A, Djuric D, Sušić V, Stanojlović O. The role of nitric oxide in convulsions induced by lindane in rats. Food Chem Toxicol. 2011 Apr;49(4):947-54.

Hsu CH, Tsai MY, Huang GS, Lin TC, Chen KP, Ho ST, Shyu LY, Li CY. Poincaré plot indexes of heart rate variability detect dynamic autonomic modulation during general anesthesia induction. Acta Anaesthesiol Taiwan. 2012 Mar;50(1):12-8.

Huang CL. Murine electrophysiological models of cardiac arrhythmogenesis. Physiol Rev. 2017;97(1):283–409.

Huikuri HV, Mäkikallio T, Airaksinen KE, Mitrani R, Castellanos A, Myerburg RJ. Measurement of heart rate variability: a clinical tool or a research toy? J Am Coll Cardiol. 1999 Dec;34(7):1878-83.

J

Jaenig W. Neurocardiology: A neurobiologist's perspective. J. Physiol. 2016;594:3955–3962.

Janković M, Savić A, Novičić M, Popović M. Deep learning approaches for human activity recognition using wearable technology. Medicinski podmladak. 2018;69:14-24.

Jansen, BH. "Nonlinear dynamics and quantitative EEG analysis." Electroencephalography and clinical neurophysiology. Supplement 1996;45: 39-56.

Jefferson AL, Himali JJ, Au R, Seshadri S, Decarli C, O'Donnell CJ et al. Relation of left ventricular ejection fraction to cognitive aging (from the Framingham heart study) Am J Cardiol. 2011;108: 1346–51.

Jeong J. EEG dynamics in patients with Alzheimer's disease. Clin Neurophysiol 2004;115:1490–505.

Jin Y, Chen C, Cao Z, Sun B, Lo IL, Liu TM, Zheng J, Sun S, Shi Y, Zhang XD. Entropy change of biological dynamics in COPD. Int J Chron Obstruct Pulmon Dis. 2017 Oct 12;12:2997-3005.

Jones SL, Svitkina TM. Axon initial segment cytoskeleton: architecture, development, and role in neuron polarity. Neural Plast. 2016;2016:6808293

K

Kamen PW, Krum H, Tonkin AM. Poincaré plot of heart rate variability allows quantitative display of parasympathetic nervous activity in humans. Clin Sci (Lond). 1996 Aug;91(2):201-8.

Kandel ER, Schwartz JH, Jessell TM, editors. Principles of neural sciences. 5th ed. New York: McGraw-Hill; 2012.

Kandratavicius L, Balista PA, Lopes-Aguiar C, Ruggiero RN, Umeoka EH, Garcia-Cairasco N, Bueno-Junior LS, Leite JP. Animal models of epilepsy: use and limitations. Neuropsychiatr Dis Treat. 2014; Sep 9;10:1693-705.

Kane MJ & Engle RW. The role of prefrontal cortex in working-memory capacity, executive attention, and general fluid intelligence: an individual-differences perspective. Psychon Bull Rev. 2002;9: 637–671.

Kannan MM and Quine SD. Ellagic acid inhibits cardiac arrhythmias, hypertrophy and hyperlipidaemia during myocardial infarction in rats. Metabolism. 2013;62:52-61.

Kannathal N, Choo ML, Acharya UR, Sadasivan PK. Entropies for detection of epilepsy in EEG. Comput Methods Programs Biomed. 2005 Dec;80(3):187-94.

Kato M, Komatsu T, Kimura T, Sugiyama F, Nakashima K, Shimada Y. Spectral analysis of heart rate variability during isoflurane anesthesia. Anesthesiology. 1992;77:669–74.

Kauffman L. Sabelli H. Mathematical Bios. Kybernetes 2003; 3:1418-1428

Kauffman LH, Sabelli H. Bios: Creative Organization Beyond Chaos, 43rd Annual Meeting of the International Society for the Systems Sciences, Asilomar, California, 27 June-2 July, 1999. pp. 358-360,

Kent BA, Strittmatter SM, Nygaard HB. Sleep and EEG Power Spectral Analysis in Three Transgenic Mouse Models of Alzheimer's Disease: APP/PS1, 3xTgAD, and Tg2576. J Alzheimers Dis. 2018;64(4):1325-1336.

Khan YU, Gotman J. Wavelet based automatic seizure detection in intracerebral electroencephalogram. Clinical Neurophysiology 2003;114: 898–908.

Kharbouch A, Shoeb A, Guttag J, Cash SS. An algorithm for seizure onset detection using intracranial EEG. Epilepsy Behavior 2011;22: 29–35

Khodabakhshi, MB. and Valiallah S. A nonlinear dynamical approach to analysis of emotions using EEG signals based on the Poincaré map function and recurrence plots. Biomedizinische Technik. Biomedical engineering 2020;65,5: 507-520.

Kirkcaldie MT, Collins JM. The axon as a physical structure in health and acute trauma. J Chem Neuroanat. 2016;76:9–18.

Kiymik MK, Akin M, Subasi A. Automatic recognition of alertness level by using wavelet transform and artificial neural network. J Neurosci Methods. 2004 Oct 30;139(2):231-40.

Kiymik MK, Subasi A, Ozcalik HR. Neural networks with periodogram and autoregressive spectral analysis methods in detection of epileptic seizure. J Med Syst. 2004 Dec;28(6):511-22.

Kligfield P. The centennial of the Einthoven electrocardiogram. J Electrocardiol. 2002;35 Suppl:123-9.

Klimesch W. Alpha-band oscillations, attentioon, and controlled access to stored information. Trends Cogn Sci. 2012;16: 606–617.

Koenig J, Kemp AH, Beauchaine TP, Thayer JF, Kaess M. Depression and resting state heart rate variability in children and adolescents - A systematic review and meta-analysis. Clin Psychol Rev. 2016 Jun;46:136-50.

Konopelski P, Ufnal M. Electrocardiography in rats: a comparison to human. Physiol Res. 2016 Nov 23;65(5):717-725.

Kopetz H. Internet of things. In: Kopetz H, editor. Real-Time Systems: Design Principles for Distributed Embedded Applications. New York, NY: Springer US 2011;307–23.

Kozelka JW, Pedley TA. Beta and mu rhythms. J Clin Neurophysiol. 1990 Apr;7(2):191-207.

Kuhlmann L, Lehnertz K, Richardson MP, Schelter B, Zaveri HP. Seizure prediction - ready for a new era. Nat Rev Neurol. 2018 Oct;14(10):618-630.

Kumar P, Agarwal JL, Kumar A. Effect of long term oral administration of L-arginine on experimentally produced myocardial ischemia in rabbits. Indian J Physiol Pharmacol. 2007;51:147–52.

Kumar P, Srivastava P, Gupta A, Bajpai M. Noninvasive recording of electrocardiogram in conscious rat: A new device. Indian J Pharmacol. 2017;49(1):116-118.

Kumar Y, Dewal M, Anand R. Epileptic seizure detection using DWT based fuzzy approximate entropy and support vector machine. Neurocomputing. 2014;133:271–9.

L

Laborde S, Mosley E, Thayer JF. Heart Rate Variability and Cardiac Vagal Tone in Psychophysiological Research - Recommendations for Experiment Planning, Data Analysis, and Data Reporting. Front Psychol. 2017 Feb 20;8:213.

Lacroix JJ, Campos FV, Frezza L, Bezanilla F. Molecular bases for the asynchronous activation of sodium and potassium channels required for nerve impulse generation. Neuron. 2013;79:651–7.

Latson TW, McCarroll SM, Mirhej MA, Hyndman VA, Whitten CW, Lipton JM. Effects of three anesthetic induction techniques on heart rate variability. J Clin Anesth. 1992;4:265–76.

LeBlanc BW, Bowary PM, Chao YC, Lii TR, & Saab CY. Electroencephalographic signatures of pain and analgesia in rats. PAIN. 2016;157(10): 2330–2340.

LeBlanc BW, Lii TR, Silverman AE, Alleyne RT, Saab CY. Cortical theta is increased while thalamocortical coherence is decreased in rat models of acute and chronic pain. Pain, 2014;155(4):773–782.

Lee WK et al. Smart ECG Monitoring Patch with Built-in R-Peak Detection for Long-Term HRV Analysis. Annals of biomedical engineering 2016; 44 (7): 2292-301.

Lehnertz K,Elger CE, Can epileptic seizures be predicted? Evidence from nonlinear time series analyses of brain elec-trical activity, Phys. Rev. Lett. 1998;80:5019—5023.

Leiser SC, Dunlop J, Bowlby MR, Devilbiss DM. Aligning strategies for using EEG as a surrogate biomarker: a review of preclinical and clinical research. Biochem Pharmacol. 2011;81(12):1408–1421.

Levenga, J et al. Sleep Behavior and EEG Oscillations in Aged Dp(16)1Yey/+ Mice: A Down Syndrome Model. Neuroscience 2018;376:117-126.

Lévesque, Maxime et al. Animal models of temporal lobe epilepsy following systemic chemoconvulsant administration. Journal of neuroscience methods 2016;260:45-52.

Levy MN and Schwartz PJ. Vagal control of the heart: Experimental basis and clinical implications . Armonk, NY: Futura Publishing Co. 1994

Li H, Zhao Q, Huang F, Cao Q, Qian Q, Johnstone SJ. Increased Beta Activity Links to Impaired Emotional Control in ADHD Adults With High IQ. J Atten Disord, 2017;21: 754-764.

Li L, Gervasi N, Girault JA. Dendritic geometry shapes neuronal cAMP signaling to the nucleus. Nat Commun. 2015;6:6319.

Li M, Sun X, Chen W. Patient-specific seizure detection method using nonlinear mode decomposition for long-term EEG signals. *Med. Biol. Eng. Comput.* 2020, *58*, 3075–3088.

Li S, Ding D & Wu J. Definitions and Epidemiology of Epilepsy. In Shorvon, S., Guerrini, R., Cook, M. & Lhatoo, S. (eds.) *Oxford Textbook of Epilepsy and Epileptic Seizures*, 2012;5:51–59.

Liang X, Xiong J, Cao Z, Wang X, Li J, Liu C. Decreased sample entropy during sleep-to-wake transition in sleep apnea patients. Physiol Meas. 2021 May 11;42(4).

Litt B, Echauz J, Prediction of epileptic seizures. The Lancet Neurology 2002;1(1):22–30.

London M, Hausser M. Dendritic computation. Annu Rev Neurosci. 2005;28:503–32.

Lothman EW, Bertram EH., III Epileptogenic effects of status epilepticus. Epilepsia. 1993;34(1):59–70.

Luo J, McQueen PG, Shi B, Lee CH, Ting CY. Wiring dendrites in layers and columns. J Neurogenet. 2016;30:69–79.

M

Ma, Yan et al. Nonlinear dynamical analysis of sleep electroencephalography using fractal and entropy approaches. Sleep medicine reviews 2018;37: 85-93.

Malik M, Xia R, Odemuyiwa O, Staunton A, Poloniecki J, Camm AJ. Influence of the recognition artefact in automatic analysis of long-term electrocardiograms on time-domain measurement of heart rate variability. Med Biol. Eng. Comput. 1993;31:539–544.

Martinerie J, Adam C, Le van Quyen M, Baulac M, Renault B, Varela FJ, Can epileptic crisis be anticipated? Nat. Med. 1998;4:173—1176.

Mason F, Scarabello A, Taruffi L, Pasini E, Calandra-Buonaura G, Vignatelli L, Bisulli F. Heart Rate Variability as a Tool for Seizure Prediction: A Scoping Review. J Clin Med. 2024 Jan 27;13(3):747.

McCauley MD, Wehrens XH. Ambulatory ECG recording in mice. J Vis Exp. 2010 May 27;(39):1739.

McCraty R. Coherence: bridging personal, social and global health. Act Nerve Super 2011;53: 85–102

Medlej Y, Asdikian R, Wadi L, Salah H, Dosh L, Hashash R, Karnib N, Medlej M, Darwish H, Kobeissy F, Obeid M. Enhanced setup for wired continuous long-term EEG monitoring in juvenile and adult rats: application for epilepsy and other disorders. BMC Neurosci. 2019 Mar 4;20(1):8.

Michaud K, Basso C, d'Amati G, et al. Diagnosis of myocardial infarction at autopsy: AECVP reappraisal in the light of the current clinical classification. Virchows Arch. 2020;476(2):179-194.

Miller EK & Cohen JD. An integrative theory of prefrontal cortex function. Annu Rev Neurosci. 2001;24: 167–202.

Miller EK. The prefrontal cortex and cognitive control. Nat Rev Neurosci. 2000;1: 59–65.

Moghim N, Corne DW. Predicting epileptic seizures in advance. PLoS One. 2014;9: e99334

Montag C, Diefenbach S. Towards homo digitalis: important research issues for psychology and the neurosciences at the dawn of the internet of things and the digital society. Sustainability 2018;10:415.

Montag C, Elhai JD, & Dagum P. On Blurry Boundaries When Defining Digital Biomarkers: How Much Biology Needs to Be in a Digital Biomarker? Frontiers in psychiatry 2021;12:740292.

Moretti DV, Fracassi C, Pievani M, Geroldi C, Binetti G, Zanetti O, Sosta K, Rossini PM, Frisoni GB. Increase of theta/gamma ratio is associated with memory impairment. Clin Neurophysiol. 2009 Feb;120(2):295-303.

Moshé SL, Perucca E, Ryvlin P, Tomson T. Epilepsy: new advances. Lancet 2014;385(9971), 884–98.

Mouchati PR, Barry JM, Holmes GL. Functional brain connectivity in a rodent seizure model of autistic-like behavior. Epilepsy Behav. 2019 Jun;95:87-94.

Murray A. Examining heart rate variability and alpha-amylase levels in predicting PTSD in combat-experienced marines (Ph.D. thesis). Alliant International University, Alhambra, CA, United States. 2012

N

Nadler JV, Perry BW, Cotman CW. Intraventricular kainic acid preferentially destroys hippocampal pyramidal cells. Nature. 1978;271(5646):676–677.

Nafea MS, Ismail ZH. Supervised Machine Learning and Deep Learning Techniques for Epileptic Seizure Recognition Using EEG Signals—A Systematic Literature Review. *Bioengineering*. 2022; 9(12):781.

Naranjo Orellana J, de la Cruz Torres B, Sarabia Cachadiña E, de Hoyo M, Domínguez Cobo S. Two new indexes for the assessment of autonomic balance in elite soccer players. Int J Sports Physiol Perform. 2015 May;10(4):452-7.

Narayanaswamy S. High resolution electrocardiography. Indian Pacing Electrophysiol J. 2002;2:50–6.

Nashef L, Ryvlin P. Sudden unexpected death in epilepsy (SUDEP): update and reflections. Neurol Clin 2009;27(4):1063–74.

Nayak CS, Anilkumar AC. EEG Normal Waveforms. In: StatPearls [Internet]. Treasure Island (FL): StatPearls Publishing; 2022 Jan.

Neafsey EJ. Prefrontal cortical control of the autonomic nervous system: anatomical and physiological observations. Prog Brain Res. 1990;85: 147–165.

Netoff T, Park Y, Parh K. Seizure prediction using cost-sensitive support vector machine. In: Proceedings of 31st Annual International Conference of the IEEE EMBS Minneapolis, Minnesota, USA, 2009; pp. 3322–3325,

Niedermeyer E. Alpha rhythms as physiological and abnormal phenomena. Int J Psychophysiol. 1997 Jun;26(1-3):31-49.

O

Olejniczak P. Neurophysiologic basis of EEG. J Clin Neurophysiol. 2006;23:186–9.

Ometov A, Shubina V, Klus L, et al. A Survey on Wearable Technology: History, State-of-the-Art and Current Challenges. Comput. Networks 2021;193:108074.

Oppenheimer SM, Cechetto DF. Cardiac chronotropic organization of the rat insular cortex. Brain Res 1990;533: 66–72.

Osorio I, Frei MG. Real-time detection, quantification, warning, and control of epileptic seizures: the foundations for a scientific epileptology. Epilepsy Behav 2009;16(3):391–6.

Overgaard CB, Dzavík V. Inotropes and vasopressors: review of physiology and clinical use in cardiovascular disease. Circulation. 2008 Sep 2;118(10):1047-56.

Owens NC & Verberne AJ. Regional hemodynamic responses to activation of the medial prefrontal cortex depressor region. Brain Res. 2001;919: 221–231.

P

Padilla-Coreano N, Bolkan SS, Pierce GM, Blackman DR, Hardin WD, Garcia-Garcia AL Direct ventral hippocampal-prefrontal input is required for anxiety-related neural activity and behavior. Neuron. 2016;89(4): 857-866.

Pappano AJ, Wier WG. Automaticity: natural excitation of the heart. In: Cardiovascular physiology. 11th ed. Mosby: Elsevier; 2019. p. 86–140.

Park Y, Luo L, Parhi KK, Netoff T. Seizure prediction with spectral power of eeg using cost-sensitive support vector machines. Epilepsia. 2011;52: 1761–1770.

Pavei J, Heinzen RG, Novakova B, Walz R, Serra AJ, Reuber M, et al. Early Seizure Detection Based on Cardiac Autonomic Regulation Dynamics. Front Physiol 2017;8:765.

Peng CK, Havlin S, Stanley HE, Goldberger AL. Quantification of scaling exponents and crossover phenomena in nonstationary heartbeat time series. *Chaos.* 1995;**5**:82–87.

Pereda AE. Electrical synapses and their functional interactions with chemical synapses. Nat Rev Neurosci. 2014;15(4):250–263.

Pereira-Junior PP, Marocolo M, Rodrigues FP, Medei E, Nascimento JH. Noninvasive method for electrocardiogram recording in conscious rats: Feasibility for heart rate variability analysis. An Acad Bras Cienc. 2010;82:431–7.

Petrosian A, Prokhorov D, Homan R, Dashei R, Wunsch D. Recurrent neural network based prediction of epileptic seizures in intra- and extracranial EEG. Neurocomputing 2000;30: 201–218

Petrosian AA, Homan R, Prokhorov D, Wunsch DC. Classification of epileptic EEG using neural network and wavelet transform. In Proceedings of the Wavelet Applications in Signal and Image Processing IV, 1996;2825:834–843.

Phan TD, Kim SH, Yang HJ, Lee GS. EEG-Based Emotion Recognition by Convolutional Neural Network with Multi-Scale Kernels. Sensors (Basel). 2021 Jul 27;21(15):5092.

Piau A, Wild K, Mattek N, Kaye J. Current state of digital biomarker technologies for real-life, home-based monitoring of cognitive function for mild cognitive impairment to mild alzheimer disease and implications for clinical care: systematic review. J Med Internet Res 2019;21:e12785.

Pincus SM. Approximate entropy as a measure of system complexity. Proc Natl Acad Sci U S A. 1991 Mar 15;88(6):2297-301.

Poil, Simon-Shlomo et al. Integrative EEG biomarkers predict progression to Alzheimer's disease at the MCI stage. Frontiers in aging neuroscience; 2013;5:58.

Pozuelo L, Tesar G, Zhang J, Penn M, Franco K, Jiang W. Depression and heart disease: what do we know, and where are we headed? Cleve Clin J Med 2009;76:59–70.

Pratt LA, Ford DE, Crum RM, Armenian HK, Gallo JJ, Eaton WW. Depression, psychotropic medication, and risk of myocardial infarction. Prospective data from the Baltimore ECA follow-up. Circulation 1996;94: 3123–3129.

R

Ramgopal S, Thome-Souza S, Jackson M, Kadish NE, Sánchez Fernández I, Klehm J, Bosl W, Reinsberger C, Schachter S, Loddenkemper T. Seizure detection, seizure prediction, and closed-loop warning systems in epilepsy. Epilepsy Behav. 2014 Aug;37:291-307.

Rao VR, Lowenstein DH. Epilepsy. Curr Biol 2015;25(17):R742–6.

Ravi S, Shreenidhi S, Shahina A, Ilakiyaselvan N, Khan AN. Epileptic seizure detection using convolutional neural networks and recurrence plots of EEG signals. *Multimed. Tools Appl.* 2022, *81*, 6585–6598.

Reichlin, Tobias et al. Advanced ECG in 2016: is there more than just a tracing?. Swiss medical weekly 2016;146:w14303.

Ren Z, Han X, Wang B. The performance evaluation of the state-of-the-art EEG-based seizure prediction models. Front Neurol. 2022 Nov 24;13:1016224.

Resstel LB & Correa FM. Involvement of the medial prefrontal cortex in central cardiovascular modulation in the rat. Auton Neurosci. 2006;126,: 130–138.

Richman J.S., Moorman J.R. Physiological time-series analysis using approximate entropy and sample entropy. Am. J. Physiol. Circ. Physiol. 2000;278:H2039–H2049.

Ritz K, van Buchem MA, Daemen MJ. The heart-brain connection: mechanistic insights and models. Netherlands Heart Journal. 2013;21(2): 55-57.

Rosengren A1, Hawken S, Ounpuu S, Sliwa K, Zubaid M, Almahmeed WA, et al. Association of psychosocial risk factors with risk of acute myocardial infarction in 11119 cases and 13648 controls from 52 countries (the INTERHEART study): case–control study. Lancet, 2004;364: 953–962.

Rosso OA, Martin MT, Plastino A. Brain electrical activity analysis using wavelet-based informational tools. Physica A 2002;313(3):587–608.

Roux B. Ion channels and ion selectivity. Essays Biochem. 2017;61:201–9.

S

Sabelli H, Kovacevic L. Quantum Bios and Biotic Complexity in the Distribution of Galaxies. Complexity 2006;11:14-25.

Sabelli H, Lawandow A. Homeobios: the pattern of heartbeats in newborns, adults, and elderly patients. Nonlinear Dynamics Psychol Life Sci. 2010 Oct;14(4):381-410.

Sabelli H, Messer J, Kovacevic L, Walthall K. Biotic patterns of heart rate variation in depressed and psychotic subjects. Nonlinear Dynamics Psychol Life Sci. 2011 Jan;15(1):11-28.

Sabelli H, Sugerman A, Kovacevic L, Kauffman L, Carlson-Sabelli L, Patel M, Konecki J. Bios data analyzer. Nonlinear Dynamics Psychol Life Sci. 2005 Oct;9(4):505-38.

Saleh M, Ambrose JA. Understanding myocardial infarction. F1000Res. 2018 Sep 3;7:F1000 Faculty Rev-1378.

Sang K, Bao C, Xin Y, Hu S, Gao X, Wang Y et al. Plastic change of prefrontal cortex mediates anxiety-like behaviors associated with chronic pain in neuropathic rats. Molecular Pain. 2018;14: 1-16

Schaltenbrand N, Lengelle R, Toussaint M, Luthringer R, Carelli G, Jacqmin A, Lainey E, Muzet A, Macher JP. Sleep stage scoring using the neural network model: comparison between visual and automatic analysis in normal subjects and patients. Sleep. 1996 Jan;19(1):26-35.

Scholz S, Schneider SL, Rose M. Differential effects of ongoing EEG beta and theta power on memory formation. PLoS One. 2017;12(2):e0171913

Schumacher J, Taylor JP, Hamilton CA et al. Quantitative EEG as a biomarker in mild cognitive impairment with Lewy bodies. Alz Res Therapy 2020;12: 82.

Seyd PA, Ahamed VT, Jacob J, Joseph P. Time and frequency domain analysis of heart rate variability and their correlations in diabetes mellitus. Int. J. Biol. Life Sci. 2008;4:24–27.

Sgoifo A, Stilli D, Medici D, Gallo P, Aimi B, Musso E. Electrode positioning for reliable telemetry ECG recordings during social stress in unrestrained rats. Physiol Behav. 1996;60:1397–401.

Shaffer F, Ginsberg J. An Overview of Heart Rate Variability Metrics and Norms. Front. Public Health. 2017;5:258..

Shahrestani S, Stewart EM, Quintana DS, Hickie IB, Guastella AJ. Heart rate variability during adolescent and adult social interactions: a meta-analysis. Biol Psychol. 2015 Feb;105:43-50.

Sharir T, Merzon K, Kruchin I, et al. Use of electrocardiographic depolarization abnormalities for detection of stress-induced ischemia as defined by myocardial perfusion imaging. Am J Cardiol. 2012;109:642–50.

Sharma AK, Reams RY, Jordan WH, Miller MA, Thacker HL, Snyder PW. Mesial temporal lobe epilepsy: pathogenesis, induced rodent models and lesions. Toxicol Pathol. 2007;35(7):984–999.

Shipp S. Structure and function of the cerebral cortex. Curr Biol. 2007;17:R443–9.

ShivkumarK, Ajijola OA, Anand I, Armour JA, Chen PS, Esler M, et al. Clinical neurocardiology defining the value of neuroscience-based cardiovascular therapeutics. J. Physiol. 2016; 594, 3911–3954.

Siddiqui F, Mohammad A, Alam MA, Naaz S, Agarwal P, Sohail SS, Madsen DØ. Deep Neural Network for EEG Signal-Based Subject-Independent Imaginary Mental Task Classification. Diagnostics (Basel). 2023 Feb 9;13(4):640.

Siddiqui MA, Ahmad U, Khan AA, Mohammad A, Badruddeen A, Khalid M, et al. Isoprenaline: a tool for inducing myocardial infarction in experimental animals. Int J Pharmacy. 2016; 6:138–144

Silalahi DK, Rizal A, Rahmawati D, Sri Aprillia B. Epileptic seizure detection using multidistance signal level difference fractal dimension and support vector machine. *J. Theor. Appl. Inf. Technol.* 2021, *99*, 909–920.

Silipo R, Marchesi C. Artificial neural networks for automatic ECG analysis. *IEEE Transactions on Signal Processing*, 1998;46(5):1417-1425.

Smits FM, Porcaro C, Cottone C, Cancelli A, Rossini PM, Tecchio F. Electroencephalographic Fractal Dimension in Healthy Ageing and Alzheimer's Disease. PLoS One. 2016 Feb 12;11(2):e0149587.

Stam CJ, van der Leij H, Keunen RWM, Tavy DLJ. Non-linear EEG changes in postanoxic encephalopathy, Theor. Biosci. 1999;118:209—218.

Stam CJ. Nonlinear dynamical analysis of EEG and MEG: review of an emerging field. Clin Neurophysiol. 2005; 116(10):2266-301.

Stanojlović O, Živanović D Experimental models of epilepsy. Medicinski pregled 2004;Vol 57: 359-362

Stuckey MI, Tulppo MP, Kiviniemi AM, Petrella RJ. Heart rate variability and the metabolic syndrome: a systematic review of the literature. Diabetes Metab Res Rev. 2014 Nov;30(8):784-93.

Subasi A. Application of adaptive neuro-fuzzy inference system for epileptic seizure detection using wavelet feature extraction. Comput Biol Med. 2007 Feb;37(2):227-44.

Sunol C, Vale C, and Rodriguez-Farre E. Polychlorocycloalkane insecticide action on GABA and glycinedependent chlorine flux. Neurotoxicology, 1998.19:573–580.

Surawicz B, Orr CM, Hermiller JB, Bell KD, Pinto RP. QRS changes during percutaneous transluminal coronary angioplasty and their possible mechanisms. J Am Coll Cardiol. 1997;30:452–8.

Suzuki S, Motogi J, Nakai H, Matsuzawa W, Takayanagi T, Umemoto T, Hirota N, Hyodo A, Satoh K, Otsuka T, Arita T, Yagi N, Yamashita T. Identifying patients with atrial fibrillation during sinus rhythm on ECG: Significance of the labeling in the artificial intelligence algorithm. Int J Cardiol Heart Vasc. 2022 Jan 11;38:100954.

T

Tang SY, Ma HP, Lin C, Lo MT, Lin LY, Chen TY, Wu CK, Chiang JY, Lee JK, Hung CS, Liu LD, Chiu YW, Tsai CH, Lin YT, Peng CK, Lin YH. Heart rhythm complexity analysis in patients with inferior ST-elevation myocardial infarction. Sci Rep. 2023 Nov 27;13(1):20861.

Tarvainen MP, Niskanen JP, Lipponen JA, Ranta-Aho PO, Karjalainen PA. Kubios HRV--heart rate variability analysis software. Comput Methods Programs Biomed. 2014;113(1):210-20.

Tavares RF, Corrêa FM, Resstel LBM. Opposite role of infralimbic and prelimbic cortex in the tachycardiac response evoked by acute restraint stress in rats. J Neurosci Res 2009;87: 2601–2607.

Thygesen K, Alpert JS, Jaffe AS, Chaitman BR, Bax JJ, Morrow DA, White HD; Executive Group on behalf of the Joint European Society of Cardiology (ESC)/American College of Cardiology (ACC)/American Heart Association (AHA)/World Heart Federation (WHF) Task Force for the Universal Definition of Myocardial Infarction. Fourth Universal Definition of Myocardial Infarction Circulation. 2018 Nov 13;138(20):e618-e651.

Toichi M, Sugiura T, Murai T, Sengoku A. A new method of assessing cardiac autonomic function and its comparison with spectral analysis and coefficient of variation of R-R interval. J Auton Nerv Syst. 1997 Jan 12;62(1-2):79-84.

Tokgozoglu SL, Batur MK, Topcuoglu MA, Saribas O, Kes S, Oto A. Effects of stroke localization on cardiac autonomic balance and sudden death. Stroke 1999;30: 1307.

Tononi G, Cirelli C. Time to be SHY? Some comments on sleep and synaptic homeostasis. Neural Plast. 2012;2012:415250.

Tsai CH, Ma HP, Lin YT, Hung CS, Huang SH, Chuang BL, Lin C, Lo MT, Peng CK, Lin YH. Usefulness of heart rhythm complexity in heart failure detection and diagnosis. Sci Rep. 2020 Sep 10;10(1):14916.

Tse G. Mechanisms of cardiac arrhythmias. J Arrhythmia. 2016;32:75–81

Tulppo MP, Mäkikallio TH, Takala TE, Seppänen T, Huikuri HV. Quantitative beat-to-beat analysis of heart rate dynamics during exercise. Am J Physiol. 1996 Jul;271(1 Pt 2):H244-52.

Turski WA, Cavalheiro EA, Schwarz M, Czuczwar SJ, Kleinrok Z, Turski L. Limbic seizures produced by pilocarpine in rats: behavioural, electroencephalographic and neuropathological study. Behav Brain Res. 1983;9(3):315–335.

Tzallas AT, Tsipouras MG, et al. Automated Epileptic Seizure Detection Methods: A Review Study. Epilepsy Histological, Electroencephalographic and Psychological Aspects 2012.

U

Upaganlawar A, Gandhi H and Balaraman R. Isoproterenol induced myocardial infarction: Protective role of natural products. J. Pharmacol. Toxicol. 2011;6:1-17.

V

Van der Wall EE. Left ventricular function plays a role in cognitive ageing. Neth Heart J. 2011;19: 447–448.

Vandecasteele K, De Cooman T, Gu Y, Cleeren E, Claes K, Paesschen WV, et al. Automated Epileptic Seizure Detection Based on Wearable ECG and PPG in a Hospital Environment. Sensors (Basel) 2017;17.pii:E2338.

Vazquez Marrufo M, Vaquero E, Cardoso MJ, Gomez, CM. Temporal evolution of alpha and beta bands during visual spatial attention. Brain Res Cogn Brain Res. 2001;12: 315–320.

Verberne AJ, Owens NC. Cortical modulation of the cardiovascular system. Prog Neurobiol 1998;54: 149–168.

Viglione SS, Walsh GO, Proceedings: Epileptic seizure prediction. Electroencephalography and clinical neurophysiology 1975;39 (4):435–436.

Vorkapić M, Janković M, Savić A, Useinović N, Rašić-Marković A, Hrnčić D, Stanojlović O, Biotic patterns in the EEG signal of lindane treated rats: ictal and preictal, *Proc. 7th Congress of Serbian Neuroscience Society*, Belgrade, Serbia, October 25-27 2017 pp. 106, 2017.

Vucević D, Hrncić D, Radosavljević T, Mladenović D, Rasić-Marković A, Loncar-Stevanović H, Djurić D, Macut D, Susić V, Stanojlović O. Correlation between electrocorticographic and

motor phenomena in lindane-induced experimental epilepsy in rats. Can J Physiol Pharmacol. 2008 Apr;86(4):173-9.

W

Wang R, Wang J, Yu H, Wei X, Yang C, Deng B. Power spectral density and coherence analysis of Alzheimer's EEG. Cogn Neurodyn. 2015;9(3):291-304.

Werhahn KJ, Hartl E, Hamann K, Breimhorst M, Noachtar S. Latency of interictal epileptiform discharges in long-term EEG recordings in epilepsy patients. Seizure. 2015;29:20–25.

Wesselius, Fons J et al. Digital biomarkers and algorithms for detection of atrial fibrillation using surface electrocardiograms: A systematic review. Computers in biology and medicine 2021;133:104404.

Williams P, White A, Ferraro D, Clark S, Staley K, Dudek FE. The use of radiotelemetry to evaluate electrographic seizures in rats with kainate-induced epilepsy. J Neurosci Methods. 2006;155(1):39–48.

Y

Yogarajan G, Alsubaie N, Rajasekaran G, Revathi T, Alqahtani MS, Abbas M, Alshahrani MM, Soufiene BO. EEG-based epileptic seizure detection using binary dragonfly algorithm and deep neural network. Sci Rep. 2023 Oct 18;13(1):17710.

Yoo, Hyun-Joon et al. "Quantification of stroke lesion volume using epidural EEG in a cerebral ischaemic rat model." Scientific reports 2021;11(1):2308.

Yuan Q, Zhou W, Li S, Cai D. Epileptic EEG classification based on extreme learning machine and nonlinear features. Epilepsy Res. 2011;96(1–2):29–38.

Z

Zaafan MA, Zaki HF, El-Brairy AI and Kenawy SA. Protective effects of atorvastatin and quercetin on isoprenaline-induced myocardial infarction in rats. Bulletin of Faculty of Pharmacy, Cairo University 2013;51:35-41.

Zambrana-Vinaroz D, Vicente-Samper JM, Sabater-Navarro JM. Validation of Continuous Monitoring System for Epileptic Users in Outpatient Settings. Sensors (Basel). 2022 Apr 9;22(8):2900.

Zappasodi F, Olejarczyk E, Marzetti L, Assenza G, Pizzella V, Tecchio F. Fractal dimension of EEG activity senses neuronal impairment in acute stroke. PLoS One. 2014 Jun 26;9(6):e100199.

Zaragoza C, Gomez-Guerrero C, Martin-Ventura JL, Blanco-Colio L, Lavin B, Mallavia B, Tarin C, Mas S, Ortiz A, Egido J. Animal models of cardiovascular diseases. J Biomed Biotechnol. 2011:497841.

Zhang R, Wang J. Discussion of some problems about rat model with myocardial infarction. Journal of Shanxi Medical University 2004;35(1):13–5

Zimetbaum PJ, Josephson ME. Use of the electrocardiogram in acute myocardial infarction. N Engl J Med. 2003 Mar 6;348(10):933-40

Zipes DP, Jalife J, Stevenson WG. Cardiac electrophysiology from cell to bedside. 7th ed. Philadelphia: Elsevier; 2018

OBJAVLJENI REZULTATI

Radovi *in extenso* u časopisima sa JCR liste:

1. **Vorkapić M**, Savić A, Janković M, Useinović N, Isaković M, Puškaš N, Stanojlović O, Hrnčić D. (2020) Alterations of medial prefrontal cortex bioelectrical activity in experimental model of isoprenaline-induced myocardial infarction. PLoS ONE 15(5): e0232530. **(M22, IF 3,240),**

Pregledni rad u časopisu Medicinski podmladak:

1. Useinović N, **Vorkapić M**, Leković A, Ademović A, Šutulović N, Grubač Ž, Rašić Marković A, Hrnčić D, Stanojlović O Osnovne karakteristike epileptiformnih pražnjenja izazvanih Lindanom kod pacova, Medicinski podmladak 2018; 69(03): str.69-75.

2. **Vorkapić M**, Useinović N, Janković M, Hrnčić D, Heart rate variabillty processing in epilepsy: The role in detection and prediction of seizures and SUDEP, *Medicinski podmladak* 2018; 69(03): pX63-68

BIOGRAFIJA AUTORA

Dr Marko Đ Vorkapić je lekar specijalista Interne medicine na Institutu za Reumatologiju u Beogradu aktuelno na subspecijalizaciji iz Reumatologije. Rodio se u Beogradu 1990. Godine. Završio je „XIII Beogradsku gimnaziju“ u Beogradu 2009. godine, a nakon toga upisao Medicinski fakultet Univerziteta u Beogradu. Fakultet je završio 2015. godine sa prosečnom ocenom 9,89. Tokom osnovnih studija više puta je nagrađivan: u tri navrata pohvalnicom dekana Medicinskog fakulteta a 2012 godine i Nagradom Zadužbine Nikole Spasića. Nakon završetka osnovnih studija upisuje doktorske akademske studije na Medicinskom fakultetu Univerziteta u Beogradu, modul Fiziološke nauke pod mentorstvom prof. dr D. Hrnčića, a nakon obaveznog lekarskog staža upisuje specijalizaciju iz Interne medicine na Medicinskom fakultetu Univerziteta u Beogradu. Godine 2019 kao jedan od “100 najboljih” sudenata biva zaposlen na konkursu Ministarstva zdravlja na Katedri za Kardiologiju Univerzitetskog Kliničkog centra Srbije gde radi u svojstvu kliničkog lekara sve do 2021. godine. 2021 godine polaže specijalistički ispit iz Interne medicine sa ocenom odličan (5) i prelazi na Institut za Reumatologiju Srbije gde 2022 godine upisuje subspecijalizaciju iz Reumatologije.

Dr Marko Vorkapić usavršavao se u oblasti Ehosonografije koštanozglobnog sistema, srca kao i krvnih sudova. Učestvovao je u brojnim domaćim i međunarodnim skupovima u oblasti Fizioloških nauka, Interne medicine, Kardiologije i Reumatologije. Bibliografija dr Vorkapića do sada broji 22 jedinice. Autor 5 in extenso radova, Učestvovao je na međunarodnim (8 izvoda) i nacionalnim skupovima (9 izvoda).

Oblasti užeg naučno-stručnog interesovanja: reumatologija, sistemske bolesti vezivnog tkiva, neurofiziologija, napredna analiza signala, neurokardiologija.

AUTHOR BIOGRAPHY

Dr Marko Vorkapić is an attending physician of internal medicine at the Institute of Rheumatology in Belgrade, and rheumatologist in training. He was born in Belgrade in 1990 and graduated from "XIII Belgrade gymnasium" in 2009 after which he attended the Medical faculty, University of Belgrade. He graduated cum laude in 2015 with an average grade of 9.89. During his graduate studies he received multiple awards. He received the Medical faculty dean award for best student three times and in 2012 he received the Nikola Spasić endowment award for best student. After graduation he went on to start doctoral studies at the Physiology department of the Medical Faculty, University of Belgrade under the mentorship of dr. Dragan Hrnčić as well as starting residency in Internal medicine at the University Clinical Center of Serbia. In 2019 he was recognized in the „100 best medical student programme" and begins working full time at the University Clinical center of Serbia, clinic for cardiology. In 2021 he finished his training in internal medicine with exellent grades and moved to work at the Institute od Rheumatology in Belgrade where he started training in rheumatology in 2022.

Dr Marko Vorkapić received further education in muskuloskeletal echosonography as well as echocardiography and vascular ultrasound. He was part of numerous international as well as national conferences in physiology, internal medicine, cardiology and rheumatology. The bibliography of dr Vorkapić consists of 22 published works. He authored 5 in extenso papers, took part in international conferences (8 abstracts) and national conferences (9 abstracts).

His professional and scientific focus is in the fields of rheumatology, autoimmune and systemic diseases, neurophysiology, advanced signal analysis and neurocardiology.

образац изјаве о ауторству

Изјава о ауторству

Име и презиме аутора: Марко Воркапић

Број индекса: FN 03/15

Изјављујем

да је докторска дисертација под насловом:

"Spectral, biotic and fractal analysis of EEG and ECG signals in experimental models of myocardial infarction and epilepsy "

- резултат сопственог истраживачког рада;
- да дисертација у целини ни у деловима није била предложена за стицање друге дипломе према студијским програмима других високошколских установа;
- да су резултати коректно наведени и
- да нисам кршио/ла ауторска права и користио/ла интелектуалну својину других лица.

Потпис аутора

У Београду, 22.05.2024

Марко Воркапић

образац изјаве о истоветности штампане и електронске верзије докторског рада

Изјава о истоветности штампане и електронске верзије докторског рада

Име и презиме аутора: Марко Воркапић

Број индекса: FN 03/15

Студијски програм: Докторске студије из медицинских наука- смер Физиолошке науке

Наслов рада: "Spectral, biotic and fractal analysis of EEG and ECG signals in experimental models of myocardial infarction and epilepsy "

Ментор: prof. dr Dragan Hrnčić, prof. dr Milica Janković

Изјављујем да је штампана верзија мог докторског рада истоветна електронској верзији коју сам предао/ла ради похрањивања у **Дигиталном репозиторијуму Универзитета у Београду.**

Дозвољавам да се објаве моји лични подаци везани за добијање академског назива доктора наука, као што су име и презиме, година и место рођења и датум одбране рада.

Ови лични подаци могу се објавити на мрежним страницама дигиталне библиотеке, у електронском каталогу и у публикацијама Универзитета у Београду.

Потпис аутора

У Београду, 22. 05. 2024

Марко Воркапић

образац изјаве о коришћењу

Изјава о коришћењу

Овлашћујем Универзитетску библиотеку „Светозар Марковић“ да у Дигитални репозиторијум Универзитета у Београду унесе моју докторску дисертацију под насловом:

“Spectral, biotic and fractal analysis of EEG and ECG signals in experimental models of myocardial infarction and epilepsy “

која је моје ауторско дело.

Дисертацију са свим прилозима предао/ла сам у електронском формату погодном за трајно архивирање.

Моју докторску дисертацију похрањену у Дигиталном репозиторијуму Универзитета у Београду и доступну у отвореном приступу могу да користе сви који поштују одредбе садржане у одабраном типу лиценце Креативне заједнице (Creative Commons) за коју сам се одлучио/ла.

1. Ауторство (CC BY)

2. Ауторство – некомерцијално (CC BY-NC)

3. Ауторство – некомерцијално – без прерада (CC BY-NC-ND)

4. Ауторство – некомерцијално – делити под истим условима (CC BY-NC-SA)

5. Ауторство – без прерада (CC BY-ND)

6. Ауторство – делити под истим условима (CC BY-SA)

(Молимо да заокружите само једну од шест понуђених лиценци. Кратак опис лиценци је саставни део ове изјаве).

Потпис аутора

У Београду, 22.05.2024

Марко Јокић

1. **Ауторство**. Дозвољавате умножавање, дистрибуцију и јавно саопштавање дела, и прераде, ако се наведе име аутора на начин одређен од стране аутора или даваоца лиценце, чак и у комерцијалне сврхе. Ово је најслободнија од свих лиценци.

2. **Ауторство – некомерцијално**. Дозвољавате умножавање, дистрибуцију и јавно саопштавање дела, и прераде, ако се наведе име аутора на начин одређен од стране аутора или даваоца лиценце. Ова лиценца не дозвољава комерцијалну употребу дела.

3. **Ауторство – некомерцијално – без прерада**. Дозвољавате умножавање, дистрибуцију и јавно саопштавање дела, без промена, преобликовања или употребе дела у свом делу, ако се наведе име аутора на начин одређен од стране аутора или даваоца лиценце. Ова лиценца не дозвољава комерцијалну употребу дела. У односу на све остале лиценце, овом лиценцом се ограничава највећи обим права коришћења дела.

4. **Ауторство – некомерцијално – делити под истим условима**. Дозвољавате умножавање, дистрибуцију и јавно саопштавање дела, и прераде, ако се наведе име аутора на начин одређен од стране аутора или даваоца лиценце и ако се прерада дистрибуира под истом или сличном лиценцом. Ова лиценца не дозвољава комерцијалну употребу дела и прерада.

5. **Ауторство – без прерада**. Дозвољавате умножавање, дистрибуцију и јавно саопштавање дела, без промена, преобликовања или употребе дела у свом делу, ако се наведе име аутора на начин одређен од стране аутора или даваоца лиценце. Ова лиценца дозвољава комерцијалну употребу дела.

6. **Ауторство – делити под истим условима**. Дозвољавате умножавање, дистрибуцију и јавно саопштавање дела, и прераде, ако се наведе име аутора на начин одређен од стране аутора или даваоца лиценце и ако се прерада дистрибуира под истом или сличном лиценцом. Ова лиценца дозвољава комерцијалну употребу дела и прерада. Слична је софтверским лиценцама, односно лиценцама отвореног кода.